UNIVERSITY OF OKLAHOMA

GRADUATE COLLEGE

NEUROIMAGING FEATURES OF NORMAL AGING IN HEALTHY ADULTS

A DISSERTATION

SUBMITTED TO THE GRADUATE FACULTY

in partial fulfillment of the requirements for the

Degree of

DOCTOR OF PHILOSOPHY

By

YUXUAN CHEN
Norman, Oklahoma
2020

NEUROIMAGING FEATURES OF NORMAL AGING IN HEALTHY ADULTS

A DISSERTATION APPROVED FOR THE
SCHOOL OF ELECTRICAL AND COMPUTER ENGINEERING

BY THE COMMITTEE CONSISTING OF

Dr. Han Yuan, Chair

Dr. John Dyer

Dr. Michael Wenger

Dr. Liangzhong Xiang

Dr. Bin Zheng

Acknowledgements

When looking back, so many wonderful memories made in the past four years, I am extremely grateful to experience such a meaningful journey in my life. Firstly, I would like to express my gratitude and appreciation to my advisor, Dr. Han Yuan, for her dedicated support and guidance as a great mentor and inspirator to lead me through my doctoral program. Meanwhile, I would like to thank Dr. John Dyer, Dr. Michael Wenger, Dr. Liangzhong Xiang, and Dr. Bin Zheng, for their consistent support and services as my advisory committee members.

I want to say "thank you" specifically to all of our collaborators: Dr. Guofa Shou, Dr. Chuang Li, Junwei Ma in Dr. Lei Ding's lab, and Lisa De Stefano, Tory Worth in Dr. Michael Wenger's lab as well as Dr. Barbara Carlson and Dr. Melissa Craft. It will be impossible for me to accomplish fruitful achievements without your unreserved support and flawless work.

Other great thanks I would like to send to my colleagues in my research lab. Thank you for getting my back at my every up and down. I could not expect more than the friendships between you, and I. Yafen Chen and Fan Zhang gave me great suggestions and advice in my research. Julia Tang was served as the best partner to help me coordinate our research project. Jesse Farrand, Josiah Rippetoe, Jesus Roque, helped me a lot to preprocess the data.

I am truly grateful to have my parents Guoqiang Chen and Ju Wang, and all my family members' support and encouragement to go through this unprecedented time and complete my degree.

This work was supported by the National Science Foundation RII Track-2 FEC 1539068, Oklahoma Center for the Advancement of Science and Technology HR16-057, National Institutes of Health NIEHS R21ES027909, and Institute for Biomedical Engineering, Science and Technology at the University of Oklahoma.

Table of Contents

List of Tables

List of Figures

Abstract

Neurodegenerative disorders, such as Alzheimer's disease (AD), have an enormous impact on the quality of life in millions of aging adults and bring a daunting financial burden to the society. Towards understanding the mechanism of AD, recent studies have emphasized the changes in large-scale brain networks related to healthy aging, with the ultimate purpose to aid in differentiating normal neurocognitive aging from neurodegenerative disorders that also arise with age. In this dissertation, my work aimed to establish a neuroimaging-based biomarker that can indicate the episodic memory performance in humans, which in the long term can be a tool to monitor the memory decline in the normal aging process early stage of Alzheimer's disease. In particular, my work focused on using wearable neural technology, i.e., electroencephalography (EEG) and functional near-infrared spectroscopy (fNIRS), to investigate the association of memory and brain connectivity pattern of default mode network (DMN).

Chapter 2 of my dissertation showed that higher brain connectivity in the posterior cingulate / precuneus area of DMN was associated with lower performance on an episodic memory task. The findings demonstrate the feasibility of using electrophysiological imaging to characterize large-scale brain networks and suggest that network connectivity changes are associated with normal aging.

Furthermore, Chapter 3 of my dissertation investigated the confounding effect of vigilance on brain network connectivity at awake resting state. I examined the characteristics of the global signal by using fNIRS and correlated the amplitude of the fNIRS global signal with vigilance measured by EEG. Results found that body positions' factor significantly affected the amplitude of the resting-state fNIRS global signal, prominently in the frequency range of 0.05 Hz - 0.1 Hz but only marginally in the very-low-frequency range of less than 0.05 Hz. More importantly, the

amplitude of the global signal in the very-low-frequency range of less than 0.05 Hz exhibited a significant negative correlation with EEG vigilance measures. For the first time, our study revealed that vigilance as a neurophysiological factor modulates the resting-state dynamics of fNIRS, which have important implications for understanding the noises and neural origins in fNIRS and possibly in fMRI signals.

In Chapter 4, my work continues to search for approaches that can minimize the confounding effect of vigilance other than regress the entire vigilance, which contains physiological noise and the neuronal component. By implementing new connectivity metrics, the significant association between memory and brain connectivity is consistent with our previous finding. More importantly, the new metrics improved the significance of the difference between two age groups and the association between age and brain connectivity. The approach of removing the confounding part of vigilance measure will increase the accuracy and sensitivity of EEG brain connectivity and indicate broad application prospects in normal and abnormal aging studies.

In summary, my dissertation systematically demonstrates the current application of portable non-invasive neuroimaging tools in the field of aging and Alzheimer's study. My work has also examined the confounding effect of vigilance on network connectivity, and further proposed a solution of calibrated network connectivity towards a more accurate neuroimaging biomarker for memory. Our results suggest that EEG would be an effective, sensitive neuroimaging tool to characterize electrophysiological features of normal aging in the human brain's large-scale networks. My findings based on multimodal neuroimaging also provide important implications in understanding the neuroimaging literature on memory and aging.

Chapter 1: Introduction

1.1 Motivation and Significance of the Study

1.1.1 State-of-the-Art in Aging and Alzheimer's Disease Study

According to a report published by Alzheimer's Association in 2020, 5.8 million Americans live with Alzheimer's disease (AD) (Hebert et al., 2013; 2020). Among the population of above 65 years old, almost one of ten people are affecting by AD (Hebert et al., 2013; 2020). With the old population keeping increasing, the aging society will aggravate the prevalence of AD nationally.

Dementia is the overall term of diseases that showed cognitive function impairment symptoms, including memory loss, language problem and problem-solving ability (2020). As a major common cause of dementia, AD accounts for 60% to 80% of the total cases. Nowadays, we are capable of gaining the knowledge that major brain changes are associated with AD except the outward behavioral manifestation. While the healthy people own more than 100 billion neurons working in the brain and 100 trillion synapses performing the role of a connection between adjacent neurons, the beta-amyloid accumulations are impeding the communications from the outside of neuron, and an abnormal form of a protein called tau tangles are hindering the nutrient transportation from the inside of neurons in the brain of patients with AD (Sato et al., 2018; Hanseeuw et al., 2019). The internal and external damage caused the outcome of neuron death and the consequence of other brain alterations, inflammation, and atrophy.

AD was not developed in a day, nor a year. This gradual process of neurodegeneration is slow at the early stages and lasting more than several decades. For some AD patients with a special gene that is widely believed to contribute significantly to this process, the significantly increased

beta-amyloid level could precede the first symptom manifestation 22 years long (Gordon et al., 2018). The very begging phase of AD is preclinical Alzheimer's. During this phase, there will have no obvious symptoms showed as compared to normal aging people. However, the subtle brain changes, mainly focus on neurobiochemical biomarkers (the levels of beta-amyloid or the glucose metabolism), can be detected by the scans of positron emission tomography or the analysis of cerebrospinal fluid. Beyond this, the possible deterioration of brain function could be enveloped by normal-appearing brain connectivity and cannot be sensitively captured by modern neuroimaging technology. Cabeze et al. provided a detailed explanation of metabolic and physiological mechanisms for brain maintenance, reserve, and compensation (Cabeza et al., 2018). Genetic and environmental factors, such as education length, physical activity, bilingualism, and so forth, endow the brain with more sources to repair impairments, resist and compensate for memory decline, as some older people perform memory tests similar to young adults.

For Alzheimer's dementia, unfortunately, there have no pharmacologic treatments approved by the U.S. Food and Drug Administration to cure or treat behavioral and psychiatric symptoms despite decades of researches on AD. Along with the difficulties of recruiting enough participation of patients and longtime observation for an investigational treatment, the most difficult problem is from the technical and pathological aspects as the biological process, and molecular changes relevant to AD is still ambiguous. Many researchers believed the trend of future treatment and intervention would be mainly focusing on the phases before the onsite of AD. This is also the starting point of my projects, though out my whole doctoral program. I devoted myself to looking for an effective and novel biomarker that would ultimately be beneficial for 1) increasing accuracy and specificity of the early diagnosis of AD, and 2) critical for monitoring the effect of investigational treatments.

1.1.2 How Aging in Adults Is Related to Alzheimer's Disease

Aging is not sufficient for the onset of Alzheimer's, and Alzheimer's is not an inevitable outcome of aging (Nelson et al., 2011). Under this premise, aging is among the greatest risk factors for AD (Hebert et al., 2010; Hebert et al., 2013). While the morbidity of AD among the population of age 65-74 is around 3%, the numbers among the age groups of 75-84 and 85 or older are 17% and 32%, respectively (Hebert et al., 2013).

Aging studies and AD studies are two different fields of research but have many intrinsic links. The findings and knowledge in one field can inspire the research in another one. Xia et al. summarized evidences in both fields based on the existing studies at the molecular, cellular and system-level (Xia et al., 2018). At the molecular level, the gene of apolipoprotein E (APOE) played a great role in AD and normal aging. Two of the three most common alleles of APOE found to have the same effect on AD and aging process (Strittmatter et al., 1993b; Seripa et al., 2006). Besides, another common pathology among both AD and aging is chronic inflammation. The intrinsic and extrinsic factors to keep the complicated balance between anti- and pro-inflammation are the key knowledge for the development and trials of AD (Shaw et al., 2013; Franceschi et al., 2017). The findings in AD research could be a benefit for the aging study and vice versa. Future more, sleep, including normal Non-rapid Eye Movement Sleep and insomnia, is the most important lifestyle with a close relationship with AD and aging (Prinz et al., 1982; Liguori et al., 2014). However, some systematic alteration, like neuron loss, happened in AD (Scheff and Price, 2006), and less likely in the process of normal aging.

The complex association between AD and aging prompts the development in studies of either AD or aging but, sometimes, confuses the investigations of AD, which mainly based on

previous aging studies and knowledge or vice versa. It is essential to understand better the different underlying mechanisms and the blurring boundaries between AD and aging.

1.1.3 How Aging Study Will Inform Intervention and Prevention Trial

The most challenging scientific problem toward AD is to figure out what its etiology is. Without a clear understanding of its pathology, it is impossible to develop effective interventions available for all AD patients. AD presents a plethora of cognitive function deteriorations. Current studies focus on the direct pathogenic factors, amyloid-beta, and tau deposition. Korczyn (2012) challenged the modern investigation to only focus on single etiology. Including the biochemical biomarkers of amyloid-beta and tau tangle, the factors as age, genetics, family history, and other mild cognitive disorder or dementia contribute to the diagnosis of AD, but none of them is an essential condition for the clinical diagnosis of AD (Korczyn et al., 2012). APOE ε4 is one of the common alleles of APOE shown that can increase the risk of AD (Strittmatter et al., 1993a), but the frequency of the presence of ε4 allele in patients with AD is only 40% (Liu et al., 2013). Especially, a newly approved AD treatment based on the "brain-gut axis" circulatory system (Wang et al., 2019) provides more possibilities and guess on the accurate etiology.

There is no doubt that the advance of aging study could benefit future investigation from pathological to clinical treatment development. First, the advances of normal aging study will boost the understanding of the gap among the transition from the normal aging process in middle-age adults to pre-clinical phases. Most researchers believe future treatment and intervention would be more effective when applied to the early stage of AD. Second, more normal aging studies would provide a more theoretical foundation to identify the abnormal process, which could increase the risk of developing AD and other dementias. Third, an aging study provides more biomarkers available for the participation screen of AD. Different biomarkers would cluster the participants

into elaborated test groups. Furthermore, this would make the clinical trials of treatments more specific, efficient, and accurate for different AD phases.

1.2 State-of-the-Art in Neuroimaging of Aging and Alzheimer's Disease

1.2.1 Significance of RSFC in Neuroimaging Studies

Resting-State Functional connectivity (RSFC) is defined as the correlation between distinct brain areas responsible for various functions in the temporal domain (Chen et al., 2020). This technology term usually refers to the interaction between different brain regions based on the measurement of the blood-oxygen-level-dependent (BOLD) in fMRI. The task activation requests the corresponding brain area to perform a special response to external stimuli or order. Moreover, this leads to the firing of plenty of neurons and followed by the increased consumption of oxygen, which leads to a decrease of deoxyhemoglobin. Brain activation, thus, can be captured by fMRI as localized increased signal intensity among single voxel. The coherence of brain activity between different brains is termed as functional brain connectivity. Furthermore, RSFC is the brain functional connectivity under the circumstance without any external stimuli.

After decades of investigation, researchers have found the RSFC within the primary sensorimotor cortex (Biswal et al., 1995b), auditory cortex, visual cortex (Hampson et al., 2002), motor and association cortices (Xiong et al., 1999; Zang et al., 2004), anterior and posterior cingulate cortex (Greicius et al., 2004b). Among all previous RSFC studies, data analysis is primarily focused on time-domain (seed-based correlation (Biswal et al., 1995b)), Kendall's correlation (Zang et al., 2004), principal component analysis (Huettel et al., 2004), independent component analysis (Beckmann et al., 2005b), and frequency-domain (Amplitude of low frequency fluctuations (ALFF) (Zou et al., 2008a; Zuo et al., 2010)) to dig the property of BOLD signal and association between RSFC and psychological or psychiatric disorders. In the data

analysis of my dissertation, the common methods in time-domain are employed, like seed-based correlation is designated to investigate the neuronal relationship between two distinct brain regions by selecting a cluster of brain source points as the representatives. Also, the independent component analysis is used to decompose the signal into several spatial-temporal patterns to map different outstanding brain functions.

1.2.2 fMRI Study of Aging/AD and Limitations

fMRI is one of the most advanced functional neuroimaging technologies (Pinti et al., 2020). This non-invasive modality allows researchers to acquire relatively high spatial resolution imaging of the human brain. Especially the RSFC in fMRI provides a reliable way to distinguish the age-related difference. Many fMRI studies demonstrated that older adults' activation is greater than the younger counterparts (Grady et al., 1995; Rypma and D'Esposito, 2000; Rypma et al., 2001; Cabeza, 2002; Satterthwaite et al., 2013). Besides, fMRI is a powerful tool in AD studies. Greicius et al. reported that the decreased hippocampal involvement was observed in a group of patients with AD compared to healthy older adults' group (Greicius et al., 2004b).

However, the tightly restrained environment limits fMRI to carry out the study of atypical development. Furthermore, it is challenging to perform cognitive tasks related to our daily lives in a narrow and noisy MRI scanner. Besides, the global signal, which is the averaged time series of the BOLD signal across all voxels, represents a time-varying of spatial homogeneity, including the effect of physiological noise (Liu et al., 2017b). However, the most common pre-processing methods, global signal removal or regression, in fMRI studies would remove neuronal components at the same time (Murphy et al., 2009; Wong et al., 2013). Moreover, this could confound some significant functional correlation and arbitrary significance (Murphy et al., 2009).

1.2.3 EEG Study of Aging/AD and Limitations

Electroencephalography (EEG) is another important neuroimaging tool. Its outstanding characteristic of high temporal resolution makes EEG become a promising tool for investigating the temporal dynamics. Previous studies indicated the universality of EEG rhythmic activity (delta band: 1-4 Hz, theta band: 4-8Hz, alpha band: 8-12Hz and beta band:12-30Hz) from early childhood (Marshall et al., 2002), to adolescents (Cragg et al., 2011), and up to advanced elderly (Mizukami and Katada, 2018).

However, the major limitation of the EEG signal is the property of relatively low spatial resolution. The current experimental level EEG devices usually contain tens of electrodes and up to 256 electrodes on a whole-head coverage. Even though the temporal domain EEG signal still has the issue of difficult to track the original neuronal source. One of the most advanced methods to solve this problem is to apply a reasonable prior constraint acquired from either fMRI or fNIRS signal and solve the so-called “inverse problem” to localize the accurate source location of the signal at every moment (Michel et al., 2004). Li et al. developed an algorithm using simultaneous fNIRS data as the spatial constraints to reconstruct the EEG signal from the temporal domain to the source level (Li et al., 2019). Besides, they applied this algorithm on the analysis of the comparison between healthy old adult and mild-AD patients.

1.2.4 fNIRS Study of Aging/AD and Limitations

fNIRS is the best alternative hemodynamic-based neuroimaging tool of fMRI. Possessing with both high temporal resolution and spatial resolution, fNIRS can substitute fMRI in most resting-state function connectivity studies. Its tolerance to head motion is favored by studies that are interested in the brain early development. In both typical and atypical early brain research, the head motions are uncontrolled during infants or children walk around, play with toys, or interact

with other individuals. Besides, fNIRS can involve a variety of elderly subjects to participant in the research of age-related effects on cortical hemodynamics during a cognitive task. Sahar et al. claim that fNIRS can robustly measure brain activity during memory encoding and retrieval in healthy subjects (Jahani et al., 2017). The significant activation was observed in the left dorsolateral prefrontal cortex during the coding, while the retrieval process resulted in activation in the dorsolateral prefrontal cortex bilaterally. This finding is consistent with previous fMRI and PET literature. Moreover, fNIRS is available on the elder adults with a variety of metal implants, pacemakers, and artificial cochleae. The novel AD biomarker with fNIRS could make clinical screening more affordable for the public.

Although fNIRS is an emerging modality as a neuroimaging tool in neuroscience, a clear consensus about the pre-processing procedure on fNIRS data has not yet be reached. Large heterogeneity in the analysis procedures is reported by Pinti and his colleagues (Pinti et al., 2019). Their systematic review summarized the pre-processing steps in 110 papers published in 2016. Except for those who did not report all the important information, there is still inconsistent opinion on almost every step in the pre-processing procedure. More than ten types of the different filters were used to filter the fNIRS data, and more than 20 different range selections were used for those bandpass filters. It is imperative to standardize the pre-processing guideline for ongoing and future fNIRS studies to avoid the confound inconsistency of results across different studies caused by the different pre-processing pipeline.

1.2.5 Complementary Features of Multimodal Neuroimaging

In Section 1.2, three popular neuroimaging tools were introduced separately. In practice, the multimodal study is a future trend for the studies relevant to the human brain. That is because the human brain is a 3-dimensional complex of brain regions. To better investigate the underlying

mechanism of normal and abnormal brain development, it is significant to capture transient temporal and accurate spatial information. Figure 1 showed the temporal and spatial parameters for EEG, fNIRS, and fMRI. Although some mathematical approaches can be used to make up its disadvantage, for example, source analysis can largely increase the spatial resolution of EEG, it still needs either fNIRS or fMRI signal to provide the priori constraints.

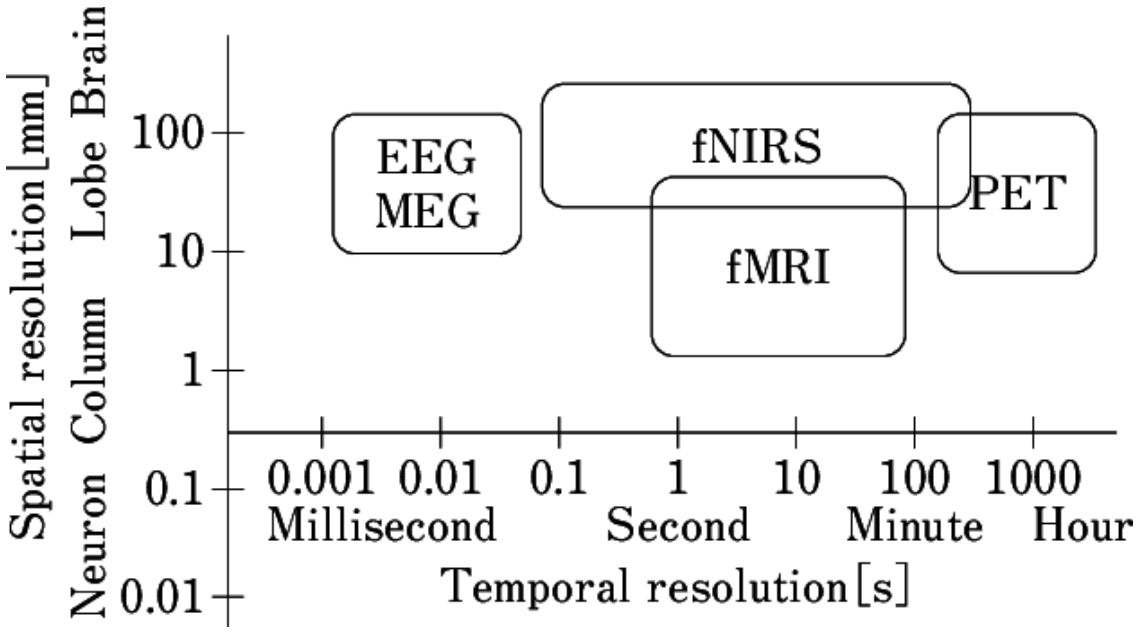

Figure 1 Comparison of features in different modalities.

Table 1 expands the comparison among EEG, fMRI, and fNIRS to every prospective. It is easy to find out that EEG and fNIRS have several places in common. Both are silent, mobile, and non-invasive neuroimaging tools. Especially the property of moderate tolerant ability to movement and permitting ferromagnetic implants make the simultaneous EEG/fNIRS modality look promising in aging and AD studies by accommodating the major restrictions for the old participants.

Table 1 Comparison of features in EEG, fNIRS, and fMRI.

	EEG	fNIRS	fMRI
Costs	Low	Moderate	High
Portability	Yes	Yes	No
Temporal Resolution	High (millisec.)	High (millisec.)	Low (sec.)
Spatial Resolution	Low (cm)	High (mm)	High (mm)
Noise	Low	Low	High
Movement Tolerance	Good	Good	Poor
Use in People with Ferromagnetic Implants	Yes	Yes	No

1.3 Organization of the Dissertation

Chapter 1 gives a brief introduction to the background of current development in Alzheimer's dementia and research. The unsuccessful clinical trials of medical treatments motivate my research from neuroimaging to assist the early diagnosis of AD in the future. Three popular neuroimaging tools are introduced to give the big picture of advantage/disadvantage comparison and why we used multimodal imaging tools.

Chapter 2 applies the EEG source analysis algorithm on our normal aging study. It reliably captures the changes of individual brain connectivity and demonstrates the significant association between brain connectivity and episodic memory. Besides, the significant relationship between brain connectivity and age is also revealed.

Chapter 3 aims to investigate the potential vigilance effect on brain connectivity measures. The simultaneous EEG/fNIRS data were acquired from 22 subjects. fNIRS-based Global signal metrics and EEG-based vigilance metrics are calculated. The frequency-domain analysis is used to determine the frequency band of interest. Well-designed statistical analysis is performed for two major factors: eye conditions (eyes-open, eyes-closed) and body positions (sitting, standing, supine). The relationship between global signal amplitude and vigilance measurements is significant.

Chapter 4 investigates the dynamic correlation between global signal amplitude and vigilance measurement at epoch-level. Long recordings of simultaneous EEG and fNIRS are divided into non-overlap 30 seconds epochs. Furthermore, the significant relationship at the individual-level continues to show up at the epoch-level. Besides, it investigates the association of brain connectivity and memory after diminishing the confounding effect of vigilance.

Chapter 5 presents the conclusion and recommendations for future investigation.

Chapter 6 summarizes all products of this work, including the presentation, publication, and manuscripts under review.

Chapter 2: Electrophysiological Resting State Brain Network and Episodic Memory in Healthy Aging Adults

2.1 Background

2.1.1 Human Memory and Brain Networks

The human brain is perhaps the most precise machine in the universe. About 100 billion neurons mass together in an organ to generate 1000 trillion synaptic joints allow us to perform extremely complicated tasks. Memory is exactly one of the most complicated tasks that human beings can excel in other mammals on earth.

In 1968, Richard Atkinson and Richard Shiffrin developed the classic memory model for posterity (Atkinson and Shiffrin, 1968). The multi-layer model categorized the memory by stages (sensory memory, Short-term memory (STM) and Long-term memory (LTM)) and types (explicit memory and implicit memory).

One major way to understand the memory is to separate them based on the stages or length of duration that memory segments could stay in our minds. This progressive relationship starting from the ephemeral sensory memory to the STM and then to the long-lasting LTM. In its literal meaning, sensory memory is the memory that humans used to sense the outside world. To avoid our memory contains only broken stream and incoherent pieces, sensory memory serves as a "cache" in the computer to allow the brain to have sufficient time to process whirlwind sensory inputs, including but not limited to auditory and visual sensory memories.

Compared to the sensory memory that could last no more than 1 second, STM could be held for several seconds and even one minute (Baddeley, 1990). Briefly, the sensory memory that we notice and pay attention shortly transformed to STM. Moreover, some of them will eventually be encoded to form LTM, which could last days, months, or years. In contrast, the sensory memory,

which did not gain attention, will be lost like a secret wind passing. Notably, the processes which we sense, explain and store information in STM are known as working memory.

Another popular way of understanding memory is in terms of the types of memory: explicit memory and implicit memory. Both are under the stage of LTM because of the relatively long-existing time and capability of being recalled. Whether the memory can be consciously remembered or not is the gold standard to distinguish explicit and implicit memory. The implicit memory is the memory we do not know how to explain why we do this or that. Thus, the major component of the implicit memory is procedural memory, such as the infants' ability to crawl and the teen's ability to ride a bicycle. Those are the memory we do not dedicate to explaining but learning by ourselves.

All those memories we can consciously and logically remember and recalled are called "explicit memory." Explicit memory, in my mind, is the way we understand and embrace the external world and environment. Semantic memory and episodic memory are the two major components. The former refers to the memory we remember about the facts and concepts, like the mathematical theorem and language. This is the way for us to communicate with others and do routine work better; the latter is our subjective experience. For example, sweet moments spent on New Year's Eve with family in a fantastic city. We usually need to remember several key components, when, where, who and doing what to tell a logic story. Exactly because of the characteristics of objectivity of episodic memory, distinguished people groups, especially between young and old adults (Damoiseaux et al., 2007), normal aging and Alzheimer disease (Tromp et al., 2015a), would perform significantly different. More details will be discussed in the next section.

As we discussed above, the term "memory" is divided and subdivided into many detailed concepts. Moreover, different brain function areas are responsible for divided memory functions.

Among those cortical cortexes, the prefrontal cortex is the main area covered for working memory, and procedural memory is replied on the striatum, etc. In particular, the posterior cingulate cortex and its attributive network, the Default Mode Network (DMN), responsible for episodic memory, are the interest region of our study. DMN includes a set of cortical regions, the inferior parietal lobule, the medial prefrontal cortex, the hippocampus and the posterior cingulate cortex/precuneus that act to be active during resting state (Raichle et al., 2001; Buckner et al., 2008).

There has emerging evidence illustrates that brain connectivity within specific brain networks, especially the DMN, demonstrates patterns that characterize the trajectory of aging and distinguish healthy aging from Alzheimer's disease in both task-specific and task-free fMRI models (Greicius et al., 2004a; Buckner et al., 2005). DMN is composed of several regions that are known to be associated with various cognitive functioning (Buckner et al., 2008; Mevel et al., 2011)(Buckner et al., 2008; Mevel et al., 2011). Posterior cingulate cortex is associated with episodic memory encoding (Natu et al., 2019), the medial prefrontal cortex is linked with social cognition (Amodio and Frith, 2006), the medial temporal lobe is reported to contribute to episodic memory and episodic future thinking (Race et al., 2011), and the parietal cortex is associated with attention function (Behrmann et al., 2004). Notably, amyloid-beta plaque, one of Alzheimer's disease pathologies, is initially deposited in DMN subsets, such as posterior cingulate cortex and hippocampus (Buckner et al., 2008; Ferreira and Busatto, 2013). Furthermore, disruptive alterations in the large-scale brain systems that support high-level cognition accompany cognitive decline at the behavior level, which is commonly observed in aging even in the absence of disease (Andrews-Hanna et al., 2007; Damoiseaux et al., 2007). Thus, the default mode network (DMN) is undoubtedly the most important area in most recent studies and aging-related studies.

2.1.2 Episodic Memory and Neurodegenerative Diseases

Episodic memory covers the personal event as well as experience in our daily life. It reflects the process of receiving, adapting, and storing information within an individual's communication with the outward environment. However, the performance of individuals could be disrupted largely by neurodegenerative diseases. The neurodegenerative diseases, including Alzheimer's disease (AD), Parkinson's disease, and other progressive diseases caused by degeneration or death of nerve cells (Fu et al., 2018). The loss of a fundamental unit of the nervous system, nerve cells, results in the incurable and irreversible characteristics of those neurodegenerative diseases.

One of the most common symptoms of neurodegenerative diseases is the loss of memory or so-called "amentia." Tracing back to the 18th century, Theodore Ribot reported the memory loss of distant events as the first characteristic of amentia among patients with dementia (Ribot, 1891). With a relentless effort of studying chronic amnesia, Alois Alzheimer founded one 51 years old patient who died after a long struggle with progressive memory loss and personality and behavior abnormalities. This case is later named "Alzheimer's disease' by his colleague Emil Kraepelin (Psychiatrie 8th edition).

Alzheimer's disease, as one of the most prevalent neurodegenerative disease, surpassed diabetes becomes the 6th leading cause of death in the US. Over 5.8 million Americans live with AD now, and this number will escalate to almost 14 million by 2050 (Alzheimer's Association, 2020). However, only 45% of people with Alzheimer's are told of their diagnosis, and 35% of those diagnosed patients were misdiagnosed as having Alzheimer's disease because of the moderate specificity of purely clinical grounded diagnosis procedure (Alzheimer's Association, 2020). Despite decades of research, we still have no cure, and we even have no way to prevent or slow down the disease after symptoms manifest. The symptoms manifestation, along with

dementia rate, neurodegeneration and abnormal amyloid deposition, are usually regarded as the onsite of the clinical stage of AD (Brier et al., 2014). While AD progresses slowly over a few decades, the relevant pathophysiological biomarkers typically precede symptomatic clinical phases over one to two decades (Gallagher and Koh, 2011; Sperling et al., 2011; Brier et al., 2014). If effective biomarkers could be identified for Alzheimer's to enable early detection of the disease, millions of patients would be able to receive early intervention or enroll in a beneficial clinical trial, and the quality of their lives could be dramatically improved.

Notwithstanding the end stage of AD is distinguishable, the earliest stage is often dismissed as the cognitive function degeneration of normal aging. The current diagnostic criteria of defining the early boundary of AD combines the feature of episodic memory decay with pathophysiological biomarkers of AD in the brain. Thus, it is clear that episodic memory played a significant role in the early diagnosis procedure of AD as well as other neurodegenerative diseases. Moreover, we focus on specifically the indivisible relationship between episodic memory and AD deterioration among neuroimaging features.

2.1.3 Episodic Memory and Age

According to Tromp's review on aging studies, age affects episodic memory from its all three phases, encoding, consolidation and retrieval (Tromp et al., 2015a). As an indispensable part of memory function, episodic memory integrated medial temporal lobe (MTL), hippocampus, and other cortical areas to enable individuals to experience external stimuli via visual, auditory, perceptual, or other ways. The large-scale brain networks are typically not uniformly affected by normal aging (Tromp et al., 2015a; Fu et al., 2018). Thus, it would be essential to laser focus on specific cortical areas, and brain networks to distinguish the subtle degeneration among age groups.

Encoding represents the general operations of transforming the external sensory, auditory, visual, and perceptual information in the arrangement of mental representation. The information and their mental representation could be an index to guide for future memory recovery and retrieval. The encoding activity involves all sensory cortices to be capable of sensing stimuli, as well as the prefrontal cortex and MTL, where the peripheral cortex, the lateral entorhinal area, and the hippocampal cortex (Tromp et al., 2015a).

Following the phase of encoding, memory storage or called "consolidation" process used to maintain the sensory content and rearrange them in the form of LTM. During this process, the neocortex and hippocampus played a big role. Especially, previous researchers found that when the contextual information is recalled, the hippocampus is always engaged actively (Piolino et al., 2008; Hoscheidt et al., 2010; Winocur et al., 2010).

The last phase of episodic memory is retrieval, which recalled the inactive LTM after days, months or even years since the LTM is consolidated. This could be the most significant process for the aging study, along with AD studies. During the retrieval process, the function network is located not only at the MTL, which involves the encoding process, but also the medial prefrontal cortex, poster cingulate cortex, and angular gyrus.

According to previous behavioral data, both encoding and retrieval processes of episodic memory displayed group-level decay when comparing older individuals with middle-age ones (Giffard et al., 2001; Gutchess et al., 2007). Nevertheless, different tasks could obscure the process of understanding the memory deficit among older adults. According to the study of Sauzéon et al., the performance of free recall right after the learning phase of healthy elderly (n=23, mean age =73.6 years old) was shown to be inferior to the performance of younger group (n=23, mean age = 22.2 years old). However, the age effect was largely diminished when comparing the results of

a yes/no recognition task, which performed 10 minutes after the learning phase (Sauzéon et al., 2016). Therefore, to benchmark the aging effect among healthy adults of different age groups is crucial for investigating the pathophysiological deterioration from healthy conditions to AD.

2.2 Motivations for This Project

With advances in medical science and health care, the world is changing into a rapidly aging society (Beard et al., 2016). Neurodegenerative disorders, such as Alzheimer's disease (AD), have an enormous impact on the quality of life in millions of aging adults and bring a daunting financial burden to the society. Although several hypotheses are currently being pursued (Ittner and Götz, 2011; Karran et al., 2011; Du et al., 2018), the lack of accurate clinical biomarkers for differentiating these disorders from normal aging has slowed the progress in establishing treatments that can be delivered early in the disease process (Golde et al., 2011; Sperling et al., 2014; Cummings et al., 2016; Crous-Bou et al., 2017).

Cognitive decline is commonly observed in aging even in the absence of diseases, affecting the functions of memory, execution, and attention (Hedden and Gabrieli, 2004; Whalley et al., 2004; Peters, 2006; Ferreira and Busatto, 2013). However, because the aging-related cognitive declines at non-pathological stage overlap with early symptom of cognitive deficit at preclinical or prodromal stage of AD (Ferreira and Busatto, 2013), early diagnosis of Alzheimer's disease is difficult to reach (Sperling et al., 2011; Fiandaca et al., 2014; Dubois et al., 2016). Therefore, in order to elucidate the pathogenesis of Alzheimer's disease, an augmenting attention has been raised to understanding normal aging (Ferreira and Busatto, 2013; Cavedo et al., 2014).

One of the first critical steps is to devise screens capable of differentiating age-related neurocognitive declines from cognitive deficits seen at preclinical or prodromal stages of a neurodegenerative disorder (Sperling et al., 2014; Cummings et al., 2016). Well-designed

experimental tasks and clinical batteries are widely deployed to detect the age-related differences in cognitive function (Donohue et al., 2014b). In addition, cognitive deficits have been observed in fMRI studies of cognitive tasks tapping into wide-ranging domains of episodic memory (Tromp et al., 2015b), working memory (Luo and Craik, 2008), attention (Madden, 1990), and executive task-switching (Cepeda et al., 2001). Nevertheless, the interpretation of task-based fMRI responses can be confounded by differences in task performance (Sheline and Raichle, 2013). Furthermore, task-based assessment of cognitive function may be biased by a number of factors that are bonded to the task design yet beyond the cognitive domains of interest (Healey et al., 2008; Grady, 2012). For example, older adults are recognized to be more susceptible to the effects of distracting interference during memory tasks (Healey et al., 2008; Grady, 2012), which suggest that a task-free strategy may be able to provide new insights.

Modern functional neuroimaging tools have dramatically shaped our knowledge of age-related changes in cognitive function. Recently, the use of task-free, resting-state functional connectivity imaging has resulted in rapidly growing literature on the nature and extent of network disruptions, which suggest the potential utility of functional connectivity as a biomarker for disease diagnosis, prognosis, and risks (Sperling, 2011; Sheline and Raichle, 2013; Brier et al., 2014). In particular, emerging evidence illustrates that brain connectivity within specific brain networks, especially the default mode network (DMN), demonstrates patterns that characterize the trajectory of aging and distinguish healthy aging from Alzheimer's disease in both task-specific and task-free fMRI models (Greicius et al., 2004a; Buckner et al., 2005).

DMN is composed of several regions which are known to be associated with various cognitive functioning (Buckner et al., 2008; Mevel et al., 2011): posterior cingulate cortex is associated with episodic memory encoding (Natu et al., 2019), the medial prefrontal cortex is

linked with social cognition (Amodio and Frith, 2006), the medial temporal lobe is reported to contribute to episodic memory and episodic future thinking (Race et al., 2011), and the parietal cortex is associated with attention function (Behrmann et al., 2004). Notably, amyloid-beta plaques, one of Alzheimer's disease pathologies, are initially deposited in DMN subsets, such as posterior cingulate cortex and hippocampus (Buckner et al., 2005). Furthermore, disruptive alterations in the large-scale brain networks that support high-level cognition are shown to accompany cognitive decline at the behavior level, which is commonly observed in aging even in the absence of disease (Andrews-Hanna et al., 2007; Damoiseaux et al., 2007).

Although functional connectivity of DMN has been suggested as a biomarker for disease diagnosis and risks, fundamental limitations exist regarding the use of magnetic resonance imaging. The blood-oxygenation-level-dependent (BOLD) signal measured by fMRI is not a direct measurement of neuronal activities (Logothetis, 2008). Therefore, the interpretation of fMRI outcomes is confounded by non-neural cerebrovascular alterations associated with the disease (D'Esposito et al., 2003; Chen, 2019). Furthermore, fMRI imaging incurs high cost and has limited accessibility. However, understanding the early pathological process related to AD, especially in the preclinical stage, requires that a large population be studied. Power analysis for the prevention trials in Alzheimer's Disease usually yielded more than 1,000 individuals are needed (Hsu and Marshall, 2017). Therefore, a more economic option for assessing the integrity of cognitive function via neuroimaging is demanded to enable more studies in large populations (Cavedo et al., 2014).

Electroencephalography (EEG), in contrast, measures neuronal activity of neural ensembles at hundreds of Hz, which is a significantly higher temporal resolution than fMRI. Recent studies from our group (Yuan et al., 2012; Yuan et al., 2013; Yuan et al., 2014; Yuan et al., 2016; O'Keeffe et al., 2017; Li et al., 2018; Yuan et al., 2018; Chen et al., 2019) and others

(Custo et al., 2017; Liu et al., 2017a) have demonstrated that network-level analysis of high-density EEG signals reveals the functional connectivity of large-scale brain networks, including the default mode network. Our previous work has developed a method to reconstruct resting state brain networks by combining a high-resolution cortical model, electrophysiological source imaging, and analysis of the temporally independent EEG microstates (Yuan et al., 2016). Such EEG-derived DMNs have been validated with the fMRI resting state networks via simultaneous EEG and fMRI in human participants (Yuan et al., 2016; Yuan et al., 2018; Chen et al., 2019). Furthermore, the large-scale networks reconstructed from EEG have been shown to detect the disease-modifying connectivity changes induced by a brain stimulation intervention (Li et al., 2018; Chen et al., 2019). Because EEG directly samples electrical neural activity, connectivity derived from EEG will not be subject to vascular coupling. Thus, the neural contribution to the fMRI derive network connectivity can be delineated separately from the vascular contribution using our EEG techniques.

In addition, as compared with fMRI, EEG provides supplementary features of economic efficiency, broad accessibility, and compatibility. Therefore, the current study aimed to examine age-related alterations in DMN in normal aging adults, towards the long-term goal of establishing an effective and economical biomarker to empower prevention studies. In our investigations, we tested the feasibility of reconstructing electrophysiological default mode network based on high-density EEG data recorded from the participants at an eyes-open resting state. Next, we compared the connectivity derived from the posterior cingulate/precuneus region of DMN with memory performance assessed by a standard cognitive battery. Our analysis tested the feasibility of creating a neuroimaging algorithm based on brain connectivity to assess the risk of pathological cognitive

decline during normal aging, which may pave the way towards an objective, low-cost and accessible technology to detect cognitive impairment at an early phase.

2.3 Hypotheses to Be Tested

The current study examines age-related alterations in DMN to establish an effective and economical biomarker to empower future longitudinal studies to advance understanding of the normal and abnormal aging process in the human brain. First, we tested the feasibility of reconstructing the electrophysiological default mode network based on high-density EEG data recorded from the participants at an eyes-open resting state. We compared the connectivity derived from the posterior cingulate/precuneus region of DMN with memory performance assessed by a standard cognitive battery. Then, we explored the feasibility of creating a neuroimaging algorithm based on brain connectivity to assess the risk of pathological cognitive decline during normal aging, which will pave the way for detecting cognitive impairment at an early phase.

2.4 Experimental Paradigm

The study protocol (shown in **Figure 2**) was approved by the Institutional Review Board at the University of Oklahoma Health Sciences Center. Middle aged and older adults were recruited from the local university community. All were initially screened by telephone screen to excluded persons with significant neurological, neuropsychiatric, sleep, substance abuse, or cardiopulmonary disorders. After obtaining their written informed consent, they next underwent a physical examination (i.e. blood pressure, temperature, pulse oximetry, heart rate) and neurophysiological assessments administrated by an advanced practice registered nurse to ensure that they were cognitively intact and with no significant chronic disease.

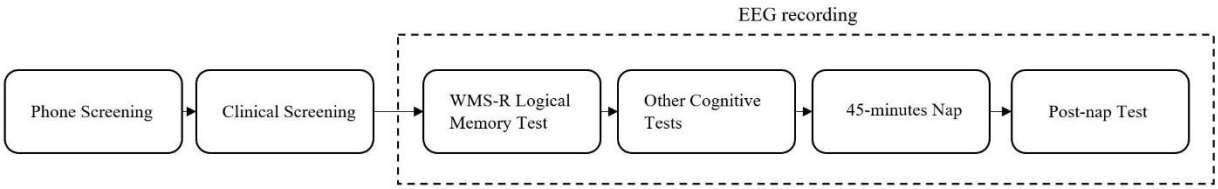

Figure 2 Experimental procedure.

As shown in **Figure 3**, the CONSORT (Consolidated Standards of Reporting Trials) flow diagram describes the progress of all participants through the trial. Briefly summarized, 190 were screened by telephone, 32 underwent clinical screening. Of the 30 met our eligibility criteria, all of them were recruited and completed the study procedure, including a battery of cognitive tests and EEG recording. Data from 1 subject was removed due to the poor quality of the neuroimaging data, resulting a final sample size of twenty-nine subjects. The resulting groups consisted of 15 middle-age adults (9F/6M, 33.5 ± 4.9 years old, and range 28-46 years old) and 14 older adults (12F/2M, 55.3 ± 4.8 years old, range 48-62 years old).

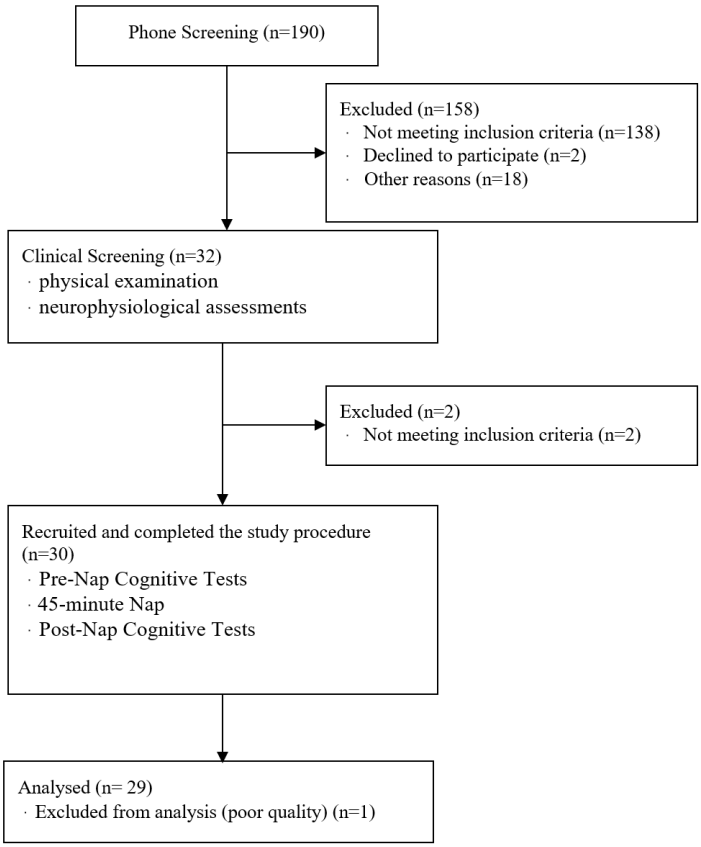

Figure 3 The porject flow chart.

All subjects completed a standardized battery of clinical neurocognitive tests, which included both subscales of the immediate and delayed memory recall subscales of the Wechsler Logical Memory Test (Wechsler, 1987), the Symbol-Digit Modalities Test (Smith, 1982) , North American Reading Test (Uttl, 2002), Stroop Color-Word Test (Stroop, 1935), Clock-Drawing Test (CLOX 1) (Royall et al., 1998; Royall et al., 2000), and the Free and Cued Selective Reminding Test (Wenger et al., 2010). During the cognitive tests, the subjects sat still on a recliner in a quiet, well-lit experiment room and the recliner was put in the upright position. A voice recorder was put 30 cm in front of subjects and turned on to record all answers from subjects for future scoring. The experimenters sat alongside the subjects to instruct them to complete the memory task and recall

sessions. The test battery was administered by a trained experimenter under a standard protocol to ensure both the consistency and accuracy of test administration and scoring. We employed the Immediate Recall score on the Logical Memory II from the Wechsler Memory Scale Fourth Edition (Wechsler, 1987) as the main score to assess the episodic memory performance, which has been well established to detect decline in prodromal dementia (Rabin et al., 2009) and detect early decline in the preclinical stages (Donohue et al., 2014a).

2.5 Data Acquisition and Preprocessing

Upon completing the clinical cognitive test batteries, a 64-channel whole-brain EEG cap based on the international 10-5 system was applied to the head of the participant. Subjects were instructed to keep still and allowed to fall asleep during the 45-min recording. The distance between the edge of EEG cap and each subject's eyebrow were measured twice to verify the cap position, once before the pre-nap recording and another time after post-nap recording. The EEG montage covered from forehead to occipital and was centered at Cz. Conductive gel was added to all electrodes to reduce the impedance below 20 kΩ throughout the recording session. In ensure a consistent fit, the front edge of the EEG cap was taped to the forehead and the distance between the edge of EEG cap and each subject's eyebrow were measured twice to verify the cap position and checked at the start and end of the recording.

The 45 minutes recordings were done with subjects lying supine in an adjustable recliner. The recording began and ended with bio-calibration, which we used to identify artifact in the EEG record. These bio-calibration were done in a standard order and involve asking them to (Oken et al.) open and close their eyes, (Oken et al.) blinks, (3) perform lateral eye movements, (Oken et al.) take deep breaths, (Oken et al.) clench their teeth, and to (Oken et al.) speak.

EEG data were recorded using a 64-channel ActiCHamp recording system (Brain Products, Munich, Germany), which consisted of two 32-channel amplifiers powered by a rechargeable battery unit. All the EEG datasets were digitized at a sampling rate of 500 Hz with a band-pass filtering of 0.1 Hz - 250 Hz. The onset and offset of the rest period were marked on the raw EEG for later truncating of the recorded signals.

The 45-minute recording was reviewed and manually scored by an certified expert with over 20 years of experience in scoring EEG sleep records, and using standard scoring criteria set by the American Academy of Sleep Medicine (AASM) (Berry et al., 2017). Briefly, the EEG data were first segmented into epochs of 30-second length and then assigned a state. Based on the frequency and amplitude of the signal, each segment was assigned of score of either awake, non-rapid eye movement sleep (Stage 1 NREM, Stage 2 NREM), Slow Wave Sleep (Stage 3 & 4 NREM), or rapid eye movement sleep (Donohue et al.). Only one person remained awake for the entire 45 minutes. In the remaining 28 subjects, all had periods of wakefulness interspersed with sleep. In order to not confuse mechanistic differences in falling and awakening from sleep, we only selected segments of the subject recording that reflected a period of wake before the onset of sleep (regardless of where and how many times this occurred in the recoding). We used these multiple segments of wakefulness within the same recording, on the same individual, to verify the reliability of the EEG-derived networks.

Preprocessing (shown in **Figure 4**) was performed with BrainVision Analyzer 2.0 (Brain Products, Munich, Germany) and MATLAB® 2015a (Mathworks, Inc., Natick, Massachusetts, United States). Bad channels and segments were removed based on impedance checks and visual inspection. The resulting recording lengths for all subjects ranged from 35 s to 180 s (mean ± std = 169.1 ± 30.5 s).

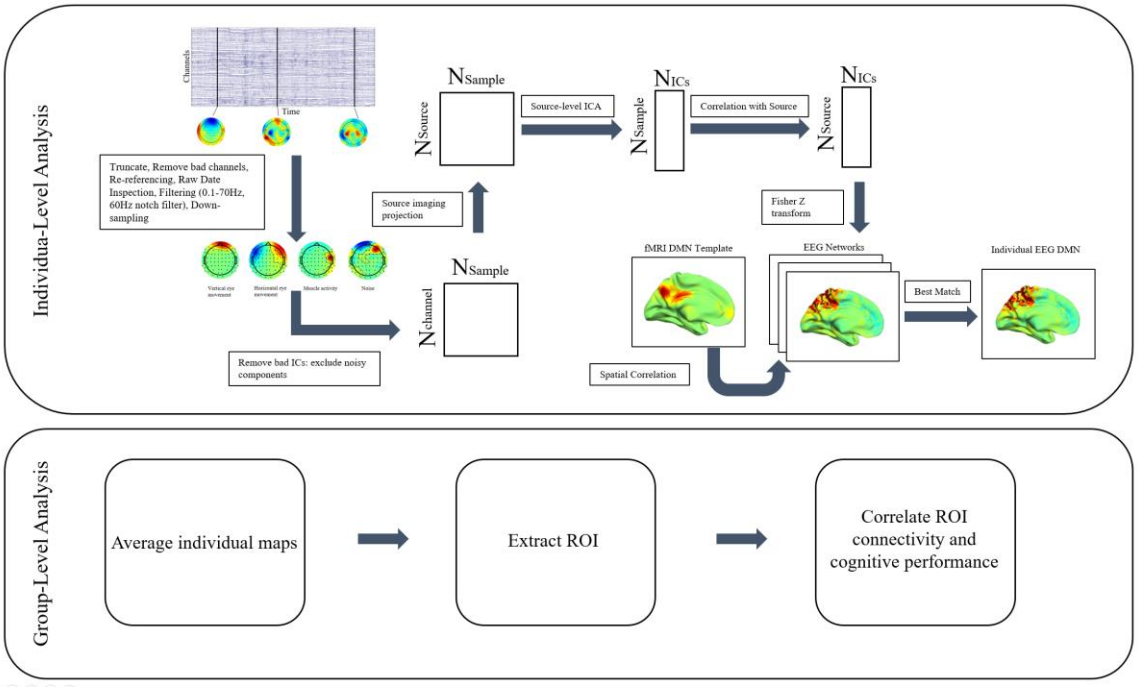

Figure 4 The schematic diagram for data processing.

Based on the sleep staging, we truncated 3-minute resting-state recording of wakefulness before any sleep onset in each subject. Five subjects fell asleep in less than 3 minutes and all recordings before sleep onset was kept. Next, the EEG data was re-referenced to the common-average reference. The continuous EEG data in each channel were band-pass filtered from 0.1 Hz to 70 Hz with an extra notch filter at 60 Hz to eliminate powerline noise. Lastly, Independent Component Analysis (ICA) was applied to remove physiological artifacts, including vertical and horizontal ocular artifacts and muscle activity. These sources of artifact were further verified by comparing the recordings against the bio-calibration records.

2.6 Electrophysiological Source Imaging.

Preprocessed EEG data were subjected to reconstruction of electrophysiological sources using a high-resolution cortical current source model. A template brain model in the MNI305 space was used as a common brain model for all subjects. The full segmentation and surface

reconstruction of structural MRI was performed using the Freesurfer suite (https://surfer.nmr.mgh.harvard.edu/), resulting in a high-definition cortical layer and the brain, skull, and scalp boundary surfaces. These surfaces were then used to construct a three-compartment Boundary Element Method (BEM) model. Conductivity values were assigned to each compartment (Zhang et al., 2006). A standard profile of electrode positions in the 64-channel montage was digitized and co-registered to the fiducial points on the template brain. The high-density cortical layer mesh was down-sampled to 10,240 vertices per hemisphere and used as the source space. Each vertex corresponded to a dipole source oriented perpendicular to the surface. A lead-field matrix was then computed via a forward calculation using the cortical source space and the 3-layer BEM model. The calculation of source imaging returned the source matrix of N_{source} x N_{sample}, where the N_{source} is the number of dipole source points and N_{sample} is number of data points in time domain. The minimum norm method (Dale and Sereno, 1993; Hämäläinen and Ilmoniemi, 1994) was used to solve the inverse problem.

2.7 Resting State Network and Connectivity

Based on the reconstructed source images, electrophysiological resting state networks were derived using the method established in Yuan et al. (2016). Considering that the participants enrolled in the study span across middle-age (28-46 years) and older age range (48-63 years), the electrophysiological network was derived in each individual prior to group-level analysis. Specifically, source images of each individual at the down-sampled EEG microstates (Lehmann et al., 1987) were temporally concatenated. Afterwards, ICA was utilized to decompose the absolute values of source-level data into 25 independent components (ICs) for every subject, with each IC representing one distinctive brain network of the corresponding subject. The time courses of brain networks were back-projected from the ICs, resulting in an activity matrix of N_{sample} x N_{IC},

where the N_{sample} is number of data points in time and N_{IC} is the number of source-level ICs. After calculating the source matrix and activity matrix, we further calculated the Pearson correlation coefficients between source matrix and activity matrix, resulting a matrix of N_{source} x N_{IC}. The connectivity value of brain networks was defined as the z-transformed correlation coefficient matrix.

For all 25 ICs, we depicted the source points on a standard brain model. Assuming each source-level IC represents one brain network, we focused on the DMN by searching for the best matched IC with a pre-defined DMN template. Specifically, the match was selected based on the spatial correlation calculated between the un-thresholded connectivity values of an EEG-derived network and the un-thresholded connectivity values of the template DMN derived from fMRI data in a separate group of healthy subjects (Yuan et al., 2016). One best match IC of highest spatial correlation coefficient was selected for every subject, which we referred as the individual-level DMN derived from EEG.

For group-level analysis, individually derived network was smoothed before averaging to mitigate the anatomical discrepancy among individuals. Connectivity values of the network matched to DMN were smoothed by employing a Gaussian filter with Full Width Half Maximum of 9 mm in FreeSurfer software. Then, the one sample t-test was used to determine the significance of DMN at the group level. Bonferroni correction was employed to control for multiple comparisons.

2.8 Association Between EEG Network Connectivity and Memory/Age

To assess the association between network connectivity and memory function, a region of interest (ROI) analysis was used. In brief, the ROI was drawn by an intersection of the group-level EEG DMN and the Yeo template of DMN (Yeo et al., 2011). Specifically, at first, the group-level

EEG DMN was obtained by performing a one sample t-test on all subjects for every single dipole source point, as described above. In addition, the output pattern of aforementioned one sample t-test was corrected by applying Bonferroni correction. The corrected EEG pattern was finally controlled by intersection with a well-established template by Yeo et al. based on fMRI data from 1,000 subjects (2011).

Episodic memory performance was quantified as the ratio of the number of first-immediate recalled items from the Wechsler Logical Memory test over the total item number during immediate recall from that same test. The Immediate Logical Memory Subscale is a standardized test that generates three scores based on the recall of two short stories. The stories involve the Anna (story 1) and Joe (story 2), each of which are divided into 25 phrases. Each story is read aloud and immediately afterwards, the subject is asked to repeat as much of the story as possible. The second story also serves as a distraction for the first, and so, after the second story about Joe, the subject is then asked to state as much as they can about the first story (Anna's Story). The sum of the three recalls is used to generate the total immediate memory score. Due to its demonstrated sensitivity for detecting prodromal dementia (Donohue et al., 2014; Rabin et al., 2009), we used the scores from the first administration of Story 1 (Anna) and to total immediate memory score to derive a measure of episodic memory performance.

Then, the EEG network connectivity averaged within the ROI was compared to the corresponding logical memory score across all subjects. The partial correlation coefficient between connectivity values and memory scores was calculated. Furthermore, the network connectivity was compared with participants' age. The Pearson correlation coefficient between averaged connectivity values in the DMN ROI and ages was calculated.

2.9 Results

Table 2 summarizes the demographic characteristics and performance on the cognitive battery. Subjects were assigned into two groups, a middle-aged group (range from 28 to 46 years old) and an older group (range from 48 to 63 years old). The WMS Logical Memory score as the primary memory function performance did not differ significantly between the middle-aged and the older adults, although the older group was associated with marginally lower memory performance ($t(27) = 1.88$, $p = 0.07$). Other cognitive scores did not differ between the age groups. The digital symbol modality as a primary assessment of working memory marginally differed among two groups ($t(27) = 1.81$, $p = 0.08$). Therefore, our later analysis of the brain network has consolidated the two age groups as one group.

The electrophysiological DMN obtained from all the middle-aged and older subjects is shown in **Figure 5**. The averaged and un-thresholded brain connectivity maps of two different resting-state segments, designated as test and re-test data, are depicted in **Figure 5** (B) and (C), respectively. After thresholding and correcting for multiple comparison on the total number of source points, the EEG DMN identified the posterior cingulate / precuneus area and the inferior parietal lobule (shown in **Figure 5** (D) and (E)), which are part of the key regions of DMN (shown in **Figure 5** A). Notably, the posterior region of EEG DMN presents stronger connectivity than the anterior regions. In addition, the un-thresholded maps of the EEG DMN showed that connectivity pattern extends to regions in the medial prefrontal cortex yet did not reach a group-level significance (**Figure 5** B).

Table 2 Participant demographics and performance variables

	Middle-age (n=15)	Older (SD) (n=14)
Mean age (year)	33.5±4.9	55.3±4.8
Age range	28-46	48-63
Female/ Male†	9/6	13/2
Age*	33.5(4.9)	55.3(4.8)
MMSE	29.4(0.2)	29.3(0.2)
WMS Logical memory (immediate recall ratio)	0.53 (0.03)	0.45 (0.03)
Digit Symbol Modalities	58.93 (2.3)	53.57 (2.1)
Stroop (word only), sec/correct%	52.6(2.7)	48.6(2.2)
CLOX1	12.3(0.5)	12.4(0.3)

Mean and standard error (in parentheses) for participant demographics; MMSE: Mini-Mental State Examination; WMS: Wechsler Memory Scale; CLOX1:The executive clock drawing task. Gender difference was analyzed by using chi-square test, † shows significant difference between middle-age and older adult group, $p<0.05$; the remaining variables were analyzed by using unpaired t-test, * shows significance difference between middle-age and older adult group, $p<0.05$.

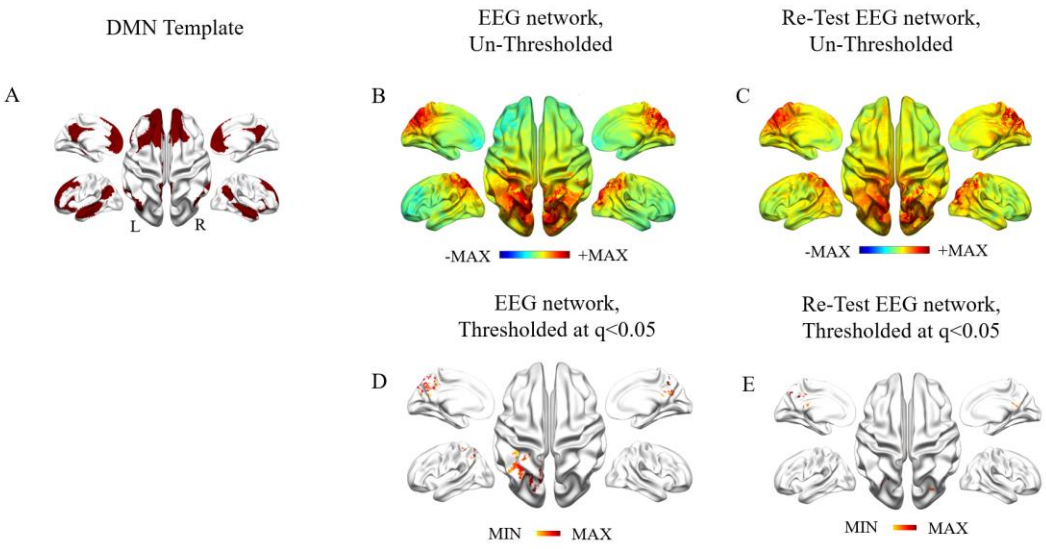

Figure 5 Group-level average of the default mode network obtained from electro-physiological source images. (A) shows the template DMN parcellation from Yeo et al., 2011. (B) and (D) show maps of EEG DMN connectivity averaged across all subjects in (B) un-thresholded and (D) thresholded manner by one sample two-sided t test, corrected for multiple comparison. Similarly, (C) and (E) show maps of EEG DMN connectivity averaged across all subjects in (C) un-thresholded and (E) thresholded manner for re-test data.

The maps of EEG DMN are consistent between the test and re-test data, as shown in **Figure 6**. The un-thresholded maps from test and re-test data yielded a spatial correlation coefficient of $r = 0.84$. The connectivity values from ROI were also consistent between the test and re-test data ($r = 0.62$, $p < 0.001$, **Figure 6**, Right Panel).

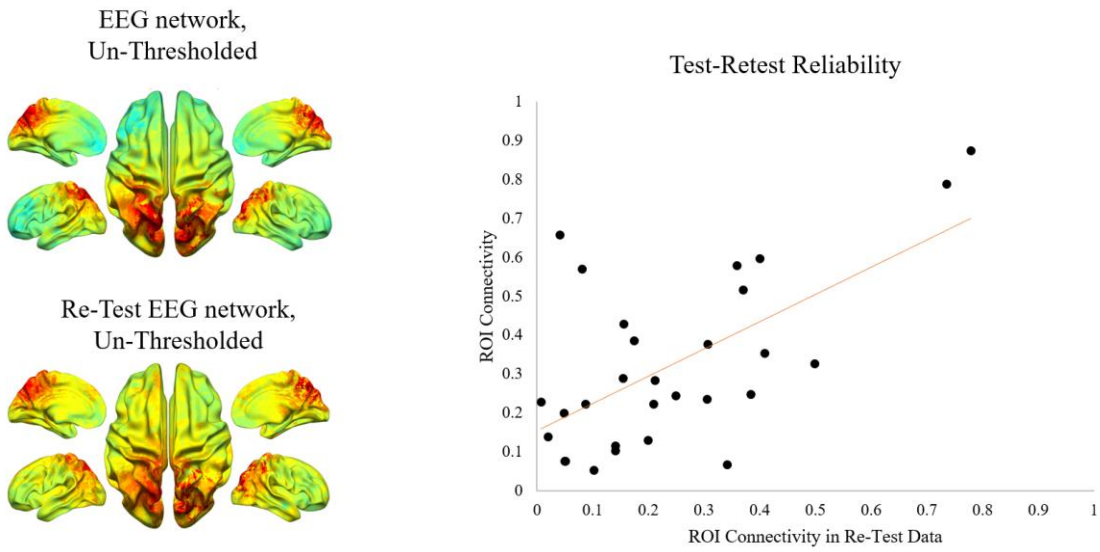

Figure 6 Test-retest reliability in EEG network. A separate EEG dataset was extracted and the network analysis and repeated. Un-thresholded EEG network maps are plotted for Test and Re-Test dataset in (A) and (B). The ROIs for test and retest data were defined by the source points of significance by one-sample two-sided t test on all subjects after multiple comparison correction. The Yeo template was further applied in conjunction to define the ROI. Then brain connectivity values averaged within corresponding ROI were extracted and plotted in (C). The correlation between all individuals' test and retest data is 0.62 ($p < 0.001$).

Furthermore, **Figure 7** shows the separately reconstructed consistent maps of DMN from the sub-group of older adults and the sub-group of middle-aged adults, which yielded a spatial correlation coefficient of r=0.66. The comparison of the connectivity patterns between the two age groups did not identify any regions with significant difference, which supports our analysis strategy of combining the two age groups as one group.

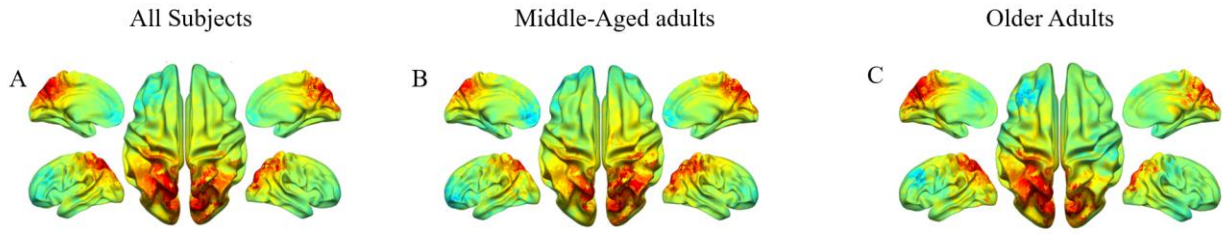

Figure 7 The un-thresholded brain connectivity averaged separately in (A) all, (B) middle-aged subjects, and (C) older subjects.

Figure 8 shows the ROI analysis comparing subjects' brain connectivity values and their memory performance. The insert plot of **Figure 8** illustrates the ROI identified by a conjunction analysis of the group-level EEG DMN and the Yeo template, i.e. the conjunction of **Figure 5** (A) and (D). The ROI primarily includes posterior cingulate area, while part of it extends to the precuneus area. After extracting the connectivity values from the ROI, a significant negative correlation was identified between the connectivity averaged from ROI and the WMSI scores among all individuals ($r = -0.47$, $p = 0.01$). This finding indicated that subjects who had a better score of episodic immediate memory recall are associated with lower connectivity in the posterior DMN areas. Since the memory performance did not reveal significant difference between the middle-aged and older adults, all subjects were pooled in the correlational analysis. Considering that ages could also contribute to the association, we adopted a partial correlation analysis and results revealed a significant correlation between memory and network connectivity ($r=-0.42$, $p=0.02$), after controlling the age factor.

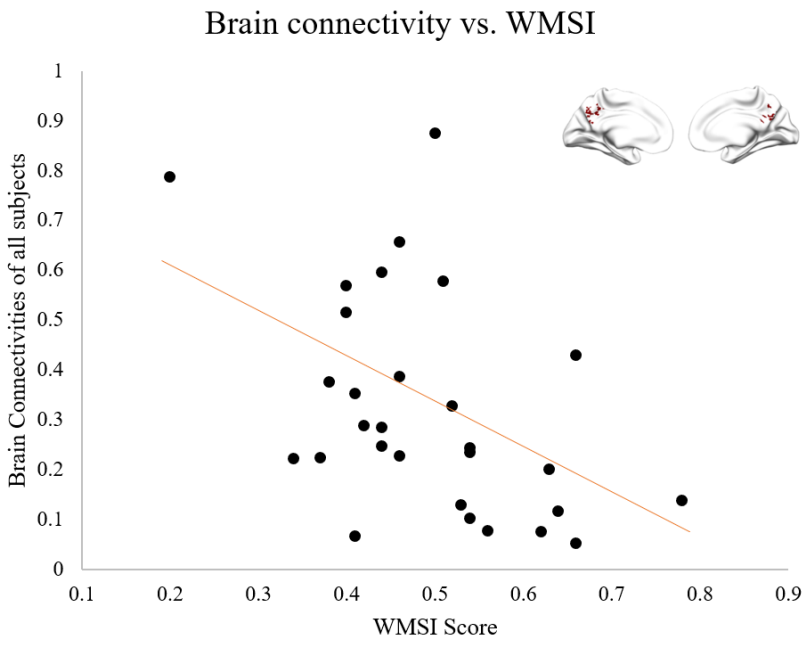

Figure 8 Functional brain connectivity is correlated with memory performance across all subjects. The insert shows ROI regions defined from EEG DMN analysis. Brain connectivity values are calculated as the z-transformed correlation coefficients between individual's source time course and IC time course, averaged within the ROI. Each dot represents one individual's brain connectivity and the corresponding Wechsler Memory Scale Immediate Recall score. Red dots indicate middle-aged subjects and blue dots indicate older adults. Black trendline represents linear relationship between these two variables among all pooled subjects ($r = -0.47$, $p = 0.01$).

In addition, we assessed the relationship between brain connectivity and the age (shown in **Figure 9**). Interestingly, older aged subjects tend to show greater connectivity in the ROI of posterior DMN. However, the association was not significant across all subjects (ages ranging from 28 to 63 years old, $r = 0.22$, $p > 0.1$). Only in the older adults' group, we found a significant correlation between the age and network connectivity in the ROI of posterior DMN ($r = 0.55$, $p = 0.04$, shown in **Figure 9**).

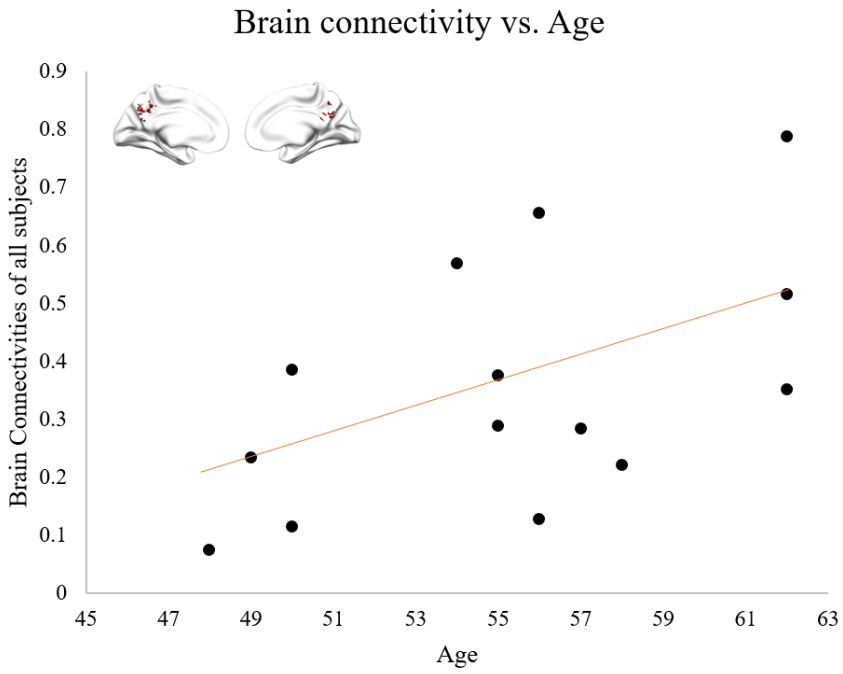

Figure 9 Functional brain connectivity is correlated with age in older adults. The insert shows ROI regions defined from EEG DMN analysis. Brain connectivity values are calculated as the z-transformed correlation coefficients between individual's source matrix and activity matrix, averaged from ROI. Each black dot represents one individual's brain connectivity and the corresponding age of years. Orange trendline represents linear relationship between these two variables ($r = 0.55$, $p = 0.04$).

The **Figure 10** shows the connectivity-memory relationship in the subset of older adults only. A similar and slightly stronger negative correlation was found in the subset of older adults ($r = -0.74$, $p = 0.003$), indicating that in the sub-group of older adults (ranging from 48 to 63 years old), better memory performance was associated with a lower connectivity in the posterior DMN ROI.

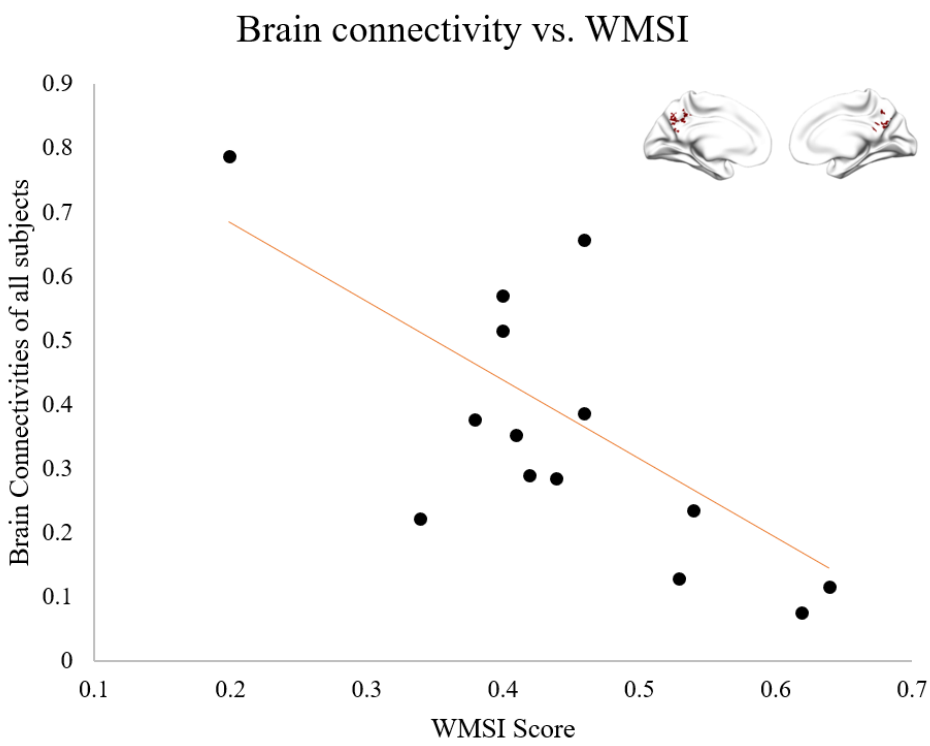

Figure 10 Functional brain connectivity is correlated with memory performance in older adults. The insert shows ROI regions defined from EEG DMN analysis. Brain connectivity values are calculated as the z-transformed correlation coefficients between individual's source matrix and activity matrix, averaged from ROI. Each black dot represents one individual's brain connectivity and the corresponding Wechsler Memory Scale Immediate Recall score. Orange trendline represents linear relationship between these two variables ($r = -0.74$, $p = 0.003$).

2.10 Discussions and Conclusions

The current study utilized EEG to investigate the association between functional connectivity of resting state brain network and memory performance across normal healthy subjects in middle-aged and older age range. Our results demonstrated that the default mode network (DMN) can be reconstructed from the cortical source images derived from EEG at rest, including regions of the precuneus, posterior cingulate cortex, and the inferior parietal lobule.

Furthermore, we found that network connectivity values within the ROI in posterior DMN were negatively correlated with episodic memory performance across healthy individuals ranging from middle-age to older-age. Meanwhile, in the sub-group of older adults, individuals' age was positively correlated with the connectivity from the same area in posterior DMN. The findings in this study reinforce our knowledge of the brain connectivity in DMN associated with advancing age. More importantly, brain connectivity assessed by this novel EEG-based neuroimaging technology is feasible to relate to many clinical batteries to benchmark normal aging. This can potentially serve as an early biomarker of neurodegenerative disorders.

To date, DMN is one of the most important brain networks in fMRI studies on aging (for a review, see (Brier et al., 2014)). A number of studies have documented that resting-state functional connectivity in the DMN is sensitive to changes among groups of individuals with AD (Greicius et al., 2004a; Wang et al., 2007; Zhang et al., 2009a), prodromal AD including mild cognitive impairment (Sorg et al., 2007; Bai et al., 2009; Petrella et al., 2011), and healthy aging (Andrews-Hanna et al., 2007; Damoiseaux et al., 2007). Earlier studies of AD have consistently reported deterioration of connectivity in DMN, as compared with the healthy elders (Greicius et al., 2004a; Wang et al., 2007; Zhang et al., 2009a) . Importantly, at the prodromal stage of AD (mild cognitive impairment), DMN connectivity was found to be abnormally impaired (Bai et al., 2008) and even associated with the risk of converting to AD-related dementia (Sorg et al., 2007). The metabolism hypothesis suggests that pathological changes in the DMN stimulate an activity-dependent or metabolism-dependent cascade that are spatially consistent with amyloid aggregations and tau pathology and, moreover, precedes and promotes the development of these AD pathology (Buckner et al., 2005), which is an important area being researched for developing intervention options. Therefore, identification of abnormal disruption of human brain networks, including

DMN and other cognitively relevant network, appears to be essential in characterizing normal aging. Such characterization is also critical for identification of early pre-clinical stages in AD and early prevention in conjunction with pharmaceutical intervention (Sperling, 2011).

Recently, an increasing number of studies have extended the investigation of DMN in normal healthy individuals across the age range from elders to younger adults, with the purpose that establishing a normal aging trajectory will aid in the early diagnostics of preclinical stages in AD (Andrews-Hanna et al., 2007; Damoiseaux et al., 2007; Sambataro et al., 2010; Ferreira et al., 2016). Consensus emerges that the connectivity within DMN was lower in the advanced elderly population (65+ years) as compared to the young adult population (Andrews-Hanna et al., 2007; Damoiseaux et al., 2007). However, literature have shown a discrepancy about the association between age and DMN across a spectrum of ages, i.e. whether positive or negative association between age and connectivity values were observed (Andrews-Hanna et al., 2007; Damoiseaux et al., 2007; Jones et al., 2011; Jockwitz et al., 2017; Zonneveld et al., 2019). Several methodological issues have been indicated to complicate the findings, including identification of subnetworks of DMN, the age range, pre-processing step such as whether or not to apply global signal regression, etc. Several of aforementioned studies (Jones et al., 2011; Zonneveld et al., 2019) applied a data-driven approach to parcellate the whole brain into units of functional networks prior to compare brain connectivity with the ages. Instead of masking out the whole DMN, the well-known resting-state network was further delineated into the anterior DMN and posterior DMN. Even though they are two subsets of DMN, each sub-network features age-related changes in both posterior and anterior areas of DMN, sometime even an opposite effect. Several studies agreed on negative association regarding anterior DMN - lower connectivity with older age (Damoiseaux et al., 2007; Jones et al., 2011; Zonneveld et al., 2019), whereas conflict findings are reported in the posterior

DMN areas. For example, Jones et al. (2011) in a study of 341 subjects aged between 64 and 91 years reported age-related increase of connectivity in the retrosplenial posterior cingulate cortex as well as age-associated decrease the medial prefrontal cortex, as part of the anterior sub-network. In addition, a much smaller increase in connectivity at the edge with cunes and lingual gyrus, mixed with predominant decrease of connectivity in the posterior cingulate cortex and precuneus, was also observed for the posterior sub-network in Jones et al. (2011). Furthermore, the age-group difference was found to be more prominent in the anterior regions than in posterior regions (Davidson and Guthrie, 2017). Likewise, another study of a large population by Zonneveld et al. (2019) (50.5 - 95.2 years of age) has employed a much finer segregation of subnetworks and concurred in a negative association with age observed in the anterior subnetwork of DMN. However, Zonneveld et al (2019) reported a contradictory finding regarding posterior DMN, i.e. an age-related increase in the retrosplenial posterior cingulate cortex. Meanwhile, a population-based study of 711 older adults (55–85 years of age) found no age-related changes in the DMN (Jockwitz et al., 2017). Importantly, in that study, the DMN was not divided into its anterior and posterior subsystems, indicating the potential relevance of investigating DMN at different scales of functional organization.

To our knowledge, our study provide the first electrophysioglocial evidence of aging effect on a large-scale brain network, the default mode network. In comparing our results with the abovementioned studies, a key methodological difference should be noted. We employed electrophysiological measurements to investigate the age-related effect in DMN, while the functional MRI studies are based on hemodynamic measurements (e.g. blood-oxygenation-level-dependent contrast), which are secondary signals that involves blood flow and oxygenation in brain tissues (Logothetis et al. 2008). Thus, the age-group differences as documented by fMRI

studies could be attritued to three possible origins - the neurons, the vasculature, or the neurovascular coupling unit (D'Esposito et al., 2003; Sweeney et al., 2018). Nonetheless, our findings based on electrophysiolgocial recordings provide direct evidence supporting the age-related changes in neuronal activities, especially at the network-level connectivtiy.

Notably, our study has employed a data-driven approach to identify the electrophysiological form of resting state brain networks and the age-association in the network connectivity, which is similar to the data-driven identification of brain networks in fMRI studies. The template that our study employed to identify the DMN should be considered as posterior DMN rather than anteriror DMN, because of the predominant coposition in the posterior cingulate cortex and precuneus, which agrees with the posterior DMN examined in Zonneveld et al. (2019) and Jones et al. (2011). Our findings (in **Figure 9**) revealed the association of age-related increase in the posterior cingulate cortex, which is similar with the positive association in posterior DMN identified by Zonneveld et al. (2019). Also, the areas of age-associated increase revealed in our restuls included additional precueus area that extends to the margin with cunes, which is partially consistent with the finding by Jones et al. (2011), i.e. an age-associated increase in the edge of cunes as part of the posterior DMN. However, Jones et al. (2011) also reported an adjacent yet predominant age-associated decrease in posterior cingulate cortex as part of the posterior DMN, which was not observed in our study. The reason of not seeing a age-related decrease could be due to the different age-range examined in our study (elaborated below), or due to a discrepency on the vascular contributions.

It is important to note a wide age range differs among these studies, which could explain their discrepancy in across-group findings. Recent studies have shifted the age inclusion towards younger range, for the purpose to establish a normal aging trajectory that will aid in the early

diagnostics of preclinical stages in AD. For example, the mean age in the study by Zonneveld et al. (2019) is 66.9 years old (ranging from 50.5 to 95.2 years), whereas the median age of the study by Jones et al. (2011) is 82 years old (ranging from 64 to 90 years). However, the age span is critical in revealing any age-related effect. In the longitudinal study by Damoiseaux et al. (Damoiseaux et al., 2012), key nodes of DMN, such as posterior cingulate cortex, did not reveal significant changes at the group level, possibly due to the short duration of follow-up (on average about three years). In comparison, our study investigated both middle-aged and older adults, which collectively ranged from 28 years to 63 years. Notably, the subgroup of older adults in our study (ranging from 48 to 63 years) overlaps with the age range in Zonneveld et al (2019). Likewise, a positive age-association in the posterior DMN was consistently observed in the subgroup of older adults in our study, although in a much smaller sample (N=14) than the large cohort studied in Zonneveld et al. (2019) (N = 2878). Furthremore, it is worthy to note that the younger sub-group in our study (ranging from 28 to 46 years) covers the middle-aged range and did not overlap with other age ranges in the above mentioned studies. It is older than the young-adult range (as in Andrews-Hanna et al., 2007 and Sperling et al., 2009), yet much younger than the elderly range (as in Jones et al., 2011 and Zonneveld et al. 2019). Our results revealed that the age-association effect in this middle-age range did not follow the trend observed in the older-adult range. Similarly, such dis-association of age-effect in the younger age range has been observed in the other studies that attempted such investigation in the adults younger than 30 years old (Andrews-Hanna et al., 2007; Sperling et al., 2009). Importantly, our investigation has extended the finding of age-disassociation to the middle-age range.

In addition to the age association, our findings stressed a functional role of PCC. Memory function has been well described as a distributed process (Mesulam, 1990), and the brain substrates

and modifiers of this process are highly variable, particularly in a cognitive aging context (Verhaeghen et al., 1993; Raz and Rodrigue, 2006; Head et al., 2008; Braskie et al., 2010). As part of a well-connected neural network underlying the memory function, PCC is involved in episodic memory encoding (Natu et al., 2019) and also is one of the most vulnerable area prone to amyloid-beta deposition (Buckner et al., 2008; Ferreira and Busatto, 2013). By defining the ROI mainly in PCC (**Figure 8**), our results have shown a significant negative correlation with memory performance on the averaged brain connectivity, which is exactly reversed to the age-association seen in our cohort. Notably, the memory-association was robust in the participant ensemble, although the memory performance did not differ significantly between two age sub-groups. Higher performance of immediate memory recall was associated with lower functional connectivity in the posterior DMN, significantly seen in the entire group (28 to 63 years old, $r = -0.47$ and $p = 0.01$) as well as in the sub-group of older adults (48 to 63 years old, $r = -0.74$ and $p = 0.003$). Previous study has suggested that different subsets of DMN were not simultaneous activated (Sestieri et al., 2011). They found the PCC / precuneus were significantly activated during memory retrieval, whereas the anterior DMN is deactivated, which points out that the functional association in posterior DMN should be delineated separately from the anterior DMN. Nonetheless, the key regions of DMN at task-less, resting state exhibit fluctuations that are coherently synchronized, which are characterized as resting state functional connectivity. Furthermore, the intrinsic connectivity of resting state brain networks, especially DMN, have been found to be associated with memory performance. The association of a steady-state functional connectivity in the default mode network with memory function is observed in both cognitively intact individuals (Wang et al., 2010; Newton et al., 2011) and diseased populations (Bai et al., 2009; Mormino et al., 2011). Notably, in these studies the resting state scans are acquired either subsequently or prior to the

function-probing tasks. It has been suggested that such changes in network-level connectivity observed in the normal aging stage occur because of insult brought by the amyloid accumulation happening at the preclinical AD-Stage (Sheline and Raichle, 2013). Thus, abnormalities in resting state functional connectivity can be detected in companion with or even before structural damage is manifested as atrophy and furthermore before cognitive decline produces clinical deterioration. In line with the model of progression events (Sheline and Raichle, 2013), our study demonstrated that reconstructed EEG source brain connectivity can reliably reveal aging effect in cognitively normal adults. Even though our EEG data was not recorded during the memory task, we observed negative association with episodic memory functioning. The finding that the greater brain connectivity is associate with worse episodic memory performance suggests a compensatory mechanism in these overall cognitively normal individuals, which is similarly observed in individuals at preclinical stage (Filippini et al., 2009) or at amnestic mild cognitive impairment stage (Qi et al., 2010). Our findings again stressed the importance of PCC as part of DMN in future aging studies to establish a full trajectory spanning normal aging, preclinical and clinical stages.

In addition, it is worthy to mention that our innovative approach of using EEG to characterize the brain networks exempted our investigation from a few controversial issues encountered in fMRI studies. With respect to the measure of neural activity, the fMRI BOLD signal is an indirect estimate whereas EEG potential is a direct estimate of neuronal activity. It is well known that BOLD signal depends on neurovascular coupling, while the latter is susceptible to aging and age-related changes (Ferreira and Busatto, 2013; Liu, 2013). Besides, regional, age-specific differences were reflected in vascular reactivity. Thus, it has been suggested that fMRI studies comparing different age groups should be carefully interpreted (Ferreira and Busatto, 2013). In addition, heterogeneous findings of aging effect on the fMRI connectivity might be

attributed to differences in pre-processing, i.e. whether removing the global signal. Global signal regression has been widely utilized to attenuate physiological nuisances and increase specificity of connectivity in most of fMRI studies (Fox et al., 2009; Jones et al., 2011). However, emerging evidences indicated that the removal global signal in the preprocessing of fMRI data might lead to spurious RSFC pattern (Murphy et al., 2009), as it may result in distance-dependent artifacts. In the study by Zonneveld et al. (2019), an ICA-based method with a high dimension of components was used to remove the noises instead of global signal regression. Likewise, in our study, we did not employ a global signal regression either; the connectivity patterns in the reconstructed EEG sources images were subject to data-driven ICA for the network analysis. Furthermore, another confounding methodological issue in fMRI studies is whether or not applying a voxel-wise gray matter correction, which has been demonstrated to alter the discovery of functional changes in fMRI, especially the aging-associated changes. As direct measurement of neural activity, our findings from EEG provide insights to cross-validate some of fMRI findings regarding the functional connectivity associated with advancing age.

Nonetheless, several limitations in our study should be acknowledged. First, some older adults outperformed middle-age adults in cognitive tests. It is also noted that a few adults recruited in the older subgroup were higher-educated than some in the middle-aged subgroup, although all participants have completed education of high-school or above. They present substantial variance of education history ranging from high school to postgraduate degrees, given a small sample recruited in our study. Another limitation is that we did not include structural measurement of volume gray matter and white matter to assess the factor of aging-related atrophy, which might contribute to the observed performance changes of memory function.

In summary, we used EEG resting state recordings to characterize the functional connectivity alteration during normal aging process. Our findings indicate that the reconstructed EEG data at source level could reflect the neuronal activity in a part of default mode network (DMN) reliably. More importantly, the reconstructed tridimensional source cortical level EEG connectivity was correlated to ages and memory performance assessed by clinical cognitive batteries. Our results indicate that EEG source imaging technology can be used in detecting brain connectivity and cognitive function alteration in healthy adults during normal aging. This pilot evidence further suggests the use of EEG-network based neuroimaging in the study of aging and Alzheimer's disease related dementia.

Chapter 3: Resting State Brain Network is Affected by Vigilance

In this chapter of my dissertation, I have investigated the effect of vigilance on resting-state brain networks, measured by multiple neuroimaging modalities. I focused my investigations using fNIRS and EEG. My findings are also relevant and have important implications for other studies using fMRI or EEG.

Recently, fNIRS has been utilized to image the hemodynamic activities in the human brain. With the advantage of economic efficiency, portability, and fewer physical constraints on the participant, fNIRS enables studying of a large-scale network in the resting-state human brain at the versatile environment and various body positions, including at bed-side or during exercise, which complements the use of fMRI in monitoring the human brain. However, like fMRI, fNIRS imaging of functional connectivity can be influenced by a strong global component. However, the nature of the global fNIRS signal has not been established. In this study, we aimed to investigate the neurophysiological origin of the global signal using simultaneous recordings of fNIRS and electroencephalogram (EEG) signals in healthy human subjects at eyes-open (EO) and eyes-closed (EC) resting conditions and at three different body positions (i.e., standing, sitting and supine). We assessed the impact of body positions on the resting-state fNIRS global signal and the relationship between the fNIRS global signal and EEG measures of vigilance in healthy human participants. As a control, we also evaluated the impact of body positions on the task-induced responses of fNIRS and EEG to auditory stimuli. Results found that the factor of body positions significantly affected the amplitude of the resting-state global signal (defined as the standard deviation of the global signal), prominently in the frequency range of 0.05 Hz - 0.1 Hz but *only marginally* in the very-low-frequency range of less than 0.05 Hz. However, the task-induced fNIRS or EEG responses did *not* differ across body positions. More importantly, the amplitude of the global

signal in the very-low-frequency range of less than 0.05 Hz exhibited a significant negative correlation with EEG vigilance measures in the EO state, which suggests that vigilance as a neurophysiological factor modulates the resting-state dynamics of fNIRS. This study is the first to investigate the relationship of resting-state fNIRS signal and EEG across body positions and revealed the neurological basis of low-frequency fNIRS global signal. Our results will have important implications for understanding the noises and neural origins in fNIRS signals, which are also relevant to the understanding of fMRI.

3.1 Background

3.1.1 Global Signal in Neuroimaging Research

The global signal was defined as the time course of fMRI blood-oxygenation-level dependent (BOLD) averaged across all voxels first by Zarahn et al. in 1997 (Zarahn et al., 1997). Regarded as a composition of various nuisance components, the global signal was removed either as a preprocessing step or a noise regressor in the analysis of general linear model. It was 2009 in a paper of Murphy et al. (2009) the first time to argue that some inspiring anti-correlated observations in a Fox et al. (2005) paper could be artifactual by introducing global signal removal (GSR). Since then, the discussion about the concern of using GSR never stops. Some studies underpin the findings in Murphy et al. (2009) with either simulation or mathematical approach (Weissenbacher et al., 2009; Saad et al., 2012).

Although the global signal is a concise concept, the arguments and investigation are keeping growing until now. According to a review of the global signal in fMRI studies, Liu et al. viewed the global signal as a time-varying measure of spatial homogeneity in the brain (Liu et al., 2017b). It does represent a combination of nuisance components that could hamper the significant findings. However, the nature of global signal itself is still unclear. For example, a previous study

compared the global signal time series which computed after different routines of regression (Wong et al., 2013). The minimal preprocessing routine was set as the baseline and the different global signal time series were divided by the one by applying minimal preprocessing routine to get a mean percent variance explained by each set of regressors (Liu et al., 2017b). They concluded that the global signal was explained 48% by Legendre polynomial and motion regressors, 31% by physiological noise regressor, and additional 14% by white matter and cerebrospinal fluid regressors. There still have 7% remaining component of global signal cannot be explained.

The global signal is treated as a measure of spatial homogeneity. All spatially widespread components are potentially become the environmental or physiological sources of global signal. By finding out that low-frequency and gradient subsystem (Liu, 2016; Power et al., 2017), motion artifact (Power et al., 2015), cardiac rate (Shmueli et al., 2007), pulse pressure (Power et al., 2017) and vascular component (He et al., 2010) are contributed to BOLD signal or significantly correlated with the global signal, neuroelectric component is also a source of BOLD global component in a study by using local field potential (Scholvinck et al., 2010). Especially, Wong et al. (2013) found the anti-correlation between EEG vigilance measurement and the stand deviation of global signal in a simultaneous EEG/fMRI study. Besides, Falaphour et al. (2016) reported the negative correlation between EEG vigilance time course and the global signal time course.

Global signal removal or regression is not a controversial method in fMRI studies, but also in recent fNIRS studies. Although, some fNIRS studies used short source-detector separation sensor to minimize the effect of physiological noise from superficial cortical layer. However, the effect of regressing out short-distance channel from raw signal is still uncertain. Brigadoi and Cooper's work give some recommendation to select the distance of electrode for infants and adults, ~2 mm and ~8mm, respectively (Brigadoi and Cooper, 2015). The fix length short source-detector

separation sensor may induce residual when subtract 5 mm measurement from corresponding 33-mm signal (Saager and Berger, 2008). Many fNIRS studies are applying different mathematical approaches to eliminate the effect of global signal. Principle component analysis, which have the highest correlation with global mean signal, is now popular method to regress first PC to lower the global effect and autocorrelation (Novi et al., 2016). Besides, partial correlation analysis is also proved to separate deep signal and shallow signal effectively without short source-detector separation sensor (Sakakibara et al., 2016). Currently, there is no advanced pre-processing routine in fNIRS studies. To minimize effect of the physiological signal with removing fNIRS global mean signal is also applied in fNIRS study (White et al., 2009). Therefore, to understand the physiological origin and potential neural component of resting-state fNIRS global signal is still very significant.

3.1.2 Vigilance and Diseases

Vigilance, as well as related terms like wakefulness, alertness, or arousal has been investigated more than decades (Jobert et al., 1994; Oken et al., 2006; Olbrich et al., 2009a). Liu and Falahpour (2020) summarized the employed vigilance metrics in previous studies, including mathematically calculation of the ratio of EEG power in the alpha band to the power in the delta and theta bands (Jobert et al. (1994), Larson-Prior et al. (2009), and Wong et al. (2013), or transformed by calculating the inverse of square root (Horovitz et al., 2008), and other metrics defined by Local field potential (Chang et al., 2016a), pupillometry (Schwalm and Rosales Jubal, 2017), and Behavioral arousal index (Chang et al., 2016a).

Many neurological disorders, such as autism, depression, and schizophrenia have been demonstrated tight association with dysregulation of arousal system (Sander et al., 2015; Jawinski et al., 2019). A recent study reported a significant correlation between the EEG-based vigilance

metrics and genetic indicator for depressive disorder, autism disorder, and Alzheimer's disease (Jawinski et al., 2019). Besides, the major neurological disorder, like schizophrenia, has been proven to have disease-related distortion in fMRI connectivity and vigilance (Calhoun et al., 2012; Wang et al., 2015). More investigations are converging the findings that the decreased vigilance level is associated with schizophrenia (Boutros et al., 2008; Razavi et al., 2013). Meanwhile, Yang et al. (2014) found the variance of global signal is lower in healthy group compared to the group of patients with schizophrenia. Since a clear consensus about vigilance and major disorders has not yet emerged, the resting-sate connectivity needs to be interpreted carefully by addressing the effect of vigilance when investigating the disease-related effect.

3.1.3 Effects of Body Positions on Measurements

fNIRS can well adopted to several different body positions compared to only laying down on scanner bed in fMRI study. The priority of fNIRS is to be the best alternative neuroimaging tool by expanding its unique advantages. Although fMRI is the most widely used, non-invasive neuroimaging modality, it is limited by the scanner environment and constraints. The fNIRS has a myriad of advantages that outperform fMRI, most notably in high portability and less sensitivity to head motion. The development of fibreless and lighter weighted wearable fNIRS system allows subjects to move freely in a naturalistic environment and to complete complicated tasks without restricting constraints. Tachtsidis et al. (Tachtsidis et al., 2004), who compared effect of three different positions on cerebral blood pressure with fNIRS and stated that standing position has the highest mean blood pressure (MBP) and supine has the lowest MBP. Although very low frequency (0.02–0.04 Hz) did not reveal any significant impact of body position, they reported that the magnitude of low frequency oscillation in oxygenated hemoglobin in the resting brain shows a significant difference between different postures in 0.04-0.15Hz. Besides, Watanabe et al. reported

that prone, supine, and sitting have significantly different effect on autonomic regulation of cardiovascular function (Watanabe et al., 2007a). All these physiological measures which affected by body positions potentially contribute to fNIRS measures and global signal component.

3.2 Motivations for This Project

Functional near-infrared spectroscopy (fNIRS) is a noninvasive functional neuroimaging technique that can monitor concentration changes in oxygenated and deoxygenated hemoglobin (HbO and HbR) in the cerebral cortex. fNIRS measurement is based on the absorption of biological tissue to light in the 700 nm to 1000 nm near-infrared spectrum. Different chromophores, such as hemoglobin, myoglobin, and cytochrome aa3, have different absorptivity (Sood et al., 2015). With the advantage of low-cost, portability, and ease to co-register with other neural recording modalities, such as an electroencephalograph (EEG), fNIRS has become an attractive means for imaging and monitoring hemodynamic signals in the human brain, which complements the use of functional magnetic resonance imaging (fMRI) in versatile environment. fNIRS has been widely applied in functional neuroimaging (Torricelli et al., 2014), cerebral monitoring in neonates (Sood et al., 2015) and brain-computer interface (Shin et al., 2017). Unlike fMRI constraining subjects to lying down on a scanner bed, fNIRS poses fewer physical constraints on the participants, thereby permitting them to be studied at different body positions during recordings.

Particularly, imaging of resting-state functional connectivity (RSFC) in the human brain has been a recent focus for neuroimaging studies, including fNIRS (Mohammadi-Nejad et al., 2018; Pinti et al., 2018). The activity of the resting brain exhibits spontaneous and large-amplitude fluctuations, which have been observed in a number of imaging modalities such as fMRI (Biswal et al., 1995a), positron emission tomography (Raichle et al., 2001; Watabe and Hatazawa, 2019), and direct measures of neuronal activity with electro- or magneto-encephalography (EEG or MEG)

(Goldman et al., 2002; Mantini et al., 2007; Brookes et al., 2011; Yuan et al., 2012; Yuan et al., 2016). The measures of resting-state cerebral hemodynamics, mostly using fMRI based on the blood-oxygenation-level dependent (BOLD) contrast, show fluctuations predominantly at a low frequency band of < 0.1 Hz (Cordes et al., 2001). The temporal synchrony across brain regions have been revealed (Beckmann et al., 2005a; Damoiseaux et al., 2006), and demonstrated to be important biomarkers for the brain at diseased conditions (Zhang and Raichle, 2010). Prior studies of RSFC in both healthy and diseased conditions can be influenced by the presence of a strong global component, which is usually observed throughout sampled voxels or sensors, thereby dominating the RSFC (Greicius et al., 2003; Fox et al., 2005; Fox et al., 2009). However, the approach of removing global signal has recently been shown to induce systematic biases and the anti-correlation enhanced by global signal regression (GSR) becomes the main concern (Fox et al., 2009; Murphy et al., 2009). Furthermore, evidences show that a neural component (Scholvinck et al., 2010; Wong et al., 2013; Wong et al., 2016) and even diagnostic information (Hahamy et al., 2014; Murphy and Fox, 2017; Yang et al., 2017) exist in the global signal, which challenges the assumption of removing it in the first place.

Like fMRI signals, fNIRS also offers the potential to examine the human brain at resting state by measuring concentration changes of HbO and HbR in the vasculature of the cortical tissues below sensing channels (Obrig and Villringer, 2003; Scholkmann et al., 2014). fNIRS has been effectively employed to characterize the resting-state brain in adults (Obrig et al., 2000; White et al., 2009; Lu et al., 2010; Mesquita et al., 2010; Zhang et al., 2010; Sasai et al., 2011) and infants (Homae et al., 2010; White et al., 2012; Molavi et al., 2013; Watanabe et al., 2017), and to assess differences between experimental groups (Keehn et al., 2013). The most common RSFC analysis of fNIRS data involves evaluating the temporal relationship between time series of the

preprocessed data from recording units, for example, through the Pearson's correlation. A global component has been observed in fNIRS measurements and commonly removed for the purpose of attenuating systematic noises at the resting state (White et al., 2009; Mesquita et al., 2010; Eggebrecht et al., 2014; Tachtsidis and Scholkmann, 2016; Duan et al., 2018). Whereas removing superficial contributions from short-distanced channels to fNIRS is increasingly employed to attenuate the systematic noises (Saager and Berger, 2005; Gagnon et al., 2011), data from both long-distanced and short-distanced channels commonly suggest a global component exist in fNIRS measurements and distribute across wide regions (Zhang et al., 2005; Kohno et al., 2007; Zhang et al., 2007; Zhang et al., 2009b; Tong and Frederick, 2010; Novi et al., 2016; Sato et al., 2016). However, the physiological nature of the fNIRS global signal has not been fully established, since the neurophysiological components in the resting-state global fNIRS signal have not been systematically investigated. Therefore, whether or not to remove the global signal in fNIRS-based RSFC analysis remains not clear.

3.3 Hypotheses to Be Tested

This study aimed to investigate the physiological underpinning of resting-state fNIRS global signal by concurrently acquiring fNIRS and EEG in whole-brain, high-density coverage. Previous studies have examined the global signal of resting-state BOLD fMRI and revealed a negative relationship between the amplitude of resting state fMRI global signal and EEG vigilance level (Wong et al., 2013; Chang et al., 2016a; Falahpour et al., 2018). Using simultaneous EEG-fMRI measures in human subjects, these studies have shown that higher vigilance states are characterized by lower global signal amplitudes, indicating that neurophysiological components exist in the global signal. Moreover, the EEG vigilance level has been linked to the fluctuations of activities in regions constituting the default mode network (Olbrich et al., 2009b), suggesting that regressing

out the resting-state global signal could potentially impact the connectivity in resting state networks. Based on the prior studies using BOLD fMRI, in the current study we hypothesize that the fNIRS global signal has a neurological component and is related to the EEG vigilance. Furthermore, considering that fNIRS is a promising technology for imaging the human brain at versatile body positions, the current study examined the impact of body positions on the fNIRS global signal at resting state conditions. In addition, as a control, the impact of body positions on evoked activities to auditory stimuli were studied.

3.4 Data Acquisition and Preprocessing

Study procedures were completed according to the Declaration of Helsinki guidelines and approved by the Institutional Review Board at the University of Oklahoma Health Sciences Center. Twenty-four healthy subjects were recruited after giving informed consent. All subjects were right-handed. Two subjects were excluded due to bad signal quality caused by excessive movement. Thus, 22 subjects' data were included in the analysis (14 males and 8 females, aged 19 to 55 years old, average age ± STD = 30.5 ± 11.5 years). Each subject participated in two separate sessions, eyes-open (EO) and eyes-closed (EC), the order of which was randomized. For each subject, two sessions occurred on different days that were within a four-week period (mean interval ± STD = 12.5 ± 14.9 days). Each session contained three recording blocks at different body positions: standing, sitting, and supine. The order of these blocks was randomized among all subjects but was kept the same for each subject at consecutive sessions. Each block contained a 10-minute resting-state part and an auditory task part that lasted 6 minutes and 30 seconds. In the resting-state part, subjects were instructed to keep as still as possible and not fall asleep. Specifically, in EO resting condition, subjects were instructed to focus on a black cross on a white background. In the auditory task part, subjects were instructed to keep still and listen to the auditory stimuli from

a pair of earbuds. During each block, fNIRS and EEG signals were recorded simultaneously. Six datasets (2 eye conditions by 3 body positions) were obtained for each subject, yielding a total of 132 datasets in the current study, which included concurrent EEG and fNIRS data of both resting state and task conditions.

3.4.1 fNIRS Data Acquisition

The fNIRS measurements were acquired with a NIRScout system (NIRX, New York, United States). 32 source probes and 32 detector probes were plugged into holders and arranged into a cap based on the international 10-5 system (Jasper, 1958). A total of 105 channels (i.e. 105 pairs of sources and detectors) were defined, covering the areas from the forehead to the occipital lobe. The inter-optode distance varied between 25mm, 27 mm and 30mm, corresponding to three different sizes of caps (54cm, 58cm, and 60 cm). The intersection between the left and right tragus and the Nasion and Inion were the center of the cap, which was denoted by the Cz position. A dark black over-cap covered the cap to block external light luminance. The absorption of near-infrared light at 760 and 850 nm was measured with a sampling rate of 1.95 Hz.

3.4.2 EEG Data Acquisition

A 64-channel, fNIRS-compatible EEG system (BrainProducts, München, Germany) was utilized to record the EEG data. To couple the EEG signal with the fNIRS hemodynamic signal, the montage of the EEG electrodes was designed to match the fNIRS montage. Every EEG channel was crossed by an adjacent pair of light source and detector. 64 EEG electrodes were also mounted onto corresponding holders. The electrode at FCz position was selected as the reference point. Two 32-channel amplifiers, which were powered by a rechargeable battery, were included in our EEG system. Electrically conductive gel was added to decrease the impedance between scalp and

electrodes. The impedances of EEG electrodes were kept under 50 kΩ throughout the recordings. All the EEG datasets were digitized with a wide band of 0.1-250 Hz at a 500 Hz sampling rate.

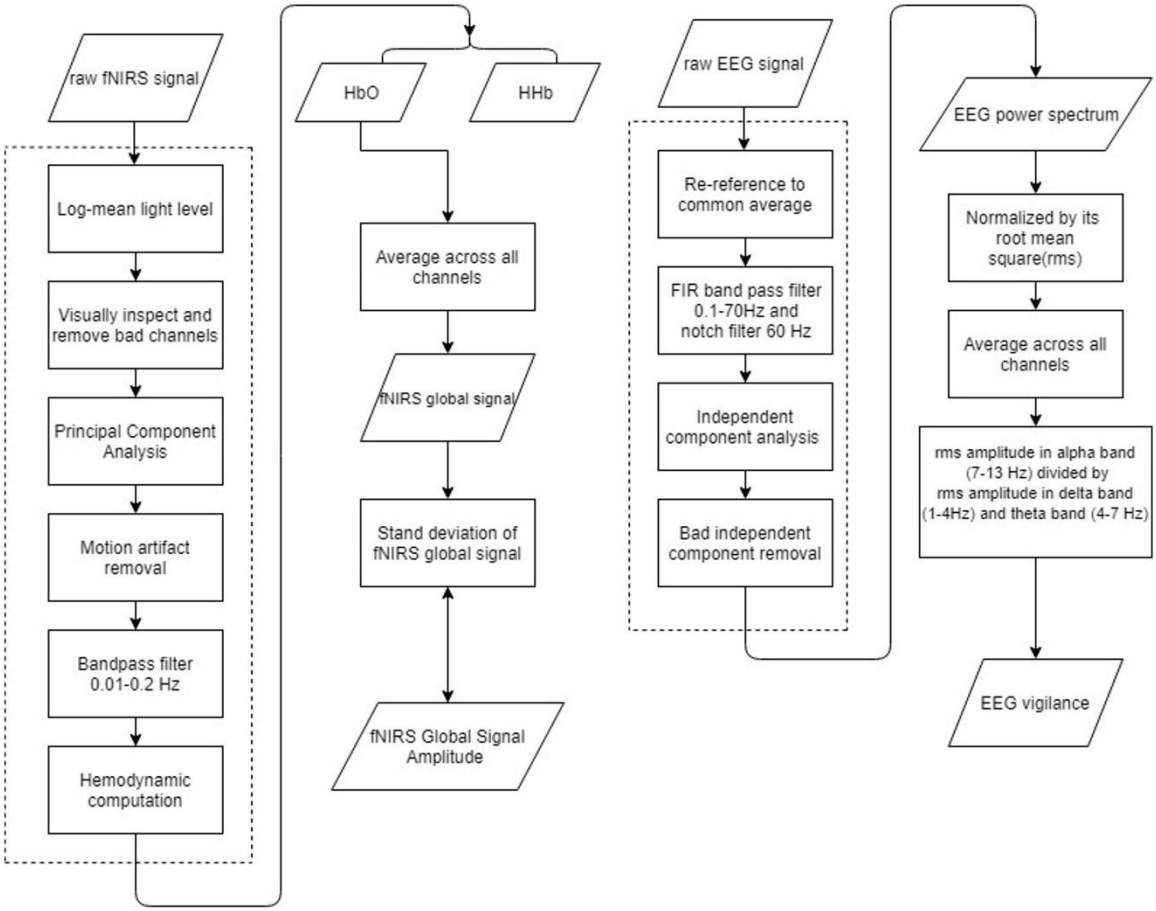

Figure 11 Flowchart of the data processing flowchart. (Left) fNIRS signal processing procedures, and (Right) EEG signal processing procedures. Dashed line circles the pre-processing procedures.

3.4.3 fNIRS and EEG Data Preprocessing

Figure 11 shows the analysis flowchart of EEG and fNIRS data. EEGLAB (Delorme and Makeig, 2004) was used for pre-processing of EEG data. After loading the raw datasets, the data was re-referenced to the common average reference. A basic FIR bandpass filter from 0.1 Hz to

70 Hz was used to filter the data in addition to a notch filter of 60 Hz. Additional ocular and muscular artifacts were removed by the independent component analysis implemented in EEGLAB. The ocular components, muscle movement components, and other artifacts were manually inspected and removed (Chaumon et al., 2015). Preprocessed EEG data were down-sampled to 250 Hz.

fNIRS data was pre-processed in HOMER2 (Huppert et al., 2009). Channels consisted of a source electrode and adjacent detector electrodes. Montages were created according to the setup of sources and detectors. Preprocessing of fNIRS data included converting raw light intensity to optical density, PCA removal (Tak and Ye, 2014), and motion artifact detection and correction. The PCA algorithm we performed here is to filter out the first principal component (Novi et al., 2016). Discontinuities and spikes existing in recordings were replaced by an average of its adjacent data segment. All channels were bandpass filtered from 0.01 to 0.2 Hz. The resulted time series were subject to hemodynamic computation via the modified Beer-Lambert law (Kocsis et al., 2006), yielding relative changes in concentrations of Oxy-Hemoglobin (HbO) and Deoxy-Hemoglobin (HbR). Differential Path Length Factor (DFP) was determined by the spectrum detected by Walter Gratzer (Med. Res. Council Labs, Hally Hill, London).

3.5 EEG-Based Vigilance Metrics

For EEG data, after removing artifacts, a spectrum was calculated by using Welch's power spectral density estimate with segments of 10 seconds and 50% overlap for each EEG channel. Then the spectrum was normalized by its overall root mean square (RMS) amplitude, resulting in the relative amplitude spectrum. Three frequency bands (delta: 1–4 Hz, theta: 4–7 Hz, alpha: 7–13 Hz) were delineated, and the RMS amplitudes were calculated separately for each band. A

measure of EEG vigilance was defined as the RMS amplitude in the alpha band divided by the sum of RMS amplitudes in the delta and theta bands.

3.6 fNIRS-Based Global Signal Metrics

After pre-processing, the fNIRS data became a measure of the relative concentration changes of Oxy-Hemoglobin and Deoxy-Hemoglobin in units of μM. Then the preprocessed fNIRS were separated into two frequency bands: the lower range of <0.05 Hz and the upper range of >0.05 Hz containing the Mayer wave, guided by inspection of power spectrum (**Figure 13**) and ANOVA tests. To calculate the global signal, the time series of relative changes in HbO or HbR were averaged across all channels covering the whole brain. Then, the amplitude of the global signal was defined by the standard deviation of the global signal time series.

3.7 Statistical Analysis

Firstly, in order to explore the effect of body position on neural recordings, as one of the main hypotheses to test in our investigation, ANOVA (standing/sitting/supine body positions) was applied on the EEG or fNIRS quantities obtained from 22 subjects, separately for the EO and EC conditions. More specifically, we performed the statistical test on each frequency bin along a continuous spectrum (**Figure 13** and **Figure 14**), as we expected a possible frequency-dependent effect of body position. Based on the delineation of frequency-dependent effect (**Figure 13**), we segregated the quantities of the fNIRS global signal in two frequency bands: $f < 0.05$ Hz and $f > 0.05$ Hz.

Next, two-way repeated measures ANOVA (standing/sitting/supine body positions X EO/EC) was applied to assess if any main effect of body position or eye condition, or interaction between the body position and the eye condition, separately in the frequency range of <0.05 Hz and >0.05 Hz and separately for HbO and HbR. Likewise, two-way repeated measures ANOVA

(standing/sitting/supine body positions X EO/EC) was tested on the EEG vigilance scores. The dimension of metrics is 22*3*2 (the subject number * position number* eye condition number). Furthermore, post-hoc analysis assessed the difference between conditions using a paired, two-sided t test. Bonferroni correction was used to correct the multiple comparison.

Furthermore, the co-variation between the global signal amplitude of fNIRS and the EEG vigilances was calculated, across all subjects and all body positions. Particularly, the co-variation analysis has excluded the frequency band of greater than 0.05 Hz which is affected by Mayer wave (Julien, 2006). Also, for the purpose of determining whether vigilance variations underlie the fluctuations in fNIRS global signal, the co-variation was only examined in the experimental conditions in which the effect of body position was not significant. Therefore, one-way ANOVA of the body position effect was assessed separately for eyes-open and eyes-closed conditions. Likewise, one-way ANOVA of the body position effect was assessed on EEG vigilance scores separately for eye conditions.

3.8 Results

The aim of the study was to investigate the neurological basis of the fNIRS resting-state global signal, if any, and the impact of body positions on the resting-state signals. The results are organized as such: the frequency-dependent impact of body positions on fNIRS and EEG signals was explored, then the factors of body positions and eye conditions were assessed in fNIRS global signal in two delineated frequency bands, and finally, the co-variation in the amplitude of fNIRS global signal and EEG vigilance was analyzed. As control results, the fNIRS and EEG task responses to auditory stimuli were included.

Firstly, spontaneous fluctuations were observed in the fNIRS global signal when subjects rested with their eyes open and closed, without any external stimuli. Representative single-session

traces of fNIRS global signals are shown in **Figure 12**, at an EC resting condition. Notably, the global signal at all three positions exhibit fluctuations with a peak frequency of ~ 0.02 Hz. Meanwhile, the data acquired from these body positions exhibited different patterns of fluctuations in the time domain, i.e. slower fluctuations are observed in the supine position and faster fluctuations in the sitting and standing positions. In terms of the amplitude, we noted that the power spectrum at the supine position showed a lowest amplitude in the frequency range of 0.05 – 0.1 Hz than those at sitting and standing positions, in the representative subject.

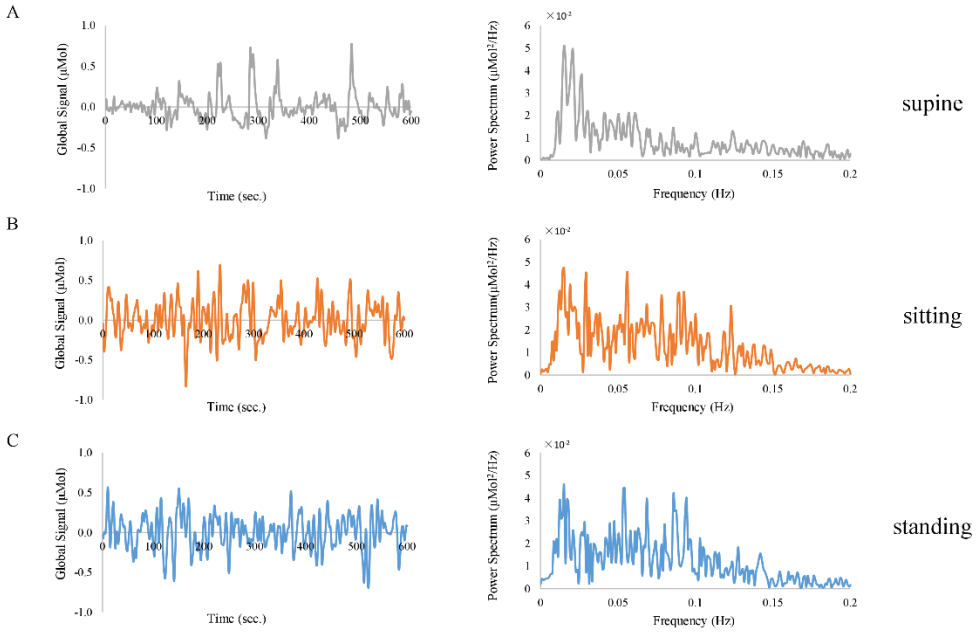

Figure 12 Representative EC single-session traces of fNIRS global signal derived from HbO signal at different positions (A) supine in grey color, (B) sitting in orange color, and (C) standing in blue color, exhibited different patterns of fluctuations in the time domain (left panel) and frequency domain (right panel).

Furthermore, the position-dependent profile of the resting-state fNIRS global signal is also prominent at the group level. **Figure 13** shows the grand average of the power spectrum of fNIRS

global signal at various resting state conditions. Notably, in the frequency range from 0.05 Hz to 0.1 Hz, the spectrums at three different body positions show largely different amplitudes. The spectrum at the standing position appears to be of highest amplitudes in 0.05 Hz - 0.1 Hz, at both EO and EC conditions (**Figure 13** A,B) in blue curves, whereas spectrum at supine are of lowest amplitudes (**Figure 13** A,B) in grey curves. In order to delineate the frequency-dependent effect of body position, we performed one-way ANOVA on the amplitude of fNIRS global signal separately in each frequency bin. At the EO condition, between 0.05 and 0.09 Hz, the effect of body position was significant on HbO ($p < 0.05$, uncorrected). Similarly, at the EC condition, the effect of body position was significant in the range from 0.07 Hz to 0.09 Hz on HbO ($p < 0.05$, uncorrected). Since the fNIRS signal in the frequency range of 0.05 Hz - 0.1 Hz has been related to a physiological noise known as the Mayer wave (Julien, 2006), our later analysis of the fNIRS global signal then focused on two distinct frequency bands, i.e. $f < 0.05$ Hz and $f > 0.05$ Hz, in order to distinguish a position-dependent impact that may be attributed to physiological noises. In HbR, we used the same frequency bands as with HbO. Noteworthy, none of HbO or HbR data showed any significant effect of body positions in a frequency bin less than 0.05 Hz ($p > 0.05$, uncorrected).

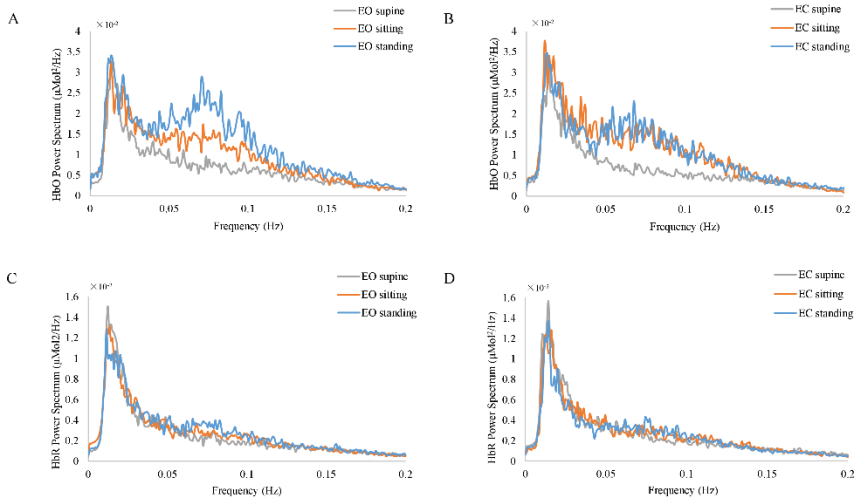

Figure 13 The grand average of the power spectrum of fNIRS global signals at various resting-state conditions, (A) and (B) shows HbO signal at EO and EC conditions. Similarly, (C) and (D) shows HbR signal at EO and EC conditions, respectively. The grey, orange, and blue curves represents supine, sitting, and standing (same in all panels).

Likewise, in the resting-state EEG, our analysis explored whether a position-dependent profile exists on the spectrum. **Figure 14** A and B show the grand average of the power spectrum at EC and EO conditions, respectively (**Figure 14** A, B). ANOVA revealed that the body position was not significant in any of the frequency bins at either EO or EC conditions ($p > 0.05$, uncorrected). Notably, although the grand average at the EC conditions appears with different amplitudes for three different conditions, it did not reach a significance level ($p = 0.067$ at $f = 10.8$ Hz, uncorrected).

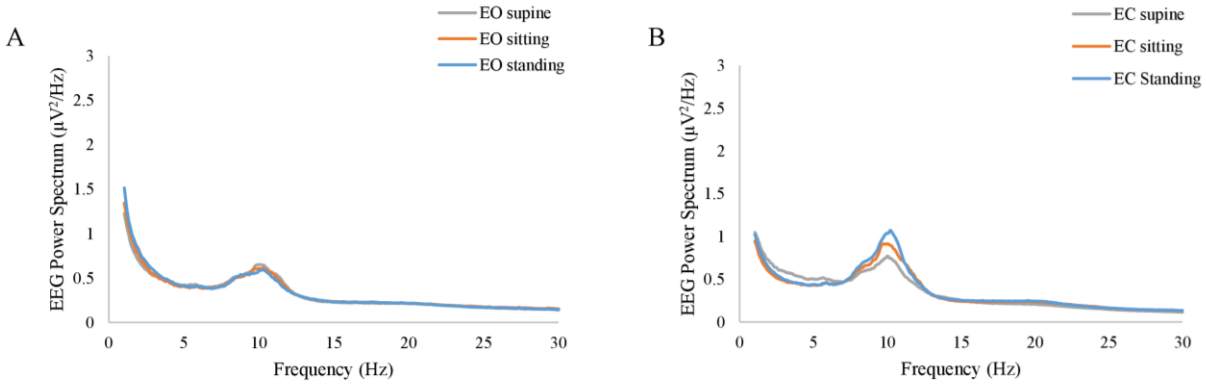

Figure 14 The grand average of the power spectrum of EEG resting-state signals at (A) EO condition. (B) EC condition. The grey, orange, and blue curves represents supine, sitting, and standing (same in both of panels).

Next, we aggregated the fNIRS and EEG quantities as the amplitude of global signal and vigilance scores, respectively. We averaged the amplitude of the fNIRS global signal (as root-mean-square) in the range of $f < 0.05$ Hz, which excludes the Mayer wave, and then separately in the range of $f > 0.05$ Hz. Meanwhile, EEG vigilance scores were calculated based on the power spectrum of resting state EEG as the ratio of alpha-band RMS divided by the sum of delta- and theta-band RMS. Two-way Repeated Measures ANOVA (body positions *eye conditions) revealed a marginal effect of body positions on fNIRS global signal amplitude in the very low frequency range of $f < 0.05$ Hz ($q = 0.10$). Meanwhile, the effect of body position was significant on the fNIRS global signal in the range of $f > 0.05$ Hz ($q < 0.001$). Noteworthy, the interaction of body positions and eye condition was not significant in fNIRS global signal amplitude in either frequency range.

Post-hoc comparison on HbO in the range of $f > 0.05$ Hz was then conducted to assess the difference between pairs of body positions (i.e. standing vs. supine, sitting vs. supine, and standing

vs. sitting) (**Figure 15** B). Analysis showed that the amplitude of fNIRS global signal for the supine position was significantly lower than the sitting position ($q < 0.01$) and standing position ($q < 0.001$), after multiple comparison correction. But amplitude of fNIRS global signal for sitting position did not differ from the standing position. Noteworthy, neither the eye factor nor the eye-position interaction was significant in fNIRS HbO or HbR data.

In terms of EEG vigilance scores (**Figure 15** E), the two-way repeated measure ANOVA found that the effect of body position, the effect of eye condition and the eye-position interaction was all significant ($q < 0.001$). Post-hoc comparisons on the EEG vigilance scores were then conducted to assess the differences. Informed by the significant interaction factor, we performed separate ANOVA analysis on the effect of body positions at separate eye condition and performed separate t-test on pairs of body positions and eye conditions. Only under EC condition, the supine position had significant smaller EEG vigilance than sitting ($q < 0.05$) and standing position ($q < 0.001$). Furthermore, regarding the eye factor (EO vs. EC), the EEG vigilance showed significance at both sitting ($q < 0.01$) and standing positions ($q < 0.001$), but not in the supine position. However, under EO condition, there was no significant effect of body position.

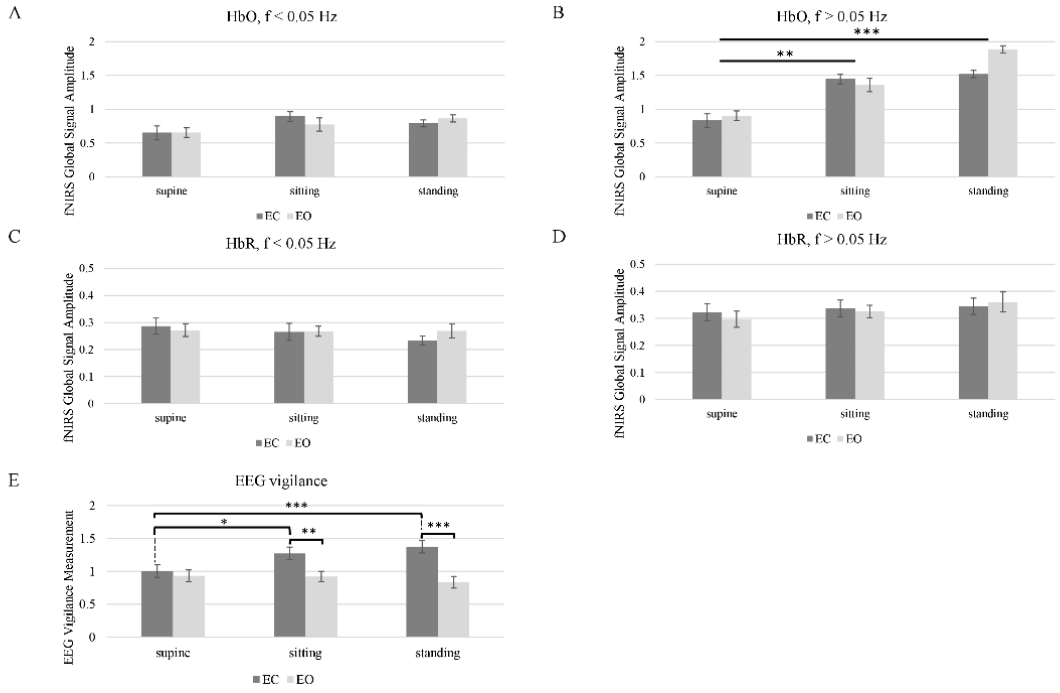

Figure 15 Statistical analysis reveals the major effects of body positions (supine, sitting, and standing) and eye conditions (EC and EO) on (A-D) fNIRS global signal amplitude and (E) EEG vigilance measurement. The amplitude of fNIRS global signal was averaged in the range of f<0.05Hz to exclude the influence of Mayer wave. A Two-way Repeated Measurement ANOVA was performed on (A) fNIRS HbO global signal amplitude, f<0.05 Hz amplitude, (B) fNIRS HbO global signal amplitude f>0.05 Hz, (C) fNIRS HbR global signal amplitude, f<0.05 Hz amplitude, (D) fNIRS HbR global signal amplitude f>0.05 Hz, and (E) EEG vigilance measurement. Error bars indicate standard error of the mean. Stars indicate significance level (* indicates $q < 0.05$, ** indicates $q < 0.01$, *** indicates $q < 0.001$).

As a next step, we examined the co-variation relationship between the fNIRS global signal and the EEG at resting state. Particularly, we compared the amplitude of fNIRS global signal in the frequency range of $f < 0.05$ Hz against the EEG vigilance scores, only at EO state when either

fNIRS or EEG quantities were not impacted by the factor of body positions. Also, we pooled data from all body positions in evaluating the correlation, since the factor of body positions was not significant. **Figure 16** shows the data of fNIRS and EEG and their correlations. Interestingly, a negative correlation was found between the HbO global signal of less than 0.05 Hz and EEG vigilance (HbO: $r = -0.38$, $q < 0.01$), while the factor of body position did not affect the EEG or fNIRS quantities. The individuals with higher global signal amplitudes were found to be with lower vigilance levels. Likewise, when subjects kept their eyes open, the correlation between the amplitude of HbR global signal ($f < 0.05$ Hz) and EEG vigilance was significant (HbR: $r = -0.40$, $q < 0.01$). Noteworthy, we did not compare fNIRS and EEG when subjects kept their eyes closed. Because EEG vigilance was significantly impacted by the three body positions at EO condition, covariation found between vigilance and fNIRS, if any, could be attributed to the position factor.

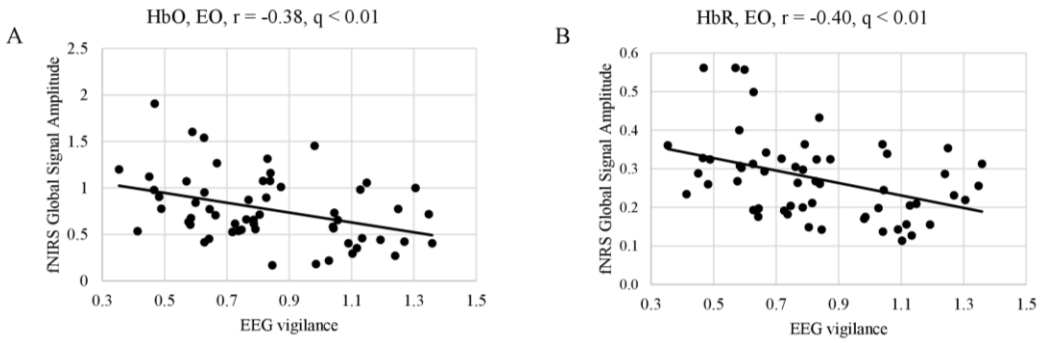

Figure 16 Amplitude of fNIRS global signal less than 0.05 Hz is highly correlated with EEG-based measure of vigilance. (A) fNIRS global signal derived from HbO signal at EO is significantly correlated ($r = -0.38$) with EEG vigilance. (B) fNIRS global signal derived from HbR signal at EO is also significantly correlated ($r = -0.40$) with EEG vigilance.

Furthermore, instead of pooling data across positions, we also examined the co-variation between fNIRS global signal and EEG per each body position as shown in **Figure 17**. Among all

body positions, results showed a consistent negative trend such that higher global signals are associated with lower vigilance states. In particular, both HbO and HbR at the standing position were significantly correlated with the EEG vigilance after multiple comparison correction (HbO: $r = -0.63$, $q < 0.05$; HbR: $r = -0.58$, $q < 0.05$). However, at other positions, the covariation did not reach significance, although a negative trend in the association was consistently noted. HbR at the supine position showed a significance-approaching correlation with EEG vigilance ($r = -0.38$, $p = 0.1$) and HbO at the sitting position also approached significance ($r = -0.35$, $p = 0.1$). However, HbO at supine position ($r = -0.12$) and HbR at sitting position ($r = -0.23$) did not show a significant correlation with EEG vigilance.

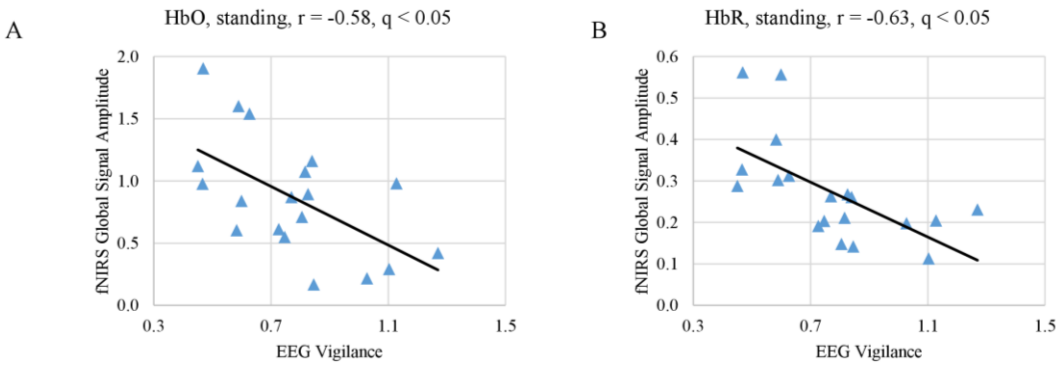

Figure 17 Amplitude of fNIRS global signal in the range of $f < 0.05$ Hz is correlated with EEG-based measure of vigilance, when subjects rested in the standing position with their eyes open. fNIRS global signal amplitudes derived from HbO signal (A) and from HbR signal (B) are both significantly correlated with EEG vigilance after multiple comparison correction (HbO: $r = -0.58$, $q < 0.05$, HbR: $r = -0.63$, $q < 0.05$).

3.9 Discussion

Our study has investigated the neurophysiological nature of the global signal of fNIRS measured at resting state. The results for the first time have demonstrated that the amplitude of the fNIRS global signal, particularly in the frequency range of $0.01< f <0.05$ Hz, is negatively correlated with EEG vigilance measures. The discovery of a neurological origin for fNIRS global signal has important implications for the processing of fNIRS signal acquired at resting state.

One of the most fundamental and critical issue in analyzing neuroimaging data is how to handle the global signal, which is defined as the time series of intensity averaged across imaging units in PET (Fox et al., 1988; Friston et al., 1990) and fMRI (Desjardins et al., 2001; Macey et al., 2004), and more recently, in fNIRS (Franceschini et al., 2006; Zeff et al., 2007; White et al., 2009; Mesquita et al., 2010). A strong presence of global signal in fMRI may lead to a massive and diffused activation pattern in task-based studies if the time series of the global signal is of similar profile with the task modulation (Kay et al., 2013; Power et al., 2015). Likewise, fNIRS studies of various tasks commonly removed a global component derived from the measurements to reveal focal activations, via linear regression and spatial filtering based on PCA/ICA decomposition (Zhang et al., 2005; Franceschini et al., 2006; Kohno et al., 2007; Zeff et al., 2007; Zhang et al., 2007; Eggebrecht et al., 2012; Eggebrecht et al., 2014; Sato et al., 2016; Zhang et al., 2016). Nonetheless, the impact of global signal is more problematic in task-free, resting state studies, as the global signal may lead to a perfusive connectivity pattern that is attributed to the global signal, no matter whichever seed region of interest is selected. Because region-specific connectivity is more desirable and because non-neuronal sources can dominantly contribute to the global signal (Glover et al., 2000; Wise et al., 2004; Birn et al., 2006; Yuan et al., 2012; Yuan et al., 2013), the analysis of resting state fMRI data has commonly included steps to attenuate the

impact of a global signal. For example, GSR removes an averaged signal of all recording units from the time series through linear regression. This procedure was originally developed for and applied to task-based fMRI data (Zarahn et al., 1997; Aguirre et al., 1998; Macey et al., 2004). Later, most resting-state fMRI studies have adopted GSR as a pre-processing approach: the global signal component is regressed out of preprocessed BOLD signals prior to computation of connectivity measures and therefore regionally focused connectivity patterns are reported (Fox et al., 2009). Similarly, in recent fNIRS studies of resting state brain, a global component has been recognized in the measurements from regularly distanced optodes (White et al., 2009; Mesquita et al., 2010; Tong and Frederick, 2010; Eggebrecht et al., 2014; Tachtsidis and Scholkmann, 2016; Duan et al., 2018) and from short-distanced optodes (White et al., 2009; Mesquita et al., 2010; Eggebrecht et al., 2014; Tachtsidis and Scholkmann, 2016; Duan et al., 2018). Till so far, there is no well-established pre-processing routine in resting state fNIRS studies although multiple efforts are being made (Huppert et al., 2009; Ye et al., 2009; Xu et al., 2014; Santosa et al., 2018). Approaches such as GSR and spatial filtering via PCA and ICA decomposition that were used in task-based fNIRS studies are also commonly adapted in resting state fNIRS studies to remove the global component, yielding regionally focused connectivity pattern (Mesquita et al., 2010; Zhang et al., 2010; Zhang et al., 2011; Sakakibara et al., 2016).

However, the removal of global signal in neuroimaging data has encountered controversial critiques, particularly in the studies of resting state functional connectivity. Because a global neurophysiological component may be present in direct neural recordings (Scholvinck et al., 2010; Wong et al., 2013; Wong et al., 2016), removing the global signal is shown to cause loss of such neural components, thereby confounding the resulted pattern of resting state functional connectivity. For example, Chen et al. (2012) found that the global signal is highly correlated with

default mode network (DMN) component. Further evidences indicated that the global signal resembles the resting-state fMRI time courses of the largest cluster when the level of global noise is low (Chen et al., 2012). Under such circumstances, GSR could mathematically mandate the presence of anti-correlation network in fMRI studies (Murphy et al., 2009). Other studies have further linked the fluctuations of global signals to the varying levels of vigilance or arousal (Chang et al., 2016a; Falahpour et al., 2018), which suggests that removing the global signal in those situations could remove an underlying behavioral factor. Therefore, the global signal regression should be very carefully applied when studying resting-state MRI (Murphy et al., 2009; Saad et al., 2012; Murphy and Fox, 2017). Until now, the nature of the fNIRS global signal has not been fully established since the neurophysiological components in the resting-state global fNIRS signal have not been systematically investigated. Our current study is the first of its kind to investigate the neuronal and non-neuronal sources in the fNIRS global signal by using concurrent fNIRS and EEG in whole-brain and high-density setup. Because both fNIRS and BOLD fMRI measure the cerebral hemodynamics, they carry similar substrates for neuronal activities while they also share common caveats due to non-neuronal sources, including respiration, cardiac pulsations, motion, etc. Like in the case of fMRI, removal of fNIRS global signal may lead to spurious results in the functional connectivity pattern, depending on whether or not there exists any neural component in the global signal of fNIRS and the amplitude level of global signal.

In this study, we have shown that fNIRS global signals acquired from the resting human brain are periodical oscillations. As shown in **Figure 12** and **Figure 13** at respective individual and group level, the resting-state fNIRS global signal resides in three ranges: dominantly less than 0.05 Hz with a peak component at ~0.02 Hz, a second peak between 0.05 and 0.1 Hz (also known as the Mayer wave) and greater than 0.1 Hz. Furthermore, our study extended investigations of the

fNIRS global signal at standing, sitting and supine positions. Indeed, periodic fluctuations were observed in the global signal at all body positions. The presence of a fluctuating fNIRS global signal with dominate activities of < 0.1 Hz suggests that the resting-state functional connectivity pattern may be affected by the global signal. Comparing with intracranial neural recordings (Leopold et al., 2003; He et al., 2008; Shmuel and Leopold, 2008), fNIRS global signal and spontaneous neural activities overlap their peaks in the range of < 0.1 Hz. Meanwhile, in comparison with fMRI, the fNIRS global signal shows a very similar spectral profile with those from BOLD fMRI. Especially, the spectrum of fNIRS at the supine position (**Figure 13** A and B**)** for both EO and EC conditions are almost identical to those reported in fMRI (e.g. **Figure 1** in (Biswal et al., 1995a). Since in our study the whole head fNIRS montage were sampled at 1.95 Hz, which is a higher frequency than BOLD fMRI (usually 0.5 Hz), the spectrum of fNIRS global signal revealed a more accurate spectrum.

Importantly, for the first time our study reported a negative correlation between the amplitude of fNIRS global signal in the range of < 0.05 Hz and the EEG vigilance based on the simultaneous recording (**Figure 16** and **Figure 17**). The negative correlation between fNIRS global signal and EEG vigilance measurement was observed at eyes open condition, when neither EEG nor fNIRS was affected by body positions (HbO and HbR in **Figure 16**). Furthermore, in a single body position at eyes-open condition, such a negative correlation between fNIRS global signal amplitude and EEG vigilance was also confirmed (HbO and HbR in **Figure 17**). The selection of frequencies f < 0.05 Hz for fNIRS is critical: it is within the range of resting state fMRI data but distinctly narrower. Previous fMRI study has demonstrated that the functional connectivity in auditory, visual and sensorimotor cortices is characterized 90% by the low-frequency band from 0 to 0.1 Hz (Cordes et al., 2001). Meanwhile, the fractional amplitude of

low-frequency fluctuation (fALFF) is defined as the ratio of power spectrum of 0.01 Hz - 0.08 Hz to that of the whole frequency band (Zou et al., 2008b). Noteworthy, one of the most studied network DMN has significantly higher fALFF than other brain regions, which indicates DMN has higher intensity of regional spontaneous brain activity in the range of 0.01 Hz - 0.08 Hz (Zou et al., 2008b). More importantly, our fNIRS signal was further narrowed to the range of < 0.05 Hz, in order to avoid the Mayor wave which is shown to depend on body positions. Because of a high sampling frequency, fNIRS was effective in preventing aliasing of high frequencies related to pulse and respiration into the range of < 0.05 Hz.

In addition, our results revealed that the power spectrum of HbO global signal depends on body positions in the range between 0.05 Hz – 0.1 Hz, regardless eyes were opened and closed (shown in **Figure 12** and **Figure 13** at respective individual and group level). Data at the standing position show the largest amplitude than the others, while the supine position is associated with lowest amplitude. These findings are consistent with previous reports by Tachtsidis et al. (Tachtsidis et al., 2004), who compared three different positions' effect on cerebral blood pressure with fNIRS. Their results showed that standing position has the highest mean blood pressure (MBP) and supine has the lowest MBP. They followed the Task Force of the European Society of Cardiology and the North American Society of Pacing and Electrophysiology (1994) to separate the frequency spectrum into 3 standard frequency bands: very low frequency (VLF: 0.02–0.04 Hz), low frequency (LF: 0.04–0.15 Hz) and high frequency (HF: 0.15–0.4 Hz). Although VLF did not reveal any significant impact of body position, their results reported that the magnitude of low frequency oscillation in HbO in the resting brain shows a significant difference between different postures in LF. Coincidentally, Mayer wave, i.e. the cyclic changes in arterial blood pressure, fall into this LF range (Muller et al., 2003; Julien, 2006). Mayer wave appears to have a close

relationship with fNIRS global signal. It is observed as oscillations of arterial pressure at ~0.1 Hz in conscious humans (Julien, 2006). Besides, it is positively related with the strength of the corresponding sympathetic nervous activity and the mean level of sympathetic nerve activity (Furlan et al., 2000). More importantly, prone, supine, and sitting have significantly different effect on autonomic regulation of cardiovascular function (Watanabe et al., 2007b). One rational speculation is that different body positions, especially the up-tilt positions, significantly affect autonomic regulation includes SNA which set the level of sympathetic vasoconstrictor tone, hence contributing to sustain arterial pressure (Julien, 2006; Scholkmann et al., 2014; Mohammadi-Nejad et al., 2018). Therefore, we regarded position-dependent effect in the Mayer wave range to be of physiological origin and discarded them for correlational analysis with EEG. Aside from the Mayer wave range, our analysis further eliminated the factor of body positions and revealed a significant correlation between the EEG vigilance and fNIRS global signal in the frequency range of <0.05 Hz (HbO and HbR in **Figure 16**). Such EEG-fNIRS association for the first time revealed a neurophysiological contribution to the fluctuations of fNIRS global signal (due to EEG vigilance), rather than a physiological factor (due to body positions).

There are abundant evidence supporting the phenomena that resting state hemodynamic signals in the range of < 0.05 Hz have neurophysiological origins. Intracortical recordings of electrical activities in human and animal studies have showed that fluctuations in the very low frequency range (including < 0.05 Hz) are widespread and coherently organized in the resting brain (Leopold et al., 2003; He et al., 2008). In addition, concurrent recordings of fMRI and electrophysiological data have shown a tight coupling relationship between the endogenous time courses of BOLD and field potentials in a resting state (Shmuel and Leopold, 2008). Previous studies show that MRI BOLD global signal amplitude is negatively correlated with EEG vigilance

measurement across the examined subjects (Wong et al., 2013; Wong et al., 2016). It was further shown that the moment-to-moment fluctuations of EEG vigilance, within individual subjects, were also negatively correlated to the amplitude of global signal in fMRI (Falahpour et al., 2018). However, so far, most fMRI studies of the resting-state brain have not carefully delineated the frequency bands due to an insufficient sampling frequency and also, the impact of body position was not investigated by fMRI due to the physical constrain.

Noteworthy, the calculation of the fNIRS global signal amplitude in our study is a reasonable adaption from the definition of global signal amplitude in previous fMRI study (Wong et al., 2013). Considering that the fNIRS optical density is converted to relative changes of HbO/HbR concentration in the stage of hemodynamic computation, the normalization in fNIRS equates the normalization in fMRI analysis (i.e. divided by the mean of fMRI time course), the calculation of fNIRS global signal in our study followed exactly the same definition in Wong et al. (2013). Our findings are consistent with previous findings on the relationship between fMRI global signal and EEG vigilance (Wong et al., 2013; Wong et al., 2016). Such discovery of a neurological component in fNIRS global in our study is novel. Importantly, our investigation adds findings from a unique perspective by showing a correlation in a carefully constrained frequency range that has excluded the possible physiological noise of blood pressure regulation.

Furthermore, our findings of a negative correlation between fNIRS global signal and EEG vigilance measures have important implications for the analysis and interpretation of fNIRS-based resting state functional connectivity. Due to such a negative correlation, removing the fNIRS global signal when studying the resting-state connectivity pattern may likely remove the vigilance signal, which could change the pattern of the resting state functional connectivity. Beyond that, Default Mode Network has been reported to be correlated with EEG vigilance scores (Olbrich et

al., 2009b). Removing fNIRS global signal therefore may attenuate activities of DMN that are correlated with vigilance fluctuations. Evidence has shown that the working memory plays a critical role in both visual rehearsal and vigilance performance (Baddeley et al., 1999). And age-related alterations and disease-related decrements (such as Alzheimer's disease) in DMN have significantly impacted working memory performance (Baddeley et al., 1999; Sambataro et al., 2010). Global signal removal might be problematic if vigilance is relevant to a diseased brain state. Therefore, the fNIRS global signal should not be treated as non-neural confound, and its removal should be carefully considered via a frequency delineation.

Last but not least, we conduct qualitative analysis and statistical analysis on auditory EEG and fNIRS responses. Our results did not observe the different body positions' effect on AEP of EEG data or task-related average of fNIRS data, at both EO and EC conditions. This excludes the concerns of environmental and systematic biases, such as the quality of data recording when subjects were positioned differently.

3.10 Conclusions

With the advantage of economic efficiency and portability, fNIRS has been proposed as a complementary option to fMRI, especially to be used in populations with contraindications to MRI scanner and in challenged environment (such as brain monitoring at bed-side or during surgery). The current study for the first time revealed the negative relationship between fNIRS global signal amplitudes and EEG vigilance scores in human participants, based on concurrent EEG and fNIRS recordings at high-density and whole-head montage. Our results stressed the significant effect of body positions on the fNIRS resting-state global signal, primarily in the frequency range of greater than 0.05 Hz yet only marginally in the range of less than 0.05 Hz. The finding of neural component in global signal suggests that such global signal should not be removed as non-neural

physiological signal, especially in studies where vigilance and related brain networks are of interest.

Chapter 4: Calibrating the Effect of Vigilance on Resting State Brain Network Using Sleep State Measurements

Since the confounding effect of vigilance and the global signal could weaken our findings with EEG-based brain connectivity measures, it would be essential to clarify and fully understand the influence of sleep stage changes on EEG and fNIRS measures. As we described previously, in order to eliminate the impact of widely distributed global signal component across the brain, many fMRI studies have adopted global signal regression (GSR) as a pre-processing approach, where the global signal component is removed as an artifact before computation of connectivity measures. However, the GSR procedure application is controversial; it may extract physiological relevant information about the brain's vigilance state. With more studies focus on brain connectivity dynamics, the temporal correlation between vigilance and the global signal is still not clear, especially in simultaneous EEG and fNIRS studies. Converging evidence has proven that the changes in vigilance can interfere with fMRI brain connectivity. Besides, the changes in vigilance could also affect the EEG measures of brain connectivity. In this study, we aimed to address the relevance of the global signal using a non-invasive neuroimaging technology, i.e., functional near-infrared spectroscopy (fNIRS). Like fMRI, fNIRS measures hemodynamic signals by probing local changes in oxygen consumption. We acquired simultaneous EEG and fNIRS signals, both in high-density configuration and whole-brain coverage, in healthy individuals at not only eye-closed resting state but also at different non-rapid eye movement (NREM) sleep stages. This is the first time to report the epoch-level temporal correlation between fNIRS global signal amplitude and EEG vigilance measurement. We deployed a novel approach by applying the subtraction of two different sleep stages to differentiate the brain connectivity alteration. We also

proposed that this method increases the sensitivity of EEG brain connectivity as a cognitive indicator for normal aging.

4.1 Motivations for This Project

Functional connectivity plays a significant role in the assessment of the resting-state brain network. Moreover, studies over an intrapersonal perspective are possible to analyze the significance of various sleep stages. In particular, the current study explores the comparison of an fNIRS-EEG simultaneous recording to understand better how an individuals' resting-state networks vary from epoch-to-epoch. Indeed, noting the responses to stimuli in the Hemodynamic response function (HRF) within a singular subject, correlated with other intrapersonal data of other subjects, can incite further implications to be made without the constraints of age, average vigilance of the testing group, and global signal. Besides, we are looking for some approaches that can minimize the confounding effect of vigilance other than regressing the entire vigilance, which contains physiological noise along with the neuronal component. To eliminate the influence of vigilance will increase EEG brain connectivity's accuracy and sensitivity and indicate broad application prospects in normal and abnormal aging studies.

4.2 Hypotheses to Be Tested

This project tested whether vigilance's fluctuation could impact the functional connectivity of the resting state brain network in the awake condition. Furthermore, I explored a new strategy to characterize the network connectivity free of the vigilance influence, based on utilizing sleep states to create a calibrated form of network connectivity. I constructed images of the network at multiple sleep states. Then I determined a formula of sleep-states-calibrated network connectivity that was shown to be an indicator for episodic memory performance.

4.3 Data Acquisition and Preprocessing

Same dataset was used here as we used before in Chapter 2. Based on some exclusion criteria, 19 healthy subjects were included in the analysis of moment-to-moment global signal and vigilance analysis (middle-aged adult group: 35.5 ± 7.2 years old, rang 28-46 years old, 4 females and 8 males; older adult group: 55.7± 6.0 years old, rang 50-63 years old, 6 females and 1 male) after excluding 10 subjects who fell asleep too quick.

And 22 healthy subjects were included in the analysis of stage-difference-based brain connectivity analysis (middle-aged adult group: 32.2 ± 3.8 years old, rang 28-40 years old, 4 females and 8 males; older adult group: 56.2 ± 4.9 years old, rang 50-63 years old, 9 females and 1 male) after excluding 7 subjects do not have long enough sleep (less than 2 minutes). The room light was turned off, with blanket and neck supporter provided. During the nap, resting state fNIRS and EEG signals were recorded simultaneously. The pulse generated by EPRIME software was sent to EEG and fNIRS systems at the same time to align those simultaneous recordings.

The fNIRS measurements were acquired with a NIRScout system (NIRX, New York, United States). A whole brain coverage of 32 sources and 32 detectors yields 105 pairs of sources and detectors, covering the areas from the forehead to the occipital lobe. The sampling rate was 1.95 Hz.

EEG data were recorded using a 64 channel fNIRS-compatible EEG system (BrainVision, North Carolina, United States). The system consisted of two 32-channel BrainVision amplifiers powered by a rechargeable battery unit. The device system was placed at the table behind the subject, which was connected using a 125 cm long cable to a BrainCap with 64 recording electrodes (BrainVision, North Carolina, United States). The EEG data were recorded at a 500 Hz sampling rate with a band of 0.1–250 Hz. Before each recording, the electrode impedances were

set below 50 kΩ, while the impedances of the reference and ground electrodes were set below 10 kΩ. The montage of whole-brain coverage EEG/fNIRS system is shown in Figure 18.

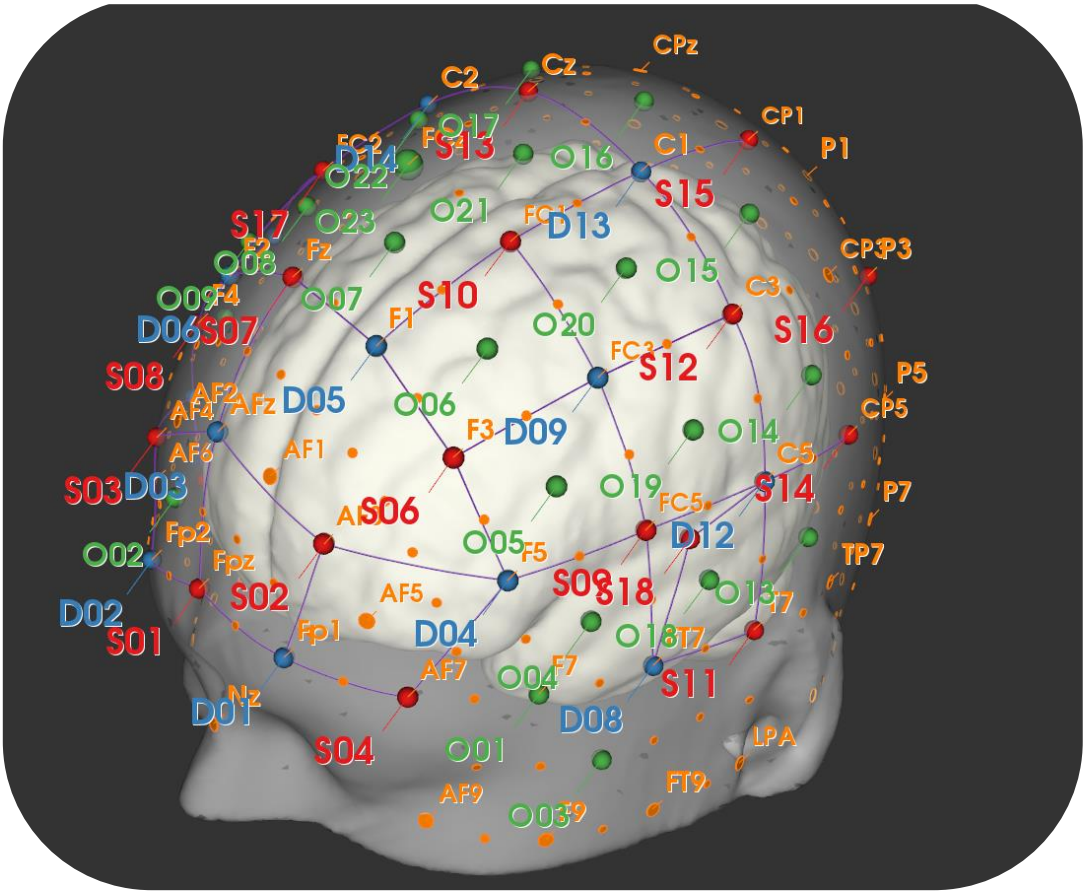

Figure 18 The montage of simultaneous EEG/fNIRS system. The green dots indicate EEG electrodes; red dots indicate fNIRS source optodes; blue dots indicate fNIRS detector optodes; purple lines indicate fNIRS channels.

Analyzer 2 (BrainVision, North Carolina, United States) was used for pre-processing of EEG data. After loading the raw datasets, the channel locations based on the international 10-5 standard electrode positions were utilized with the FCz position selected as the reference point. Therefore, the original topography is a circular map with its center at the reference point. The data

was re-referenced to the common average. A basic FIR bandpass filter from 0.1 Hz to 70 Hz was used to filter the data in addition of notch filter of 60 Hz.

The fNIRS data was pre-processed in HOMER2 (Huppert et al., 2009). Channels consisted of a source electrode and adjacent detector electrodes. Montages were created according to the setup of sources and detectors. Preprocessing of fNIRS data included converting raw light intensity to optical density, PCA removal, and motion artifact detection and correction. Discontinuities and spikes existing in recordings were replaced by an average of its adjacent data segment. All channels were bandpass filtered from 0.01 to 0.2 Hz. The resulted time series were subject to hemodynamic computation via the modified Beer-Lambert law (Kocsis et al., 2006), yielding relative changes in concentrations of Oxy-Hemoglobin (HbO) and Deoxy-Hemoglobin (HbR). Differential Path Length Factor (DFP) was determined by the spectrum detected by Walter Gratzer (Med. Res. Council Labs, Hally Hill, London). Hemodynamic computation allows us to relate the changes in light to changes in relative concentrations of hemoglobin through the modified Beer–Lambert law. Differential Path Length Factor (DFP) was determined by the spectrum detected by Walter Gratzer (Med. Res. Council Labs, Hally Hill, London). Finally, concentration change of hemoglobin will be calculated.

4.4 Polysomnography Based on EEG

Every data was segmented in tens of 30s epochs, starting from the EPRIME marker. All epochs were scored by a certified expert (B.W.C.) according to the American Academy of Sleep Medicine. Non-rapid eyes movement (NREM) stage 1, 2, and 3 indicate the deeper level of sleep status. Among the 29 subjects, 28 fell into sleep, 22 subjects fell into NREM stage 2, and 11 subjects fell into slow wave sleep (NREM stage 3 and 4).

4.5 EEG-Based Vigilance Metrics

To assess the epoch-to-epoch relationship between data from two independent modalities, we calculated the correlation between global signal amplitude and vigilance measurement per each 30s epoch, and per each subject. The r value was z-transformed by fisher transform, then we ran a two-sided, t-test versus zero value per each stage for every subject. In the random effect model, the random factor of subjects was at different levels for four different stages.

After pre-processing, the fNIRS data is a measure of the relative concentration changes of HbO and HbR in units of μM. The baseline for the concentration change is the mean of the absolute concentration plus noise offset. To calculate the global signal, the time series of relative changes in HbO or HbR were averaged across all channels covering the whole brain. Then, the amplitude of the global signal was defined by the standard deviation of the global signal time series.

For EEG data, a spectrogram was calculated for each EEG channel with Welch's power spectral estimate, and potentially motion-contaminated time points in the spectrogram were removed. For each remaining time point in the spectrogram, a relative amplitude spectrum was computed by normalizing the spectrum with its overall root mean square (rms) amplitude (square root of the sum of squares across all frequency bins). Relative EEG amplitudes were then computed as the rms amplitude in the following frequency bands (delta band: 1–4 Hz, theta band: 4–7 Hz, alpha band: 7–13 Hz). A measure of vigilance was defined as the rms amplitude in the alpha band divided by the rms amplitude in the delta and theta bands.

4.6 Resting State Connectivity Metrics

The resting-state connectivity is described in Section 2.7. We used the same procedure to calculate the brain connectivity pattern for N1, and N2 stages. Besides, two different ROI masks were defined by a conjunction analysis of the group-level EEG DMN pattern and the Yeo template.

The ROI masks of N1 and N2 are shown in Figure 23 A and B, respectively. We defined the new individual connectivity metrics by using two parts. The first part is to apply N1-ROI-mask on N1 stage connectivity. And then apply N2-ROI-mask on N2 stage connectivity. The new metrics is defined by using the N1 ROI connectivity from N1-ROI-mask minus the N2 ROI connectivity from N2-ROI-mask.

4.7 Statistical Analysis

For each subject, we calculated the temporal correlation between global signal amplitudes and vigilance measurements using Pearson's correlation coefficient across 30-s epochs. The coefficients were then transformed to z-scores, and subject to t-test to evaluate within- and inter-group differences. T test was performed on 30-s epoch level correlations between global signal amplitude and vigilance measurement, for all subjects, middle-age group, and older adult group. Furthermore, two-sample unpaired t-test was performed to compare middle-age and older groups. Bonferroni-corrections were used to minimize experiment-wise Type 1 error.

4.8 Results

Figure 19 demonstrates the fluctuation of fNIRS HbO global signal in one representative subject (black line). Each black dot indicates the global signal amplitude calculated from its corresponding 30-s epoch. The amplitude of the global signal varies from epoch to epoch. We further align the fluctuation with the sleep stage segmentation. As shown in the secondary axis (right y-axis), the sleep data was segmented into awake, NREM stage 1, 2, and 3. The red squared curve shows the subject gradually fell into slow wave (deep) sleep and woke up at the end of the recording. The amplitude of the fNIRS global signal is higher when compared to NREM stages. The sleep stages will be quantitively assessed by vigilance level with EEG measurement later.

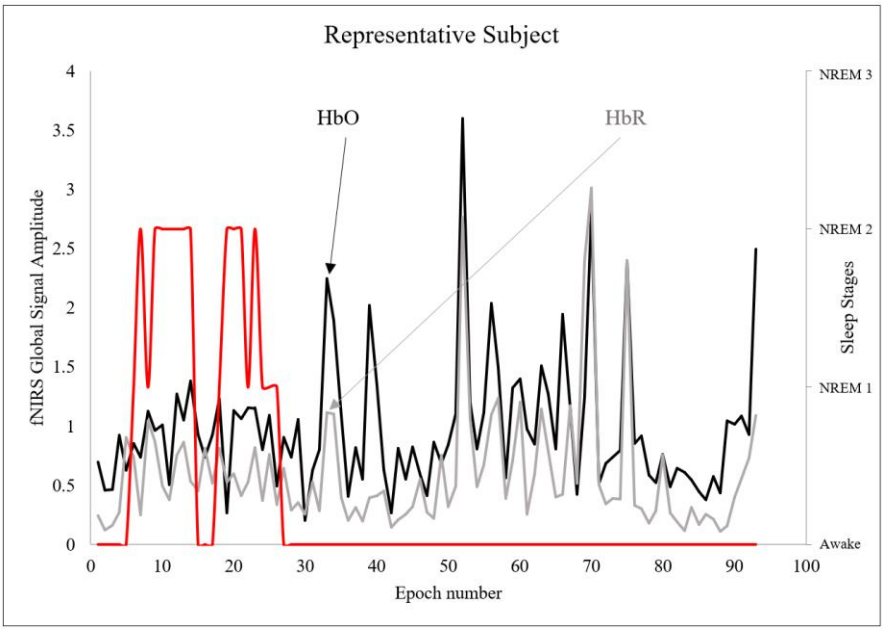

Figure 19 Moment-to-moment fluctuations of fNIRS HbO (black solid line) and HbR (gray solid line) global signal amplitude in one representative subject. Epochs of sleep scores are plotted in the red line.

The representative relationship between fNIRS global signal amplitude and EEG vigilance measurement was shown in Figure 20. The global signal amplitude calculated from HbO and HbR were displayed in Figure 20 A and B, respectively. Every dot represents the global signal amplitude and vigilance measurement of a 30-s epoch. The resting-state wakefulness cluster had a long range of the vigilance level. The result indicates that a negative correlation, i.e. higher fNIRS-derived global signal amplitudes are associated with lower EEG-derived vigilance states (less alertness). With the increased EEG vigilance measurement under wakefulness, the amplitude of global signal decreased.

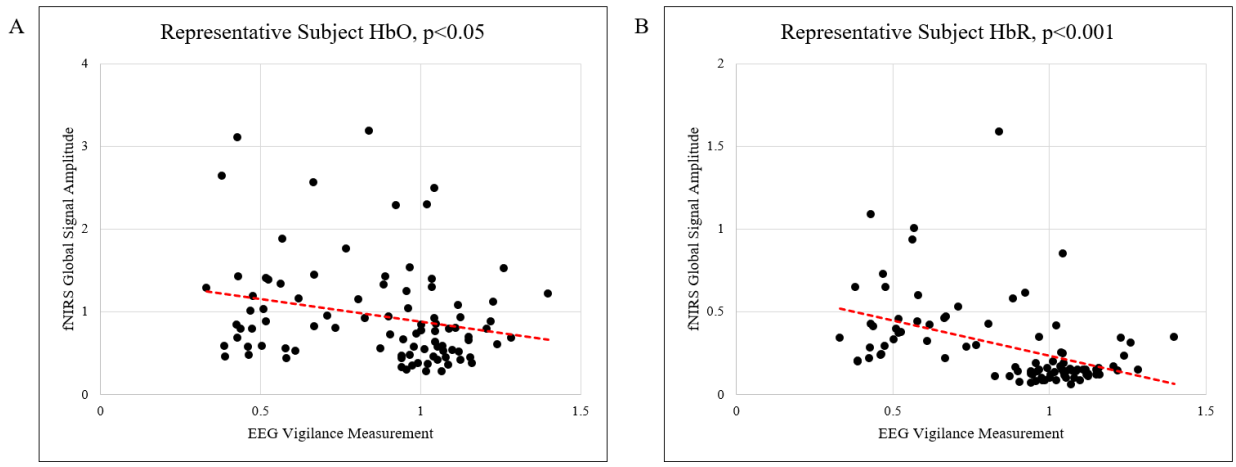

Figure 20 The relationship between fNIRS global signal amplitude and EEG vigilance measurement in a representative subject, for (A) HbO ($r = -0.24$, $p < 0.001$) and (B) HbR ($r = -0.45$, $p < 0.001$).

One-sample t-test results show the z-transformed correlation coefficients which derived from all subjects' both HbO and HbR data are significant different from zero (HbO: $t(17) = -2.88$, $q<0.05$, HbR: $t(17) = -2.96$, $q<0.05$). We ran a two-sample unpaired t-test on middle-age and older groups, there is no significance between them for both HbO and HbR data ($p>0.1$ for both).

Table 3 Group-level correlation between fNIRS global signal and vigilance

		All (n=19)		Middle-age (n=12)		Older (n=7)		Middle-age vs. Older
		M ± SD	t (vs. 0)	M ± SD	t (vs. 0)	M ± SD	t (vs. 0)	t
r (GS, Vigi.), Wakefulness	HbO	-0.24±0.37	-2.88**	-0.25±0.34	-2.50*	-0.23±0.43	-1.46	0.05
	HbR	-0.28±0.41	-2.96**	-0.24±0.40	-1.99	-0.35±0.47	-2.15	0.67

** $p < 0.05$ after Bonferroni-corrections, * $p < 0.05$ before Bonferroni-corrections

In Chapter 2, the relationships between Memory performance and memory/age are investigated. Figure 21 further demonstrated the trajectory of memory alterations with aging. 16.

Although the memory performance did NOT differ between middle-aged and older adults, their relationships between memory performance and age of years follow distinct trend. The two subgroups were separately fitted by lines. Blue line and red line represent the older group and the middle-aged group, respectively. WMSI scores stand for the Wechsler Memory Scale Immediate Recall score. Only in the older group, a significant negative relationship was found between the age and the memory performance scores ($r = -0.75$, $p = 0.002$).

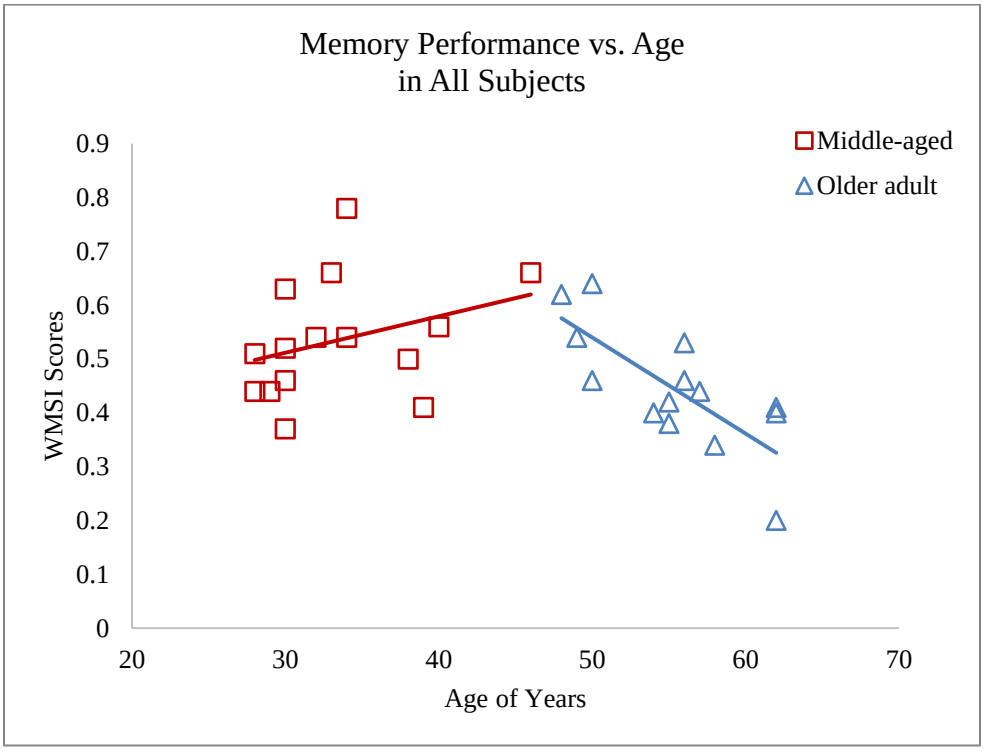

Figure 21 The relationship between memory performance and age of years differs in middle-aged and older adults. The two subgroups were separately fitted by lines. Blue line and red line represent the older group and the middle-aged group, respectively. Only in the older group, a negative relationship was found between the age and the memory performance scores ($r = -0.75$, $p = 0.002$). WMSI scores stand for the Wechsler Memory Scale Immediate Recall score.

Besides, Figure 22 shows the temporal covariation between brain connectivity and vigilance. The wakefulness stages before first sleep onsite were selected and divided into many 30s epochs. The brain connectivity calculated from every 30s-epoch and depicted as the orange curve in Figure 22 A. Meanwhile, the epoch-level vigilance assessed by EEG is shown as the blue curve. A significant co-variation was observed between time-course brain connectivity and vigilance (r= 0.54, p=0.003) as displayed in Figure 22 B.

A

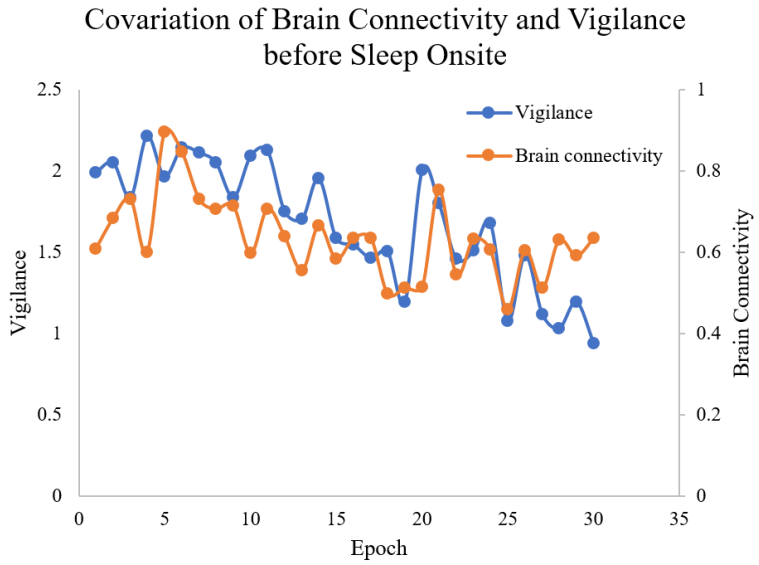

B

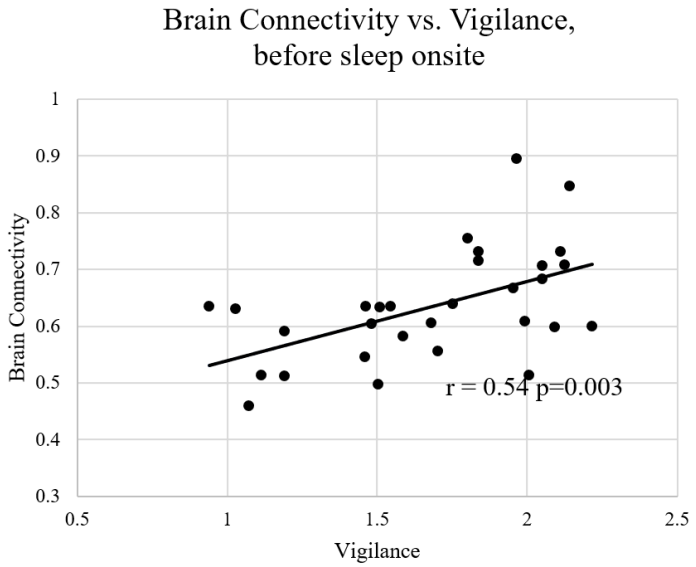

Figure 22 (A) Temporal Covariation of brain connectivity and vigilance before sleep onsite within one representative subject. (B) The epoch-level brain connectivity is correlated with vigilance within one representative subject (r= 0.54, p=0.003).

To examine this possibility, we investigated the relationship between brain connectivity based on the stage difference metrics and memory function assessed by WMS-D (delay recall) score. First, the ROI mask of N1 stage and N2 stage defined by the t-test versus 0 across corresponding available subjects are shown in Figure 23 A and B, respectively. The result in Figure 23 C reveals a significant correlation between memory and brain connectivity (r=0.58, p=0.006).

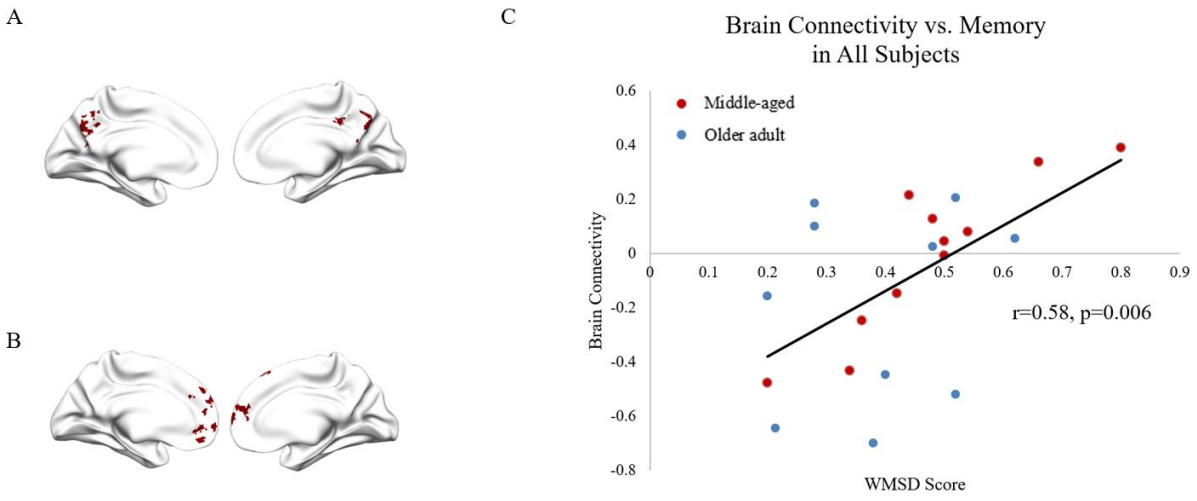

Figure 23 The ROI masks of (A) N1 stage and (B) N2 stage defined by the t-test versus 0 across corresponding available subjects. (C) Functional brain connectivity is correlated with memory performance in all adults. Each dot represents one individual's brain connectivity and the corresponding Wechsler Memory Scale Delay Recall score. Red dots and blue dots represent middle-aged and older adult groups, respectively. Black trend line represents linear relationship between these two variables (r = -0.58, p = 0.006).

4.9 Conclusion and Discussion

In this chapter, we found that when healthy subjects at wakeful rest, the moment-to-moment dynamics of fNIRS global signal and vigilance are also negatively correlated, consistent with what we found at the individual level. Our findings suggest that vigilance fluctuations may be the physiological factor underlying the variations in resting-state global brain activities, measured by fNIRS hemodynamic signals. Thus, removing any global signal components in studies of functional connectivity dynamics should be interpreted with caution. Besides, the brain connectivity shows a significant association with memory after implementing new connectivity metrics to minimize the stand error of vigilance. This supports our previous finding and verifies that EEG brain connectivity is a sensitive biomarker for aging study.

The BOLD global signal regression has been under debate for over a decade. While introduced to enhance the detection of system-specific correlations, it may affect the topography in functional connectivity (Fox et al., 2009; Murphy et al., 2009). In the past decade, the BOLD global signal fluctuation has been proved to correlate with arousal (Liu et al., 2018a), sleep depth (McAvoy et al., 2017), and especially vigilance negatively (Wong et al., 2013).

This study investigated the correlation between fNIRS global signal amplitude and EEG vigilance measurement by utilizing a simultaneous fNIRS and EEG system. Our result demonstrated a negative correlation based on the fNIRS HbO and EEG recording under an eyes-closed resting state. This is consistent with the previous fMRI study (Wong et al., 2013) and our previous study (Yuxuan et al., 2017). Notably, we investigated this correlation on an epoch-level within each subject compared to all previous studies conducted on the subject level. Based on our knowledge, this is the first time to report the within-subject level correlation between fNIRS global

signal and vigilance with fNIRS. This is also the first time to investigate the global signal under Non-REM stages with fNIRS modality.

In our opinion, the global changes in cerebral blood flow and oxygen metabolism reflect the fluctuations in vigilance as a person transitions from lighter to deeper stages of sleep. Studies with the Kety-Schmidt technique and positron emission tomography have found the global reduction in cerebral blood flow, oxygen metabolism and glucose metabolism from wakefulness to slow-wave sleep (Madsen et al., 1991a; Madsen et al., 1991b; Braun et al., 1997). A recent fMRI study also reported that the mean BOLD global signal increases with sleep depth in the gray matter (McAvoy et al., 2018). McAvoy et al. interpret their findings with the descent of deoxyhemoglobin. Our finding is consistent with their study to some extent. In the future, we can investigate changes in deoxyhemoglobin as well to testify their finding with fNIRS.

Compared with previous studies that were only able to investigate the subject-level correlation between global signal amplitude and vigilance, this study emphasizes the fluctuations within and between subjects. This could provide us with a novel solution to pre-process fNIRS data, especially those studies with a sleep task. Overall, our study has the potential to facilitate the understanding of the human brain's lateralized organization, which changes during Non-REM sleep and has been mapped with the hemispherical differences in the global BOLD signal's spontaneous fluctuations (McAvoy et al., 2016; McAvoy et al., 2017).

Regarding the influence of arousal level, previous studies demonstrated that resting-state fMRI signal varies with the changes of arousal or vigilance (Fukunaga et al., 2006; Horovitz et al., 2008; Larson-Prior et al., 2009). Chang et al. proposed a time-varying spatial fMRI pattern to tract the fluctuation of the arousal level (Chang et al., 2016b). The spatial pattern was validated by electrophysiology and behavioral measure. Moreover, it was implemented to track the continuous

arousal changes and increase the sensitivity of fMRI. However, the regression of arousal fluctuation would be problematic in practice. One study published on Nature Communication reported that the basal forebrain's nucleus basalis is involved in arousal regulation, and the cortical activity measured by fMRI is associated with the changes of arousal level (Liu et al., 2018b). Instead of regressing out the whole vigilance fluctuation, we proposed a novel metrics of EEG brain connectivity under sleep to benchmark episodic memory function with normal aging. Notably, one previous study reported the electrophysiological evidence of DMN disassociation during deep sleep (Horovitz et al., 2009). The finding of brain connectivity between frontal and posterior regions are lost during deep sleep might be informative of the decreased level of consciousness characteristic of deep sleep. These findings support our hypothesis that vigilance contributes to the confounding effect of the widespread global component. With removing the confounding part of vigilance measure, the sensitivity of EEG brain connectivity gains improvement.

Chapter 5: Summary and Perspectives

In my dissertation, EEG and fNIRS are applied to a series of investigations surrounding fundamental scientific questions (the relationship between global signal and vigilance) and clinical diagnostic application (association between brain connectivity and age or episodic memory). Specifically, we used EEG resting-state recordings to characterize functional connectivity changes during the normal aging process. EEG source-based brain connectivity shows a significant association with age and episodic memory, one of the most important and promising cognitive function for aging and AD studies. This indicates the reconstructed EEG data at source level could reflect the neuronal activity in DMN reliably. EEG source imaging technology can be used in detecting brain connectivity and cognitive function alteration in healthy adults during normal aging.

To better interpret our findings, my work continues to examine the confounding effect of vigilance by correlating vigilance level with a well-defined global signal, which presents a major mixture of physiological noise and a portion of the neuronal component. Since the vigilance is a confounding component for EEG acquisition, getting rid of vigilance could eliminate the interference and benefit for elaborating the significant findings.

This work continues to investigate the relationship between fNIRS global signal and vigilance at the epoch level. Our result reveals that the moment-to-moment dynamics of fNIRS global signal and vigilance are still negatively correlated. This suggests that vigilance fluctuations may be the physiological factor underlying the variations in resting-state global brain activities, measured by fNIRS hemodynamic signals. Importantly, a calibrated formula based on varying sleep states was proposed and demonstrated to provide a more accurate characterization of memory function.

In summary, my dissertation systematically demonstrates the current application of portable non-invasive neuroimaging tools in the field of aging and Alzheimer's study. My work has also examined the confounding effect of vigilance on network connectivity, and further proposed a solution of calibrated network connectivity towards a more accurate neuroimaging biomarker for memory. Our results suggest that EEG would be an effective, sensitive neuroimaging tool to characterize electrophysiological features of normal aging in large-scale networks of the human brain. My findings based on multimodal neuroimaging also provide important implications in understanding the neuroimaging literature on memory and aging.

Future work will need to focus on understanding the deeper mechanism of modulation on cognitive functions during the transition from wakefulness to NREM sleep stages. EEG and fNIRS are effective bedside monitoring modalities for the sleep study. As taking advantage of portability and movement tolerance into account, they would be able to play a more significant role in the interdisciplinary study by combing sleep, aging, and human brain connectivity. Not only limited to DMN, but more specific large-scale brain networks could also be highlighted by the alteration of brain connectivity during the transition from high vigilance stages to low vigilance stages or reversely. The subtle changes of functional brain connectivity hidden behind the transient process of transition between distinct vigilance stages would largely increase the sensitivity of detecting abnormal functional brain development. Not limited to episodic memory, other cognitive functions, especially different forms of attention, could also be an effective biomarker in the future aging study. With reliable measures and preprocessing pipeline, fNIRS will be a promising neuroimaging tool to cross-validate the findings in EEG studies. The combination of EEG, fNIRS or other modality will provide more possibility to probe the underlying mechanism of aging and pathology of neurodegenerative disease.

Chapter 6: Products of This Work

Peer-Review Publications

1. [Under Review] **Chen Y**, Tang J, DeStefano LA, Wenger M, Ding L, Craft MA, Carlson BW, Yuan H: Electrophysiological Resting State Brain Network and Episodic Memory in Healthy Aging Adults. *NeuroImaging*.
2. [Under Review] **Chen Y**, Tang J, Chen Y, Farrand J, Yuan H: Amplitude of fNIRS Resting-State Global Signal is Related to EEG Vigilance Measures: A Simultaneous fNIRS and EEG Study. *Frontiers in Neuroscience*.
3. [In preparation] **Chen Y**, Yuan H: Calibrating the Effect of Vigilance on Resting State Brain Networks by Sleep State Alterations.
4. [Under Review] Zhang F, Cheong D, **Chen Y**, Khan A, Ding L, Yuan H*: Correcting Physiological Noises in Functional Near-Infrared Spectroscopy. *IEEE Transactions on Biomedical Engineering*.
5. Shou G, Yuan H, Li C, **Chen Y**, Chen Y, Ding L. Whole-brain electrophysiological functional connectivity dynamics in resting-state EEG. *Journal of Neural Engineering*, 2020. DOI: doi: 10.1088/1741-2552/ab7ad3.
6. **Chen Y**, Farrand J, Tang J, Chen Y, O'Keeffe J, Shou G, Ding L, Yuan H: Relationship between Amplitude of Resting-State fNIRS Global Signal and EEG Vigilance Measures. Conf Proc IEEE Eng Med Biol Soc. 2017; 2017: 537 - 540. doi:10.1109/EMBC.2017.8036880.

Published Conference abstracts

1. Chen Y, Roque J, Tang J, Craft M, Carlson B, Yuan H. Fluctuations of Hemodynamic Global Signal Are Correlated with Vigilance States in Middle-age and Older Adults: A Simultaneous EEG and fNIRS Study. *Society for Neuroscience Annual Meeting 2019, Chicago, US, 2019.*
2. Chen Y, Tang J, DeStefano LA, Ding L, Craft MA, Wenger M, Carlson BW, Yuan H*: Fluctuations of Hemodynamic Global Signal Are Correlated with Vigilance States in Middle-aged and Older Adults: A Simultaneous EEG and fNIRS Study. *41st Annual International Conference of the IEEE Engineering in Medicine and Biology Society, Berlin, Germany, 2019.*
3. Chen Y, Roque J Tang J, Craft M, Carlson B, Yuan H. Fluctuations of Hemodynamic Global Signal Are Correlated with Vigilance States: A Simultaneous EEG and fNIRS study *41st Annual International Conference of the IEEE Engineering in Medicine and Biology Society, Berlin, Germany, 2019*
4. Chen Y, Chen Y, Tang J, O'Keeffe J, Shou G, Ding L, Yuan H*: Different Body Positions Affect Amplitude of Resting-State fNIRS Global Signal and EEG Vigilance Measures. *6th Biennial Conference on Resting State and Brain Connectivity, Montreal, Canada, 2018.*
5. Tang J, Chen Y, Yuan H*: Characterizing Cognitive Memory Function in Middle-Aged and Older Adults. *50th Annual Meeting of the Biomedical Engineering Society, Atlanta, Georgia, October 17, 2018.*
6. Tang J, Chen Y, DeStefano L, Worth T, Craft MA, Carlson BW, Wenger M, Ding L, and Yuan H*: Multimodal Characterization of Cognitive Memory Function in Middle-Aged

and Older Adults. *2nd OU-OUHSC Biomedical Engineering Symposium, Oklahoma City, OK, March 29, 2018.*

7. Chen Y, Chen Y, Tang J, O'Keeffe J, Shou G, Ding L, Yuan H*: Relationship between Amplitude of Resting-State fNIRS Global Signal and EEG Vigilance Measures. *2nd OU-OUHSC Biomedical Engineering Symposium, Oklahoma City, OK, March 29, 2018.*
8. Chen Y, Tang J, DeStefano L, Craft MA, Carlson BW, Wenger M, Ding L, and Yuan H*: EEG Fluctuations of Wake and Sleep in Middle Aged and Older Adults. *2nd OU-OUHSC Biomedical Engineering Symposium, Oklahoma City, OK, 2018.*
9. Lee J, Chen Y, Tang J, Chen Y, O'Keeffe J, Shou G, Ding L, Yuan H, Multimodal Imaging of Human Brain Auditory Responses Using Simultaneous EEG and fNIRS *2nd OU-OUHSC Biomedical Engineering Symposium, Oklahoma City, OK, 2018.*
10. Farrand J, Chen Y, Tang J, Chen Y, O'Keeffe J, Shou G, Ding L, Yuan H*: Multimodal Imaging of Human Brain Auditory Responses Using Simultaneous EEG and fNIRS. *1st OU-OUHSC Biomedical Engineering Symposium, Oklahoma City, OK, 2017*
11. Chen Y, Farrand J, Tang J, Chen Y, O'Keeffe J, Shou G, Ding L, Yuan H*: Amplitude of Resting-State fNIRS Global Signal is related to EEG Vigilance Measures *1st OU-OUHSC Biomedical Engineering Symposium, Oklahoma City, OK, 2017.*
12. Chen Y, Farrand J, Tang J, Chen Y, O'Keeffe J, Shou G, Ding L, Yuan H, Amplitude of Resting-State fNIRS Global Signal is related to EEG Vigilance Measures, *8th International IEEE EMBS Conference on Neural Engineering* 2017.

13. Chen Y, Farrand J, Tang J, Chen Y, O'Keeffe J, Shou G, Ding L, Yuan H*: Amplitude of Resting-State fNIRS Global Signal is related to EEG Vigilance Measures *8th International IEEE EMBS Neural Engineering Conference, Shang Hai, China, 2017.*
14. Chen Y, Farrand J, Tang J, Chen Y, O'Keeffe J, Shou G, Ding L, Yuan H, Amplitude of Resting-State fNIRS Global Signal is related to EEG Vigilance Measures *1st OU-OUHSC Biomedical Engineering Symposium 2017*.

Poster Presentations

1. Chen Y, Tang J, DeStefano L, Ding L, Craft M, Wenger M, Carlson B, Yuan H, EEG Fluctuations of Default Mode Network in Middle-Aged and Older Adults *3rd OU-OUHSC Biomedical Engineering Symposium, Oklahoma City, OK, 2019*
2. Chen Y, Roque J Tang J, Craft M, Carlson B, Yuan H. Fluctuations of Hemodynamic Global Signal Are Correlated with Vigilance States: A Simultaneous EEG and fNIRS study *41st Annual International Conference of the IEEE Engineering in Medicine and Biology Society, Berlin, Germany, 2019*
3. Chen Y, Chen Y, Tang J, O'Keefee J, Shou G, Ding L, Yuan H. Different Body Positions Affect Amplitude of Resting-State fNIRS Global Signal and EEG Vigilance Measures *Sixth Biennial Conference on Resting State and Brain Connectivity,2018.*
4. Chen Y, Tang J, O'Keefee J, Shou G, Ding L, Yuan H. Relationship between Amplitude of Resting-State fNIRS Global Signal and EEG Vigilance Measures. *OU graduate research day, 2018.*

5. Chen Y, Tang J, O'Keefee J, Shou G, Ding L, Yuan H. Relationship between Amplitude of Resting-State fNIRS Global Signal and EEG Vigilance Measures. *2nd OU-OUHSC Biomedical Engineering Symposium, 2018.*
6. Chen Y, Carlson B, Craft M, DeStefano L, Worth T, Tang J, Ding L, Yuan H. EEG Fluctuation of Wake and Sleep in Different Age Healthy Groups *2nd OU-OUHSC Biomedical Engineering Symposium, 2018.*
7. Chen Y, Farrand J, Tang J, Chen Y, O'Keeffe J, Shou G, Ding L, Yuan H*: Amplitude of Resting-State fNIRS Global Signal is related to EEG Vigilance Measures, *8th International IEEE EMBS Conference on Neural Engineering 2017.*
8. Chen Y, Farrand J, Tang J, Chen Y, O'Keeffe J, Shou G, Ding L, Yuan H: Amplitude of Resting-State fNIRS Global Signal is related to EEG Vigilance Measures, *1st OU-OUHSC Biomedical Engineering Symposium 2017*.

Oral Presentations

1. Chen Y, Tang J, DeStefano L, Ding L, Craft M, Wenger M, Carlson B, Yuan H, Electrophysiological Resting State Brain Network and Episodic Memory Changes in Healthy Aging Adults. *OCNS Research Retreat, Oklahoma City, OK, 2020*
2. Chen Y, Yuan H, Wearable Technology Assists Diagnosis of Alzheimer's Disease. *Three Minute Thesis*, Norman, OK, 2020

References

Aguirre, G.K., Zarahn, E., and D'Esposito, M. (1998). The variability of human, BOLD hemodynamic responses. *Neuroimage* 8(4)**,** 360-369. doi: 10.1006/nimg.1998.0369.

Amodio, D.M., and Frith, C.D. (2006). Meeting of minds: the medial frontal cortex and social cognition. *Nature Reviews Neuroscience* 7(4)**,** 268-277. doi: 10.1038/nrn1884.

Andrews-Hanna, J.R., Snyder, A.Z., Vincent, J.L., Lustig, C., Head, D., Raichle, M.E., et al. (2007). Disruption of large-scale brain systems in advanced aging. *Neuron* 56(5)**,** 924-935. doi: 10.1016/j.neuron.2007.10.038.

Association, A.s. (2020). 2020 Alzheimer's disease facts and figures. *Alzheimer's & Dementia* 16(3)**,** 391-460. doi: 10.1002/alz.12068.

Atkinson, R.C., and Shiffrin, R.M. (1968). "Human Memory: A Proposed System and its Control Processes," in *Psychology of Learning and Motivation*, eds. K.W. Spence & J.T. Spence. Academic Press), 89-195.

Baddeley, A., Cocchini, G., Della Sala, S., Logie, R.H., and Spinnler, H. (1999). Working memory and vigilance: evidence from normal aging and Alzheimer's disease. *Brain Cogn* 41(1)**,** 87-108. doi: 10.1006/brcg.1999.1097.

Baddeley, A.D. (1990). "The development of the concept of working memory: Implications and contributions of neuropsychology," in *Neuropsychological impairments of short-term memory*. (New York, NY, US: Cambridge University Press), 54-73.

Bai, F., Watson, D.R., Yu, H., Shi, Y., Yuan, Y., and Zhang, Z. (2009). Abnormal resting-state functional connectivity of posterior cingulate cortex in amnestic type mild cognitive impairment. *Brain Res* 1302**,** 167-174. doi: 10.1016/j.brainres.2009.09.028.

Bai, F., Zhang, Z., Yu, H., Shi, Y., Yuan, Y., Zhu, W., et al. (2008). Default-mode network activity distinguishes amnestic type mild cognitive impairment from healthy aging: a combined structural and resting-state functional MRI study. *Neurosci Lett* 438(1)**,** 111-115. doi: 10.1016/j.neulet.2008.04.021.

Beard, J.R., Officer, A., de Carvalho, I.A., Sadana, R., Pot, A.M., Michel, J.-P., et al. (2016). The World report on ageing and health: a policy framework for healthy ageing. *Lancet (London, England)* 387(10033)**,** 2145-2154. doi: 10.1016/S0140-6736(15)00516-4.

Beckmann, C.F., DeLuca, M., Devlin, J.T., and Smith, S.M. (2005a). Investigations into resting-state connectivity using independent component analysis. *Philos Trans R Soc Lond B Biol Sci* 360(1457)**,** 1001-1013. doi: 10.1098/rstb.2005.1634.

Beckmann, C.F., DeLuca, M., Devlin, J.T., and Smith, S.M. (2005b). Investigations into resting-state connectivity using independent component analysis. *Philosophical Transactions of the Royal Society B: Biological Sciences* 360(1457)**,** 1001-1013. doi: doi:10.1098/rstb.2005.1634.

Behrmann, M., Geng, J.J., and Shomstein, S. (2004). Parietal cortex and attention. *Current Opinion in Neurobiology* 14(2)**,** 212-217. doi: https://doi.org/10.1016/j.conb.2004.03.012.

Berry, R.B., Brooks, R., Gamaldo, C., Harding, S.M., Lloyd, R.M., Quan, S.F., et al. (2017). AASM Scoring Manual Updates for 2017 (Version 2.4). *Journal of clinical sleep medicine : JCSM : official publication of the American Academy of Sleep Medicine* 13(5)**,** 665-666. doi: 10.5664/jcsm.6576.

Birn, R.M., Diamond, J.B., Smith, M.A., and Bandettini, P.A. (2006). Separating respiratory-variation-related fluctuations from neuronal-activity-related fluctuations in fMRI. *Neuroimage* 31(4)**,** 1536-1548. doi: 10.1016/j.neuroimage.2006.02.048.

Biswal, B., Yetkin, F.Z., Haughton, V.M., and Hyde, J.S. (1995a). Functional connectivity in the motor cortex of resting human brain using echo-planar MRI. *Magn Reson Med* 34(4)**,** 537-541.

Biswal, B., Zerrin Yetkin, F., Haughton, V.M., and Hyde, J.S. (1995b). Functional connectivity in the motor cortex of resting human brain using echo-planar mri. *Magnetic Resonance in Medicine* 34(4)**,** 537-541. doi: 10.1002/mrm.1910340409.

Boutros, N.N., Arfken, C., Galderisi, S., Warrick, J., Pratt, G., and Iacono, W. (2008). The status of spectral EEG abnormality as a diagnostic test for schizophrenia. *Schizophrenia research* 99(1-3)**,** 225-237.

Braskie, M.N., Small, G.W., and Bookheimer, S.Y. (2010). Vascular health risks and fMRI activation during a memory task in older adults. *Neurobiology of Aging* 31(9)**,** 1532-1542. doi: https://doi.org/10.1016/j.neurobiolaging.2008.08.016.

Braun, A.R., Balkin, T.J., Wesenten, N.J., Carson, R.E., Varga, M., Baldwin, P., et al. (1997). Regional cerebral blood flow throughout the sleep-wake cycle. An H2(15)O PET study. *Brain* 120 (Pt 7)**,** 1173-1197.

Brier, M.R., Thomas, J.B., and Ances, B.M. (2014). Network dysfunction in Alzheimer's disease: refining the disconnection hypothesis. *Brain connectivity* 4(5)**,** 299-311. doi: 10.1089/brain.2014.0236.

Brigadoi, S., and Cooper, R.J. (2015). How short is short? Optimum source-detector distance for short-separation channels in functional near-infrared spectroscopy. *Neurophotonics* 2(2)**,** 025005. doi: 10.1117/1.NPh.2.2.025005.

Brookes, M.J., Woolrich, M., Luckhoo, H., Price, D., Hale, J.R., Stephenson, M.C., et al. (2011). Investigating the electrophysiological basis of resting state networks using

magnetoencephalography. *Proc Natl Acad Sci U S A* 108(40)**,** 16783-16788. doi: 10.1073/pnas.1112685108.

Buckner, R.L., Andrews-Hanna, J.R., and Schacter, D.L. (2008). The brain's default network: anatomy, function, and relevance to disease. *Ann N Y Acad Sci* 1124**,** 1-38. doi: 10.1196/annals.1440.011.

Buckner, R.L., Snyder, A.Z., Shannon, B.J., LaRossa, G., Sachs, R., Fotenos, A.F., et al. (2005). Molecular, structural, and functional characterization of Alzheimer's disease: evidence for a relationship between default activity, amyloid, and memory. *J Neurosci* 25(34)**,** 7709-7717. doi: 10.1523/jneurosci.2177-05.2005.

Cabeza, R. (2002). Hemispheric asymmetry reduction in older adults: the HAROLD model. *Psychol Aging* 17(1)**,** 85-100. doi: 10.1037//0882-7974.17.1.85.

Cabeza, R., Albert, M., Belleville, S., Craik, F.I.M., Duarte, A., Grady, C.L., et al. (2018). Maintenance, reserve and compensation: the cognitive neuroscience of healthy ageing. *Nat Rev Neurosci* 19(11)**,** 701-710. doi: 10.1038/s41583-018-0068-2.

Calhoun, V.D., Sui, J., Kiehl, K., Turner, J.A., Allen, E.A., and Pearlson, G. (2012). Exploring the psychosis functional connectome: aberrant intrinsic networks in schizophrenia and bipolar disorder. *Frontiers in psychiatry* 2**,** 75.

Cavedo, E., Lista, S., Khachaturian, Z., Aisen, P., Amouyel, P., Herholz, K., et al. (2014). The Road Ahead to Cure Alzheimer's Disease: Development of Biological Markers and Neuroimaging Methods for Prevention Trials Across all Stages and Target Populations. *J Prev Alzheimers Dis* 1(3)**,** 181-202. doi: 10.14283/jpad.2014.32.

Cepeda, N.J., Kramer, A.F., and Gonzalez de Sather, J.C.M. (2001). Changes in executive control across the life span: Examination of task-switching performance. *Developmental Psychology* 37(5)**,** 715-730. doi: 10.1037/0012-1649.37.5.715.

Chang, C., Leopold, D.A., Scholvinck, M.L., Mandelkow, H., Picchioni, D., Liu, X., et al. (2016a). Tracking brain arousal fluctuations with fMRI. *Proc Natl Acad Sci U S A* 113(16)**,** 4518-4523. doi: 10.1073/pnas.1520613113.

Chang, C., Leopold, D.A., Schölvinck, M.L., Mandelkow, H., Picchioni, D., Liu, X., et al. (2016b). Tracking brain arousal fluctuations with fMRI. *Proceedings of the National Academy of Sciences* 113(16)**,** 4518-4523. doi: 10.1073/pnas.1520613113.

Chen, G., Chen, G., Xie, C., Ward, B.D., Li, W., Antuono, P., et al. (2012). A method to determine the necessity for global signal regression in resting-state fMRI studies. *Magn Reson Med* 68(6)**,** 1828-1835. doi: 10.1002/mrm.24201.

Chen, J.J. (2019). Functional MRI of brain physiology in aging and neurodegenerative diseases. *Neuroimage* 187**,** 209-225. doi: 10.1016/j.neuroimage.2018.05.050.

Chen, K., Azeez, A., Chen, D.Y., and Biswal, B.B. (2020). Resting-State Functional Connectivity: Signal Origins and Analytic Methods. *Neuroimaging Clinics of North America* 30(1)**,** 15-23. doi: https://doi.org/10.1016/j.nic.2019.09.012.

Chen, Y., Cha, Y.H., Li, C., Shou, G., Gleghorn, D., Ding, L., et al. (2019). Multimodal Imaging of Repetitive Transcranial Magnetic Stimulation Effect on Brain Network: A Combined Electroencephalogram and Functional Magnetic Resonance Imaging Study. *Brain Connect* 9(4)**,** 311-321. doi: 10.1089/brain.2018.0647.

Cordes, D., Haughton, V.M., Arfanakis, K., Carew, J.D., Turski, P.A., Moritz, C.H., et al. (2001). Frequencies contributing to functional connectivity in the cerebral cortex in "resting-state" data. *AJNR Am J Neuroradiol* 22(7)**,** 1326-1333.

Cragg, L., Kovacevic, N., McIntosh, A.R., Poulsen, C., Martinu, K., Leonard, G., et al. (2011). Maturation of EEG power spectra in early adolescence: a longitudinal study. *Developmental Science* 14(5)**,** 935-943. doi: 10.1111/j.1467-7687.2010.01031.x.

Crous-Bou, M., Minguillón, C., Gramunt, N., and Molinuevo, J.L. (2017). Alzheimer's disease prevention: from risk factors to early intervention. *Alzheimer's Research & Therapy* 9(1)**,** 71. doi: 10.1186/s13195-017-0297-z.

Cummings, J., Aisen, P.S., DuBois, B., Frölich, L., Jack, C.R., Jones, R.W., et al. (2016). Drug development in Alzheimer's disease: the path to 2025. *Alzheimer's Research & Therapy* 8(1)**,** 39. doi: 10.1186/s13195-016-0207-9.

Custo, A., Van De Ville, D., Wells, W.M., Tomescu, M.I., Brunet, D., and Michel, C.M. (2017). Electroencephalographic Resting-State Networks: Source Localization of Microstates. *Brain connectivity* 7(10)**,** 671-682. doi: 10.1089/brain.2016.0476.

D'Esposito, M., Deouell, L.Y., and Gazzaley, A. (2003). Alterations in the BOLD fMRI signal with ageing and disease: a challenge for neuroimaging. *Nat Rev Neurosci* 4(11)**,** 863-872. doi: 10.1038/nrn1246.

Dale, A.M., and Sereno, M.I. (1993). Improved Localizadon of Cortical Activity by Combining EEG and MEG with MRI Cortical Surface Reconstruction: A Linear Approach. *J Cogn Neurosci* 5(2)**,** 162-176. doi: 10.1162/jocn.1993.5.2.162.

Damoiseaux, J.S., Beckmann, C.F., Arigita, E.J.S., Barkhof, F., Scheltens, P., Stam, C.J., et al. (2007). Reduced resting-state brain activity in the “default network” in normal aging. *Cerebral Cortex* 18(8)**,** 1856-1864. doi: 10.1093/cercor/bhm207.

Damoiseaux, J.S., Prater, K.E., Miller, B.L., and Greicius, M.D. (2012). Functional connectivity tracks clinical deterioration in Alzheimer's disease. *Neurobiol Aging* 33(4)**,** 828.e819-830. doi: 10.1016/j.neurobiolaging.2011.06.024.

Damoiseaux, J.S., Rombouts, S.A., Barkhof, F., Scheltens, P., Stam, C.J., Smith, S.M., et al. (2006). Consistent resting-state networks across healthy subjects. *Proc Natl Acad Sci U S A* 103(37)**,** 13848-13853. doi: 10.1073/pnas.0601417103.

Davidson, J.G.S., and Guthrie, D.M. (2017). Older Adults With a Combination of Vision and Hearing Impairment Experience Higher Rates of Cognitive Impairment, Functional Dependence, and Worse Outcomes Across a Set of Quality Indicators. *Journal of Aging and Health* 31(1)**,** 85-108. doi: 10.1177/0898264317723407.

Desjardins, A.E., Kiehl, K.A., and Liddle, P.F. (2001). Removal of confounding effects of global signal in functional MRI analyses. *Neuroimage* 13(4)**,** 751-758. doi: 10.1006/nimg.2000.0719.

Donohue, M.C., Sperling, R.A., Salmon, D.P., Rentz, D.M., Raman, R., Thomas, R.G., et al. (2014a). The preclinical Alzheimer cognitive composite: measuring amyloid-related decline. *JAMA Neurol* 71(8)**,** 961-970. doi: 10.1001/jamaneurol.2014.803.

Donohue, M.C., Sperling, R.A., Salmon, D.P., Rentz, D.M., Raman, R., Thomas, R.G., et al. (2014b). The preclinical Alzheimer cognitive composite: measuring amyloid-related decline. *JAMA neurology* 71(8)**,** 961-970. doi: 10.1001/jamaneurol.2014.803.

Du, X., Wang, X., and Geng, M. (2018). Alzheimer's disease hypothesis and related therapies. *Translational Neurodegeneration* 7(1)**,** 2. doi: 10.1186/s40035-018-0107-y.

Duan, L., Zhao, Z., Lin, Y., Wu, X., Luo, Y., and Xu, P. (2018). Wavelet-based method for removing global physiological noise in functional near-infrared spectroscopy. *Biomed Opt Express* 9(8)**,** 3805-3820. doi: 10.1364/BOE.9.003805.

Dubois, B., Hampel, H., Feldman, H.H., Scheltens, P., Aisen, P., Andrieu, S., et al. (2016). Preclinical Alzheimer's disease: Definition, natural history, and diagnostic criteria. *Alzheimers Dement* 12(3)**,** 292-323. doi: 10.1016/j.jalz.2016.02.002.

Eggebrecht, A.T., Ferradal, S.L., Robichaux-Viehoever, A., Hassanpour, M.S., Dehghani, H., Snyder, A.Z., et al. (2014). Mapping distributed brain function and networks with diffuse optical tomography. *Nat Photonics* 8(6)**,** 448-454. doi: 10.1038/nphoton.2014.107.

Eggebrecht, A.T., White, B.R., Ferradal, S.L., Chen, C., Zhan, Y., Snyder, A.Z., et al. (2012). A quantitative spatial comparison of high-density diffuse optical tomography and fMRI cortical mapping. *Neuroimage* 61(4)**,** 1120-1128. doi: 10.1016/j.neuroimage.2012.01.124.

Falahpour, M., Chang, C., Wong, C.W., and Liu, T.T. (2018). Template-based prediction of vigilance fluctuations in resting-state fMRI. *Neuroimage* 174**,** 317-327. doi: 10.1016/j.neuroimage.2018.03.012.

Ferreira, L.K., and Busatto, G.F. (2013). Resting-state functional connectivity in normal brain aging. *Neuroscience & Biobehavioral Reviews* 37(3)**,** 384-400. doi: https://doi.org/10.1016/j.neubiorev.2013.01.017.

Ferreira, L.K., Regina, A.C.B., Kovacevic, N., Martin, M.d.G.M., Santos, P.P., Carneiro, C.d.G., et al. (2016). Aging Effects on Whole-Brain Functional Connectivity in Adults Free of

Cognitive and Psychiatric Disorders. *Cerebral Cortex* 26(9)**,** 3851-3865. doi: 10.1093/cercor/bhv190.

Fiandaca, M.S., Mapstone, M.E., Cheema, A.K., and Federoff, H.J. (2014). The critical need for defining preclinical biomarkers in Alzheimer's disease. *Alzheimers Dement* 10(3 Suppl)**,** S196-212. doi: 10.1016/j.jalz.2014.04.015.

Filippini, N., MacIntosh, B.J., Hough, M.G., Goodwin, G.M., Frisoni, G.B., Smith, S.M., et al. (2009). Distinct patterns of brain activity in young carriers of the APOE-epsilon4 allele. *Proc Natl Acad Sci U S A* 106(17)**,** 7209-7214. doi: 10.1073/pnas.0811879106.

Fox, M.D., Snyder, A.Z., Vincent, J.L., Corbetta, M., Van Essen, D.C., and Raichle, M.E. (2005). The human brain is intrinsically organized into dynamic, anticorrelated functional networks. *Proc Natl Acad Sci U S A* 102(27)**,** 9673-9678. doi: 10.1073/pnas.0504136102.

Fox, M.D., Zhang, D., Snyder, A.Z., and Raichle, M.E. (2009). The global signal and observed anticorrelated resting state brain networks. *J Neurophysiol* 101(6)**,** 3270-3283. doi: 10.1152/jn.90777.2008.

Fox, P.T., Mintun, M.A., Reiman, E.M., and Raichle, M.E. (1988). Enhanced detection of focal brain responses using intersubject averaging and change-distribution analysis of subtracted PET images. *J Cereb Blood Flow Metab* 8(5)**,** 642-653. doi: 10.1038/jcbfm.1988.111.

Franceschi, C., Garagnani, P., Vitale, G., Capri, M., and Salvioli, S. (2017). Inflammaging and 'Garb-aging'. *Trends Endocrinol Metab* 28(3)**,** 199-212. doi: 10.1016/j.tem.2016.09.005.

Franceschini, M.A., Joseph, D.K., Huppert, T.J., Diamond, S.G., and Boas, D.A. (2006). Diffuse optical imaging of the whole head. *J Biomed Opt* 11(5)**,** 054007. doi: 10.1117/1.2363365.

Friston, K.J., Frith, C.D., Liddle, P.F., Dolan, R.J., Lammertsma, A.A., and Frackowiak, R.S. (1990). The relationship between global and local changes in PET scans. *J Cereb Blood Flow Metab* 10(4)**,** 458-466. doi: 10.1038/jcbfm.1990.88.

Fu, H., Hardy, J., and Duff, K.E. (2018). Selective vulnerability in neurodegenerative diseases. *Nature Neuroscience* 21(10)**,** 1350-1358. doi: 10.1038/s41593-018-0221-2.

Fukunaga, M., Horovitz, S.G., van Gelderen, P., de Zwart, J.A., Jansma, J.M., Ikonomidou, V.N., et al. (2006). Large-amplitude, spatially correlated fluctuations in BOLD fMRI signals during extended rest and early sleep stages. *Magn Reson Imaging* 24(8)**,** 979-992. doi: 10.1016/j.mri.2006.04.018.

Furlan, R., Porta, A., Costa, F., Tank, J., Baker, L., Schiavi, R., et al. (2000). Oscillatory patterns in sympathetic neural discharge and cardiovascular variables during orthostatic stimulus. *Circulation* 101(8)**,** 886-892.

Gagnon, L., Perdue, K., Greve, D.N., Goldenholz, D., Kaskhedikar, G., and Boas, D.A. (2011). Improved recovery of the hemodynamic response in diffuse optical imaging using short optode separations and state-space modeling. *Neuroimage* 56(3)**,** 1362-1371. doi: 10.1016/j.neuroimage.2011.03.001.

Gallagher, M., and Koh, M.T. (2011). Episodic memory on the path to Alzheimer's disease. *Curr Opin Neurobiol* 21(6)**,** 929-934. doi: 10.1016/j.conb.2011.10.021.

Giffard, B., Desgranges, B., Nore-Mary, F., Lalevée, C., de la Sayette, V., Pasquier, F., et al. (2001). The nature of semantic memory deficits in Alzheimer's disease: new insights from hyperpriming effects. *Brain* 124(Pt 8)**,** 1522-1532. doi: 10.1093/brain/124.8.1522.

Glover, G.H., Li, T.Q., and Ress, D. (2000). Image-based method for retrospective correction of physiological motion effects in fMRI: RETROICOR. *Magn Reson Med* 44(1)**,** 162-167.

Golde, T.E., Schneider, L.S., and Koo, E.H. (2011). Anti-aβ therapeutics in Alzheimer's disease: the need for a paradigm shift. *Neuron* 69(2)**,** 203-213. doi: 10.1016/j.neuron.2011.01.002.

Goldman, R.I., Stern, J.M., Engel, J., Jr., and Cohen, M.S. (2002). Simultaneous EEG and fMRI of the alpha rhythm. *Neuroreport* 13(18)**,** 2487-2492. doi: 10.1097/01.wnr.0000047685.08940.d0.

Gordon, B.A., Blazey, T.M., Su, Y., Hari-Raj, A., Dincer, A., Flores, S., et al. (2018). Spatial patterns of neuroimaging biomarker change in individuals from families with autosomal dominant Alzheimer's disease: a longitudinal study. *Lancet Neurol* 17(3)**,** 241-250. doi: 10.1016/s1474-4422(18)30028-0.

Grady, C. (2012). The cognitive neuroscience of ageing. *Nature reviews. Neuroscience* 13(7)**,** 491-505. doi: 10.1038/nrn3256.

Grady, C.L., McIntosh, A.R., Horwitz, B., Maisog, J.M., Ungerleider, L.G., Mentis, M.J., et al. (1995). Age-related reductions in human recognition memory due to impaired encoding. *Science* 269(5221)**,** 218-221. doi: 10.1126/science.7618082.

Greicius, M.D., Krasnow, B., Reiss, A.L., and Menon, V. (2003). Functional connectivity in the resting brain: a network analysis of the default mode hypothesis. *Proc Natl Acad Sci U S A* 100(1)**,** 253-258. doi: 10.1073/pnas.0135058100.

Greicius, M.D., Srivastava, G., Reiss, A.L., and Menon, V. (2004a). Default-mode network activity distinguishes Alzheimer's disease from healthy aging: evidence from functional MRI. *Proc Natl Acad Sci U S A* 101(13)**,** 4637-4642. doi: 10.1073/pnas.0308627101.

Greicius, M.D., Srivastava, G., Reiss, A.L., and Menon, V. (2004b). Default-mode network activity distinguishes Alzheimer's disease from healthy aging: Evidence from

functional MRI. *Proceedings of the National Academy of Sciences of the United States of America* 101(13)**,** 4637. doi: 10.1073/pnas.0308627101.

Gutchess, A.H., Kensinger, E.A., Yoon, C., and Schacter, D.L. (2007). Ageing and the self-reference effect in memory. *Memory* 15(8)**,** 822-837. doi: 10.1080/09658210701701394.

Hahamy, A., Calhoun, V., Pearlson, G., Harel, M., Stern, N., Attar, F., et al. (2014). Save the global: global signal connectivity as a tool for studying clinical populations with functional magnetic resonance imaging. *Brain Connect* 4(6)**,** 395-403. doi: 10.1089/brain.2014.0244.

Hämäläinen, M.S., and Ilmoniemi, R.J. (1994). Interpreting magnetic fields of the brain: minimum norm estimates. *Medical & Biological Engineering & Computing* 32(1)**,** 35-42. doi: 10.1007/bf02512476.

Hampson, M., Peterson, B.S., Skudlarski, P., Gatenby, J.C., and Gore, J.C. (2002). Detection of functional connectivity using temporal correlations in MR images. *Hum Brain Mapp* 15(4)**,** 247-262. doi: 10.1002/hbm.10022.

Hanseeuw, B.J., Betensky, R.A., Jacobs, H.I.L., Schultz, A.P., Sepulcre, J., Becker, J.A., et al. (2019). Association of Amyloid and Tau With Cognition in Preclinical Alzheimer Disease: A Longitudinal Study. *JAMA Neurology* 76(8)**,** 915-924. doi: 10.1001/jamaneurol.2019.1424.

He, B.J., Snyder, A.Z., Zempel, J.M., Smyth, M.D., and Raichle, M.E. (2008). Electrophysiological correlates of the brain's intrinsic large-scale functional architecture. *Proc Natl Acad Sci U S A* 105(41)**,** 16039-16044. doi: 10.1073/pnas.0807010105.

He, H., Shin, D., and Liu, A. (Year). "Resting state BOLD fluctuations in large draining veins are highly correlated with the global mean signal", in: *Proceedings of the 18th Annual Meeting of the ISMRM*).

Head, D., Rodrigue, K.M., Kennedy, K.M., and Raz, N. (2008). Neuroanatomical and cognitive mediators of age-related differences in episodic memory. *Neuropsychology* 22(4)**,** 491-507. doi: 10.1037/0894-4105.22.4.491.

Healey, M.K., Campbell, K.L., and Hasher, L. (2008). "Chapter 22 Cognitive aging and increased distractibility: Costs and potential benefits," in *Progress in Brain Research,* eds. W.S. Sossin, J.-C. Lacaille, V.F. Castellucci & S. Belleville. Elsevier), 353-363.

Hebert, L.E., Bienias, J.L., Aggarwal, N.T., Wilson, R.S., Bennett, D.A., Shah, R.C., et al. (2010). Change in risk of Alzheimer disease over time. *Neurology* 75(9)**,** 786-791. doi: 10.1212/WNL.0b013e3181f0754f.

Hebert, L.E., Weuve, J., Scherr, P.A., and Evans, D.A. (2013). Alzheimer disease in the United States (2010-2050) estimated using the 2010 census. *Neurology* 80(19)**,** 1778-1783. doi: 10.1212/WNL.0b013e31828726f5.

Hedden, T., and Gabrieli, J.D.E. (2004). Insights into the ageing mind: a view from cognitive neuroscience. *Nature Reviews Neuroscience* 5(2)**,** 87-96. doi: 10.1038/nrn1323.

Homae, F., Watanabe, H., Otobe, T., Nakano, T., Go, T., Konishi, Y., et al. (2010). Development of global cortical networks in early infancy. *J Neurosci* 30(14)**,** 4877-4882. doi: 10.1523/JNEUROSCI.5618-09.2010.

Horovitz, S.G., Braun, A.R., Carr, W.S., Picchioni, D., Balkin, T.J., Fukunaga, M., et al. (2009). Decoupling of the brain's default mode network during deep sleep. *Proceedings of the National Academy of Sciences of the United States of America* 106(27)**,** 11376-11381. doi: 10.1073/pnas.0901435106.

Horovitz, S.G., Fukunaga, M., de Zwart, J.A., van Gelderen, P., Fulton, S.C., Balkin, T.J., et al. (2008). Low frequency BOLD fluctuations during resting wakefulness and light sleep: a

simultaneous EEG-fMRI study. *Hum Brain Mapp* 29(6)**,** 671-682. doi: 10.1002/hbm.20428.

Hoscheidt, S.M., Nadel, L., Payne, J., and Ryan, L. (2010). Hippocampal activation during retrieval of spatial context from episodic and semantic memory. *Behav Brain Res* 212(2)**,** 121-132. doi: 10.1016/j.bbr.2010.04.010.

Hsu, D., and Marshall, G.A. (2017). Primary and Secondary Prevention Trials in Alzheimer Disease: Looking Back, Moving Forward. *Curr Alzheimer Res* 14(4)**,** 426-440. doi: 10.2174/1567205013666160930112125.

Huettel, S.A., Song, A.W., and McCarthy, G. (2004). *Functional magnetic resonance imaging*. Sinauer Associates Sunderland, MA.

Huppert, T.J., Diamond, S.G., Franceschini, M.A., and Boas, D.A. (2009). HomER: a review of time-series analysis methods for near-infrared spectroscopy of the brain. *Appl Opt* 48(10)**,** D280-298.

Ittner, L.M., and Götz, J. (2011). Amyloid-β and tau — a toxic pas de deux in Alzheimer's disease. *Nature Reviews Neuroscience* 12(2)**,** 67-72. doi: 10.1038/nrn2967.

Jahani, S., Fantana, A.L., Harper, D., Ellison, J.M., Boas, D.A., Forester, B.P., et al. (2017). fNIRS can robustly measure brain activity during memory encoding and retrieval in healthy subjects. *Sci Rep* 7(1)**,** 9533. doi: 10.1038/s41598-017-09868-w.

Jasper, H.H. (1958). The Ten-Twenty Electrode System of the International Federation. . *Electroencephalography and Clinical Neurophysiology* 10**,** 371-375.

Jawinski, P., Kirsten, H., Sander, C., Spada, J., Ulke, C., Huang, J., et al. (2019). Human brain arousal in the resting state: a genome-wide association study. *Molecular psychiatry* 24(11)**,** 1599-1609.

Jobert, M., Schulz, H., Jähnig, P., Tismer, C., Bes, F., and Escola, H. (1994). A computerized method for detecting episodes of wakefulness during sleep based on the alpha slow-wave index (ASI). *Sleep* 17(1)**,** 37-46.

Jockwitz, C., Caspers, S., Lux, S., Eickhoff, S.B., Jutten, K., Lenzen, S., et al. (2017). Influence of age and cognitive performance on resting-state brain networks of older adults in a population-based cohort. *Cortex* 89**,** 28-44. doi: 10.1016/j.cortex.2017.01.008.

Jones, D.T., Machulda, M.M., Vemuri, P., McDade, E.M., Zeng, G., Senjem, M.L., et al. (2011). Age-related changes in the default mode network are more advanced in Alzheimer disease. *Neurology* 77(16)**,** 1524-1531. doi: 10.1212/WNL.0b013e318233b33d.

Julien, C. (2006). The enigma of Mayer waves: Facts and models. *Cardiovasc Res* 70(1)**,** 12-21. doi: 10.1016/j.cardiores.2005.11.008.

Karran, E., Mercken, M., and Strooper, B.D. (2011). The amyloid cascade hypothesis for Alzheimer's disease: an appraisal for the development of therapeutics. *Nature Reviews Drug Discovery* 10(9)**,** 698-712. doi: 10.1038/nrd3505.

Kay, K.N., Rokem, A., Winawer, J., Dougherty, R.F., and Wandell, B.A. (2013). GLMdenoise: a fast, automated technique for denoising task-based fMRI data. *Front Neurosci* 7**,** 247. doi: 10.3389/fnins.2013.00247.

Keehn, B., Wagner, J.B., Tager-Flusberg, H., and Nelson, C.A. (2013). Functional connectivity in the first year of life in infants at-risk for autism: a preliminary near-infrared spectroscopy study. *Front Hum Neurosci* 7**,** 444. doi: 10.3389/fnhum.2013.00444.

Kocsis, L., Herman, P., and Eke, A. (2006). The modified Beer-Lambert law revisited. *Phys Med Biol* 51(5)**,** N91-98. doi: 10.1088/0031-9155/51/5/N02.

Kohno, S., Miyai, I., Seiyama, A., Oda, I., Ishikawa, A., Tsuneishi, S., et al. (2007). Removal of the skin blood flow artifact in functional near-infrared spectroscopic imaging data through independent component analysis. *J Biomed Opt* 12(6)**,** 062111. doi: 10.1117/1.2814249.

Korczyn, A.D., Vakhapova, V., and Grinberg, L.T. (2012). Vascular dementia. *J Neurol Sci* 322(1-2)**,** 2-10. doi: 10.1016/j.jns.2012.03.027.

Larson-Prior, L.J., Zempel, J.M., Nolan, T.S., Prior, F.W., Snyder, A.Z., and Raichle, M.E. (2009). Cortical network functional connectivity in the descent to sleep. *Proc Natl Acad Sci U S A* 106(11)**,** 4489-4494. doi: 10.1073/pnas.0900924106.

Lehmann, D., Ozaki, H., and Pal, I. (1987). EEG alpha map series: brain micro-states by space-oriented adaptive segmentation. *Electroencephalogr Clin Neurophysiol* 67(3)**,** 271-288. doi: 10.1016/0013-4694(87)90025-3.

Leopold, D.A., Murayama, Y., and Logothetis, N.K. (2003). Very slow activity fluctuations in monkey visual cortex: implications for functional brain imaging. *Cereb Cortex* 13(4)**,** 422-433.

Li, C., Yuan, H., Shou, G., Cha, Y.-H., Sunderam, S., Besio, W., et al. (2018). Cortical Statistical Correlation Tomography of EEG Resting State Networks. *Frontiers in Neuroscience* 12(365). doi: 10.3389/fnins.2018.00365.

Li, R., Nguyen, T., Potter, T., and Zhang, Y. (2019). Dynamic cortical connectivity alterations associated with Alzheimer's disease: An EEG and fNIRS integration study. *NeuroImage. Clinical* 21**,** 101622-101622. doi: 10.1016/j.nicl.2018.101622.

Liguori, C., Romigi, A., Nuccetelli, M., Zannino, S., Sancesario, G., Martorana, A., et al. (2014). Orexinergic system dysregulation, sleep impairment, and cognitive decline in Alzheimer disease. *JAMA Neurol* 71(12)**,** 1498-1505. doi: 10.1001/jamaneurol.2014.2510.

Liu, C.-C., Liu, C.-C., Kanekiyo, T., Xu, H., and Bu, G. (2013). Apolipoprotein E and Alzheimer disease: risk, mechanisms and therapy. *Nature reviews. Neurology* 9(2)**,** 106-118. doi: 10.1038/nrneurol.2012.263.

Liu, Q., Farahibozorg, S., Porcaro, C., Wenderoth, N., and Mantini, D. (2017a). Detecting large-scale networks in the human brain using high-density electroencephalography. *Human Brain Mapping* 38(9)**,** 4631-4643. doi: 10.1002/hbm.23688.

Liu, T.T. (2013). Neurovascular factors in resting-state functional MRI. *NeuroImage* 80**,** 339-348. doi: 10.1016/j.neuroimage.2013.04.071.

Liu, T.T. (2016). Noise contributions to the fMRI signal: An overview. *Neuroimage* 143**,** 141-151. doi: 10.1016/j.neuroimage.2016.09.008.

Liu, T.T., Nalci, A., and Falahpour, M. (2017b). The global signal in fMRI: Nuisance or Information? *NeuroImage* 150**,** 213-229. doi: 10.1016/j.neuroimage.2017.02.036.

Liu, X., de Zwart, J.A., Scholvinck, M.L., Chang, C., Ye, F.Q., Leopold, D.A., et al. (2018a). Subcortical evidence for a contribution of arousal to fMRI studies of brain activity. *Nat Commun* 9(1)**,** 395. doi: 10.1038/s41467-017-02815-3.

Liu, X., de Zwart, J.A., Schölvinck, M.L., Chang, C., Ye, F.Q., Leopold, D.A., et al. (2018b). Subcortical evidence for a contribution of arousal to fMRI studies of brain activity. *Nature Communications* 9(1)**,** 395. doi: 10.1038/s41467-017-02815-3.

Logothetis, N.K. (2008). What we can do and what we cannot do with fMRI. *Nature* 453(7197)**,** 869-878. doi: 10.1038/nature06976.

Lu, C.-M., Zhang, Y.-J., Biswal, B.B., Zang, Y.-F., Peng, D.-L., and Zhu, C.-Z. (2010). Use of fNIRS to assess resting state functional connectivity. *Journal of Neuroscience Methods* 186(2)**,** 242-249. doi: https://doi.org/10.1016/j.jneumeth.2009.11.010.

Luo, L., and Craik, F.I.M. (2008). Aging and Memory: A Cognitive Approach. *The Canadian Journal of Psychiatry* 53(6)**,** 346-353. doi: 10.1177/070674370805300603.

Macey, P.M., Macey, K.E., Kumar, R., and Harper, R.M. (2004). A method for removal of global effects from fMRI time series. *Neuroimage* 22(1)**,** 360-366. doi: 10.1016/j.neuroimage.2003.12.042.

Madden, D.J. (1990). Adult age differences in attentional selectivity and capacity. *European Journal of Cognitive Psychology* 2(3)**,** 229-252. doi: 10.1080/09541449008406206.

Madsen, P.L., Schmidt, J.F., Holm, S., Vorstrup, S., Lassen, N.A., and Wildschiodtz, G. (1991a). Cerebral oxygen metabolism and cerebral blood flow in man during light sleep (stage 2). *Brain Res* 557(1-2)**,** 217-220.

Madsen, P.L., Schmidt, J.F., Wildschiodtz, G., Friberg, L., Holm, S., Vorstrup, S., et al. (1991b). Cerebral O2 metabolism and cerebral blood flow in humans during deep and rapid-eye-movement sleep. *J Appl Physiol (1985)* 70(6)**,** 2597-2601. doi: 10.1152/jappl.1991.70.6.2597.

Mantini, D., Perrucci, M.G., Del Gratta, C., Romani, G.L., and Corbetta, M. (2007). Electrophysiological signatures of resting state networks in the human brain. *Proc Natl Acad Sci U S A* 104(32)**,** 13170-13175. doi: 10.1073/pnas.0700668104.

Marshall, P.J., Bar-Haim, Y., and Fox, N.A. (2002). Development of the EEG from 5 months to 4 years of age. *Clinical Neurophysiology* 113(8)**,** 1199-1208. doi: https://doi.org/10.1016/S1388-2457(02)00163-3.

McAvoy, M., Mitra, A., Coalson, R.S., d'Avossa, G., Keidel, J.L., Petersen, S.E., et al. (2016). Unmasking Language Lateralization in Human Brain Intrinsic Activity. *Cereb Cortex* 26(4)**,** 1733-1746. doi: 10.1093/cercor/bhv007.

McAvoy, M., Mitra, A., Tagliazucchi, E., Laufs, H., and Raichle, M.E. (2017). Mapping visual dominance in human sleep. *Neuroimage* 150**,** 250-261. doi: 10.1016/j.neuroimage.2017.02.053.

McAvoy, M.P., Tagliazucchi, E., Laufs, H., and Raichle, M.E. (2018). Human non-REM sleep and the mean global BOLD signal. *J Cereb Blood Flow Metab***,** 271678X18791070. doi: 10.1177/0271678X18791070.

Mesquita, R.C., Franceschini, M.A., and Boas, D.A. (2010). Resting state functional connectivity of the whole head with near-infrared spectroscopy. *Biomed Opt Express* 1(1)**,** 324-336. doi: 10.1364/BOE.1.000324.

Mesulam, M.M. (1990). Large-scale neurocognitive networks and distributed processing for attention, language, and memory. *Ann Neurol* 28(5)**,** 597-613. doi: 10.1002/ana.410280502.

Mevel, K., Chételat, G., Eustache, F., and Desgranges, B. (2011). The default mode network in healthy aging and Alzheimer's disease. *International journal of Alzheimer's disease* 2011**,** 535816-535816. doi: 10.4061/2011/535816.

Michel, C.M., Murray, M.M., Lantz, G., Gonzalez, S., Spinelli, L., and Grave de Peralta, R. (2004). EEG source imaging. *Clinical Neurophysiology* 115(10)**,** 2195-2222. doi: https://doi.org/10.1016/j.clinph.2004.06.001.

Mizukami, K., and Katada, A. (2018). EEG frequency characteristics in healthy advanced elderly. *Journal of Psychophysiology* 32(3)**,** 131-139. doi: 10.1027/0269-8803/a000190.

Mohammadi-Nejad, A.R., Mahmoudzadeh, M., Hassanpour, M.S., Wallois, F., Muzik, O., Papadelis, C., et al. (2018). Neonatal brain resting-state functional connectivity imaging modalities. *Photoacoustics* 10**,** 1-19. doi: 10.1016/j.pacs.2018.01.003.

Molavi, B., May, L., Gervain, J., Carreiras, M., Werker, J.F., and Dumont, G.A. (2013). Analyzing the resting state functional connectivity in the human language system using near infrared spectroscopy. *Front Hum Neurosci* 7**,** 921. doi: 10.3389/fnhum.2013.00921.

Mormino, E.C., Smiljic, A., Hayenga, A.O., Onami, S.H., Greicius, M.D., Rabinovici, G.D., et al. (2011). Relationships between β-amyloid and functional connectivity in different components of the default mode network in aging. *Cereb Cortex* 21(10)**,** 2399-2407. doi: 10.1093/cercor/bhr025.

Muller, T., Reinhard, M., Oehm, E., Hetzel, A., and Timmer, J. (2003). Detection of very low-frequency oscillations of cerebral haemodynamics is influenced by data detrending. *Med Biol Eng Comput* 41(1)**,** 69-74.

Murphy, K., Birn, R.M., Handwerker, D.A., Jones, T.B., and Bandettini, P.A. (2009). The impact of global signal regression on resting state correlations: are anti-correlated networks introduced? *Neuroimage* 44(3)**,** 893-905. doi: 10.1016/j.neuroimage.2008.09.036.

Murphy, K., and Fox, M.D. (2017). Towards a consensus regarding global signal regression for resting state functional connectivity MRI. *Neuroimage* 154**,** 169-173. doi: 10.1016/j.neuroimage.2016.11.052.

Natu, V.S., Lin, J.-J., Burks, A., Arora, A., Rugg, M.D., and Lega, B. (2019). Stimulation of the Posterior Cingulate Cortex Impairs Episodic Memory Encoding. *The Journal of Neuroscience* 39(36)**,** 7173. doi: 10.1523/JNEUROSCI.0698-19.2019.

Nelson, P.T., Head, E., Schmitt, F.A., Davis, P.R., Neltner, J.H., Jicha, G.A., et al. (2011). Alzheimer's disease is not "brain aging": neuropathological, genetic, and epidemiological human studies. *Acta Neuropathol* 121(5)**,** 571-587. doi: 10.1007/s00401-011-0826-y.

Newton, A.T., Morgan, V.L., Rogers, B.P., and Gore, J.C. (2011). Modulation of steady state functional connectivity in the default mode and working memory networks by cognitive load. *Hum Brain Mapp* 32(10)**,** 1649-1659. doi: 10.1002/hbm.21138.

Novi, S.L., Rodrigues, R.B., and Mesquita, R.C. (2016). Resting state connectivity patterns with near-infrared spectroscopy data of the whole head. *Biomed Opt Express* 7(7)**,** 2524-2537. doi: 10.1364/BOE.7.002524.

O'Keeffe, J., Carlson, B., DeStefano, L., Wenger, M., Craft, M., Hershey, L., et al. (2017). EEG fluctuations of wake and sleep in mild cognitive impairment. *Conf Proc IEEE Eng Med Biol Soc* 2017**,** 3612-3615. doi: 10.1109/embc.2017.8037639.

Obrig, H., Neufang, M., Wenzel, R., Kohl, M., Steinbrink, J., Einhaupl, K., et al. (2000). Spontaneous low frequency oscillations of cerebral hemodynamics and metabolism in human adults. *Neuroimage* 12(6)**,** 623-639. doi: 10.1006/nimg.2000.0657.

Obrig, H., and Villringer, A. (2003). Beyond the visible--imaging the human brain with light. *J Cereb Blood Flow Metab* 23(1)**,** 1-18. doi: 10.1097/01.WCB.0000043472.45775.29.

Oken, B.S., Salinsky, M.C., and Elsas, S. (2006). Vigilance, alertness, or sustained attention: physiological basis and measurement. *Clinical neurophysiology* 117(9)**,** 1885-1901.

Olbrich, S., Mulert, C., Karch, S., Trenner, M., Leicht, G., Pogarell, O., et al. (2009a). EEG-vigilance and BOLD effect during simultaneous EEG/fMRI measurement. *Neuroimage* 45(2)**,** 319-332.

Olbrich, S., Mulert, C., Karch, S., Trenner, M., Leicht, G., Pogarell, O., et al. (2009b). EEG-vigilance and BOLD effect during simultaneous EEG/fMRI measurement. *Neuroimage* 45(2)**,** 319-332. doi: 10.1016/j.neuroimage.2008.11.014.

Peters, R. (2006). Ageing and the brain. *Postgrad Med J* 82(964)**,** 84-88. doi: 10.1136/pgmj.2005.036665.

Petrella, J.R., Sheldon, F.C., Prince, S.E., Calhoun, V.D., and Doraiswamy, P.M. (2011). Default mode network connectivity in stable vs progressive mild cognitive impairment. *Neurology* 76(6)**,** 511-517. doi: 10.1212/WNL.0b013e31820af94e.

Pinti, P., Scholkmann, F., Hamilton, A., Burgess, P., and Tachtsidis, I. (2019). Current Status and Issues Regarding Pre-processing of fNIRS Neuroimaging Data: An Investigation of Diverse Signal Filtering Methods Within a General Linear Model Framework. *Frontiers in Human Neuroscience* 12(505). doi: 10.3389/fnhum.2018.00505.

Pinti, P., Tachtsidis, I., Hamilton, A., Hirsch, J., Aichelburg, C., Gilbert, S., et al. (2018). The present and future use of functional near-infrared spectroscopy (fNIRS) for cognitive neuroscience. *Ann N Y Acad Sci*. doi: 10.1111/nyas.13948.

Pinti, P., Tachtsidis, I., Hamilton, A., Hirsch, J., Aichelburg, C., Gilbert, S., et al. (2020). The present and future use of functional near-infrared spectroscopy (fNIRS) for cognitive neuroscience. *Ann N Y Acad Sci* 1464(1)**,** 5-29. doi: 10.1111/nyas.13948.

Piolino, P., Desgranges, B., Hubert, V., Bernard, F.A., Matuszewski, V., Chételat, G., et al. (2008). Reliving lifelong episodic autobiographical memories via the hippocampus: a correlative resting PET study in healthy middle-aged subjects. *Hippocampus* 18(5)**,** 445-459. doi: 10.1002/hipo.20406.

Power, J.D., Plitt, M., Laumann, T.O., and Martin, A. (2017). Sources and implications of whole-brain fMRI signals in humans. *Neuroimage* 146**,** 609-625. doi: 10.1016/j.neuroimage.2016.09.038.

Power, J.D., Schlaggar, B.L., and Petersen, S.E. (2015). Recent progress and outstanding issues in motion correction in resting state fMRI. *Neuroimage* 105**,** 536-551. doi: 10.1016/j.neuroimage.2014.10.044.

Prinz, P.N., Vitaliano, P.P., Vitiello, M.V., Bokan, J., Raskind, M., Peskind, E., et al. (1982). Sleep, EEG and mental function changes in senile dementia of the Alzheimer's type. *Neurobiology of Aging* 3(4)**,** 361-370. doi: https://doi.org/10.1016/0197-4580(82)90024-0.

Qi, Z., Wu, X., Wang, Z., Zhang, N., Dong, H., Yao, L., et al. (2010). Impairment and compensation coexist in amnestic MCI default mode network. *Neuroimage* 50(1)**,** 48-55. doi: 10.1016/j.neuroimage.2009.12.025.

Rabin, L.A., Paré, N., Saykin, A.J., Brown, M.J., Wishart, H.A., Flashman, L.A., et al. (2009). Differential memory test sensitivity for diagnosing amnestic mild cognitive impairment and predicting conversion to Alzheimer's disease. *Neuropsychology, development, and cognition. Section B, Aging, neuropsychology and cognition* 16(3)**,** 357-376. doi: 10.1080/13825580902825220.

Race, E., Keane, M.M., and Verfaellie, M. (2011). Medial temporal lobe damage causes deficits in episodic memory and episodic future thinking not attributable to deficits in narrative construction. *The Journal of neuroscience : the official journal of the Society for Neuroscience* 31(28)**,** 10262-10269. doi: 10.1523/JNEUROSCI.1145-11.2011.

Raichle, M.E., MacLeod, A.M., Snyder, A.Z., Powers, W.J., Gusnard, D.A., and Shulman, G.L. (2001). A default mode of brain function. *Proc Natl Acad Sci U S A* 98(2)**,** 676-682. doi: 10.1073/pnas.98.2.676.

Raz, N., and Rodrigue, K.M. (2006). Differential aging of the brain: Patterns, cognitive correlates and modifiers. *Neuroscience & Biobehavioral Reviews* 30(6)**,** 730-748. doi: https://doi.org/10.1016/j.neubiorev.2006.07.001.

Razavi, N., Jann, K., Koenig, T., Kottlow, M., Hauf, M., Strik, W., et al. (2013). Shifted coupling of EEG driving frequencies and fMRI resting state networks in schizophrenia spectrum disorders. *PLoS One* 8(10)**,** e76604.

Ribot, T. (1891). *Les maladies de la mémoire.* Baillière.

Royall, D.R., Chiodo, L.K., and Polk, M.J. (2000). Correlates of disability among elderly retirees with "subclinical" cognitive impairment. *The Journals of Gerontology: Series A: Biological Sciences and Medical Sciences* 55(9)**,** M541-M546. doi: 10.1093/gerona/55.9.M541.

Royall, D.R., Cordes, J.A., and Polk, M. (1998). CLOX: an executive clock drawing task. *J Neurol Neurosurg Psychiatry* 64(5)**,** 588-594. doi: 10.1136/jnnp.64.5.588.

Rypma, B., and D'Esposito, M. (2000). Isolating the neural mechanisms of age-related changes in human working memory. *Nat Neurosci* 3(5)**,** 509-515. doi: 10.1038/74889.

Rypma, B., Prabhakaran, V., Desmond, J.E., and Gabrieli, J.D. (2001). Age differences in prefrontal cortical activity in working memory. *Psychology and aging* 16(3)**,** 371.

Saad, Z.S., Gotts, S.J., Murphy, K., Chen, G., Jo, H.J., Martin, A., et al. (2012). Trouble at rest: how correlation patterns and group differences become distorted after global signal regression. *Brain Connect* 2(1)**,** 25-32. doi: 10.1089/brain.2012.0080.

Saager, R., and Berger, A. (2008). Measurement of layer-like hemodynamic trends in scalp and cortex: implications for physiological baseline suppression in functional near-infrared spectroscopy. *J Biomed Opt* 13(3)**,** 034017. doi: 10.1117/1.2940587.

Saager, R.B., and Berger, A.J. (2005). Direct characterization and removal of interfering absorption trends in two-layer turbid media. *J Opt Soc Am A Opt Image Sci Vis* 22(9)**,** 1874-1882.

Sakakibara, E., Homae, F., Kawasaki, S., Nishimura, Y., Takizawa, R., Koike, S., et al. (2016). Detection of resting state functional connectivity using partial correlation analysis: A study using multi-distance and whole-head probe near-infrared spectroscopy. *Neuroimage* 142**,** 590-601. doi: 10.1016/j.neuroimage.2016.08.011.

Sambataro, F., Murty, V.P., Callicott, J.H., Tan, H.Y., Das, S., Weinberger, D.R., et al. (2010). Age-related alterations in default mode network: impact on working memory performance. *Neurobiol Aging* 31(5)**,** 839-852. doi: 10.1016/j.neurobiolaging.2008.05.022.

Sander, C., Hensch, T., Wittekind, D.A., Boettger, D., and Hegerl, U. (2015). Assessment of wakefulness and brain arousal regulation in psychiatric research. *Neuropsychobiology* 72(3-4)**,** 195-205.

Santosa, H., Zhai, X., Fishburn, F., and Huppert, T. (2018). The NIRS Brain AnalyzIR Toolbox. *Algorithms* 11(5)**,** 73.

Sasai, S., Homae, F., Watanabe, H., and Taga, G. (2011). Frequency-specific functional connectivity in the brain during resting state revealed by NIRS. *Neuroimage* 56(1)**,** 252-257. doi: 10.1016/j.neuroimage.2010.12.075.

Sato, C., Barthélemy, N.R., Mawuenyega, K.G., Patterson, B.W., Gordon, B.A., Jockel-Balsarotti, J., et al. (2018). Tau Kinetics in Neurons and the Human Central Nervous System. *Neuron* 97(6)**,** 1284-1298.e1287. doi: 10.1016/j.neuron.2018.02.015.

Sato, T., Nambu, I., Takeda, K., Aihara, T., Yamashita, O., Isogaya, Y., et al. (2016). Reduction of global interference of scalp-hemodynamics in functional near-infrared spectroscopy

using short distance probes. *Neuroimage* 141**,** 120-132. doi: 10.1016/j.neuroimage.2016.06.054.

Satterthwaite, T.D., Elliott, M.A., Gerraty, R.T., Ruparel, K., Loughead, J., Calkins, M.E., et al. (2013). An improved framework for confound regression and filtering for control of motion artifact in the preprocessing of resting-state functional connectivity data. *NeuroImage* 64**,** 240-256. doi: https://doi.org/10.1016/j.neuroimage.2012.08.052.

Sauzéon, H., N'Kaoua, B., Pala, P.A., Taillade, M., Auriacombe, S., and Guitton, P. (2016). Everyday-like memory for objects in ageing and Alzheimer's disease assessed in a visually complex environment: The role of executive functioning and episodic memory. *J Neuropsychol* 10(1)**,** 33-58. doi: 10.1111/jnp.12055.

Scheff, S.W., and Price, D.A. (2006). Alzheimer's disease-related alterations in synaptic density: neocortex and hippocampus. *J Alzheimers Dis* 9(3 Suppl)**,** 101-115. doi: 10.3233/jad-2006-9s312.

Scholkmann, F., Kleiser, S., Metz, A.J., Zimmermann, R., Mata Pavia, J., Wolf, U., et al. (2014). A review on continuous wave functional near-infrared spectroscopy and imaging instrumentation and methodology. *Neuroimage* 85 Pt 1**,** 6-27. doi: 10.1016/j.neuroimage.2013.05.004.

Scholvinck, M.L., Maier, A., Ye, F.Q., Duyn, J.H., and Leopold, D.A. (2010). Neural basis of global resting-state fMRI activity. *Proc Natl Acad Sci U S A* 107(22)**,** 10238-10243. doi: 10.1073/pnas.0913110107.

Seripa, D., Franceschi, M., Matera, M.G., Panza, F., Kehoe, P.G., Gravina, C., et al. (2006). Sex Differences in the Association of Apolipoprotein E and Angiotensin-Converting Enzyme Gene Polymorphisms With Healthy Aging and Longevity: A Population-Based Study

From Southern Italy. *The Journals of Gerontology: Series A* 61(9)**,** 918-923. doi: 10.1093/gerona/61.9.918.

Sestieri, C., Corbetta, M., Romani, G.L., and Shulman, G.L. (2011). Episodic memory retrieval, parietal cortex, and the default mode network: functional and topographic analyses. *The Journal of neuroscience : the official journal of the Society for Neuroscience* 31(12)**,** 4407-4420. doi: 10.1523/JNEUROSCI.3335-10.2011.

Shaw, A.C., Goldstein, D.R., and Montgomery, R.R. (2013). Age-dependent dysregulation of innate immunity. *Nat Rev Immunol* 13(12)**,** 875-887. doi: 10.1038/nri3547.

Sheline, Y.I., and Raichle, M.E. (2013). Resting state functional connectivity in preclinical Alzheimer's disease. *Biol Psychiatry* 74(5)**,** 340-347. doi: 10.1016/j.biopsych.2012.11.028.

Shin, J., Kwon, J., Choi, J., and Im, C.H. (2017). Performance enhancement of a brain-computer interface using high-density multi-distance NIRS. *Sci Rep* 7(1)**,** 16545. doi: 10.1038/s41598-017-16639-0.

Shmuel, A., and Leopold, D.A. (2008). Neuronal correlates of spontaneous fluctuations in fMRI signals in monkey visual cortex: Implications for functional connectivity at rest. *Hum Brain Mapp* 29(7)**,** 751-761. doi: 10.1002/hbm.20580.

Shmueli, K., van Gelderen, P., de Zwart, J.A., Horovitz, S.G., Fukunaga, M., Jansma, J.M., et al. (2007). Low-frequency fluctuations in the cardiac rate as a source of variance in the resting-state fMRI BOLD signal. *Neuroimage* 38(2)**,** 306-320. doi: 10.1016/j.neuroimage.2007.07.037.

Smith, A. (1982). *Symbol digit modalities test.* Western Psychological Services Los Angeles, CA.

Sood, B.G., McLaughlin, K., and Cortez, J. (2015). Near-infrared spectroscopy: applications in neonates. *Semin Fetal Neonatal Med* 20(3)**,** 164-172. doi: 10.1016/j.siny.2015.03.008.

Sorg, C., Riedl, V., Muhlau, M., Calhoun, V.D., Eichele, T., Laer, L., et al. (2007). Selective changes of resting-state networks in individuals at risk for Alzheimer's disease. *Proc Natl Acad Sci U S A* 104(47)**,** 18760-18765. doi: 10.1073/pnas.0708803104.

Sperling, R. (2011). Potential of functional MRI as a biomarker in early Alzheimer's disease. *Neurobiol Aging* 32 Suppl 1**,** S37-43. doi: 10.1016/j.neurobiolaging.2011.09.009.

Sperling, R., Mormino, E., and Johnson, K. (2014). The evolution of preclinical Alzheimer's disease: implications for prevention trials. *Neuron* 84(3)**,** 608-622. doi: 10.1016/j.neuron.2014.10.038.

Sperling, R.A., Aisen, P.S., Beckett, L.A., Bennett, D.A., Craft, S., Fagan, A.M., et al. (2011). Toward defining the preclinical stages of Alzheimer's disease: recommendations from the National Institute on Aging-Alzheimer's Association workgroups on diagnostic guidelines for Alzheimer's disease. *Alzheimers Dement* 7(3)**,** 280-292. doi: 10.1016/j.jalz.2011.03.003.

Strittmatter, W.J., Saunders, A.M., Schmechel, D., Pericak-Vance, M., Enghild, J., Salvesen, G.S., et al. (1993a). Apolipoprotein E: high-avidity binding to beta-amyloid and increased frequency of type 4 allele in late-onset familial Alzheimer disease. *Proc Natl Acad Sci U S A* 90(5)**,** 1977-1981. doi: 10.1073/pnas.90.5.1977.

Strittmatter, W.J., Weisgraber, K.H., Huang, D.Y., Dong, L.M., Salvesen, G.S., Pericak-Vance, M., et al. (1993b). Binding of human apolipoprotein E to synthetic amyloid beta peptide: isoform-specific effects and implications for late-onset Alzheimer disease. *Proceedings of the National Academy of Sciences of the United States of America* 90(17)**,** 8098-8102. doi: 10.1073/pnas.90.17.8098.

Stroop, J.R. (1935). Studies of interference in serial verbal reactions. *Journal of Experimental Psychology* 18(6)**,** 643-662. doi: 10.1037/h0054651.

Sweeney, M.D., Kisler, K., Montagne, A., Toga, A.W., and Zlokovic, B.V. (2018). The role of brain vasculature in neurodegenerative disorders. *Nat Neurosci* 21(10)**,** 1318-1331. doi: 10.1038/s41593-018-0234-x.

Tachtsidis, I., Elwell, C.E., Leung, T.S., Lee, C.W., Smith, M., and Delpy, D.T. (2004). Investigation of cerebral haemodynamics by near-infrared spectroscopy in young healthy volunteers reveals posture-dependent spontaneous oscillations. *Physiol Meas* 25(2)**,** 437-445.

Tachtsidis, I., and Scholkmann, F. (2016). False positives and false negatives in functional near-infrared spectroscopy: issues, challenges, and the way forward. *Neurophotonics* 3(3)**,** 031405. doi: 10.1117/1.NPh.3.3.031405.

Tong, Y., and Frederick, B.D. (2010). Time lag dependent multimodal processing of concurrent fMRI and near-infrared spectroscopy (NIRS) data suggests a global circulatory origin for low-frequency oscillation signals in human brain. *Neuroimage* 53(2)**,** 553-564. doi: 10.1016/j.neuroimage.2010.06.049.

Torricelli, A., Contini, D., Pifferi, A., Caffini, M., Re, R., Zucchelli, L., et al. (2014). Time domain functional NIRS imaging for human brain mapping. *Neuroimage* 85 Pt 1**,** 28-50. doi: 10.1016/j.neuroimage.2013.05.106.

Tromp, D., Dufour, A., Lithfous, S., Pebayle, T., and Després, O. (2015a). Episodic memory in normal aging and Alzheimer disease: Insights from imaging and behavioral studies. *Ageing Res Rev* 24(Pt B)**,** 232-262. doi: 10.1016/j.arr.2015.08.006.

Tromp, D., Dufour, A., Lithfous, S., Pebayle, T., and Després, O. (2015b). Episodic memory in normal aging and Alzheimer disease: Insights from imaging and behavioral studies. *Ageing Research Reviews* 24**,** 232-262. doi: https://doi.org/10.1016/j.arr.2015.08.006.

Uttl, B. (2002). North American Adult Reading Test: age norms, reliability, and validity. *J Clin Exp Neuropsychol* 24(8)**,** 1123-1137. doi: 10.1076/jcen.24.8.1123.8375.

Verhaeghen, P., Marcoen, A., and Goossens, L. (1993). Facts and Fiction About Memory Aging: A Quantitative Integration of Research Findings. *Journal of Gerontology* 48(4)**,** P157-P171. doi: 10.1093/geronj/48.4.P157.

Wang, H.-L.S., Rau, C.-L., Li, Y.-M., Chen, Y.-P., and Yu, R. (2015). Disrupted thalamic resting-state functional networks in schizophrenia. *Frontiers in behavioral neuroscience* 9**,** 45.

Wang, K., Liang, M., Wang, L., Tian, L., Zhang, X., Li, K., et al. (2007). Altered functional connectivity in early Alzheimer's disease: a resting-state fMRI study. *Hum Brain Mapp* 28(10)**,** 967-978. doi: 10.1002/hbm.20324.

Wang, L., Laviolette, P., O'Keefe, K., Putcha, D., Bakkour, A., Van Dijk, K.R., et al. (2010). Intrinsic connectivity between the hippocampus and posteromedial cortex predicts memory performance in cognitively intact older individuals. *Neuroimage* 51(2)**,** 910-917. doi: 10.1016/j.neuroimage.2010.02.046.

Wang, X., Sun, G., Feng, T., Zhang, J., Huang, X., Wang, T., et al. (2019). Sodium oligomannate therapeutically remodels gut microbiota and suppresses gut bacterial amino acids-shaped neuroinflammation to inhibit Alzheimer's disease progression. *Cell Research* 29(10)**,** 787-803. doi: 10.1038/s41422-019-0216-x.

Watabe, T., and Hatazawa, J. (2019). Evaluation of Functional Connectivity in the Brain Using Positron Emission Tomography: A Mini-Review. *Front Neurosci* 13**,** 775. doi: 10.3389/fnins.2019.00775.

Watanabe, H., Shitara, Y., Aoki, Y., Inoue, T., Tsuchida, S., Takahashi, N., et al. (2017). Hemoglobin phase of oxygenation and deoxygenation in early brain development measured using fNIRS. *Proceedings of the National Academy of Sciences of the United States of America* 114(9)**,** E1737-E1744. doi: 10.1073/pnas.1616866114.

Watanabe, N., Reece, J., and Polus, B.I. (2007a). Effects of body position on autonomic regulation of cardiovascular function in young, healthy adults. *Chiropractic & osteopathy* 15**,** 19-19. doi: 10.1186/1746-1340-15-19.

Watanabe, N., Reece, J., and Polus, B.I. (2007b). Effects of body position on autonomic regulation of cardiovascular function in young, healthy adults. *Chiropr Osteopat* 15**,** 19. doi: 10.1186/1746-1340-15-19.

Wechsler, D. (1987). Manual for the Wechsler memory scale-revised. *San Antonio, TX: Psychological Corporation*.

Weissenbacher, A., Kasess, C., Gerstl, F., Lanzenberger, R., Moser, E., and Windischberger, C. (2009). Correlations and anticorrelations in resting-state functional connectivity MRI: a quantitative comparison of preprocessing strategies. *Neuroimage* 47(4)**,** 1408-1416. doi: 10.1016/j.neuroimage.2009.05.005.

Wenger, M.K., Negash, S., Petersen, R.C., and Petersen, L. (2010). Modeling and Estimating Recall Processing Capacity: Sensitivity and Diagnostic Utility in Application to Mild Cognitive Impairment. *J Math Psychol* 54(1)**,** 73-89. doi: 10.1016/j.jmp.2009.04.012.

Whalley, L.J., Fox, H.C., Wahle, K.W., Starr, J.M., and Deary, I.J. (2004). Cognitive aging, childhood intelligence, and the use of food supplements: possible involvement of n−3 fatty acids. *The American Journal of Clinical Nutrition* 80(6)**,** 1650-1657. doi: 10.1093/ajcn/80.6.1650.

White, B.R., Liao, S.M., Ferradal, S.L., Inder, T.E., and Culver, J.P. (2012). Bedside optical imaging of occipital resting-state functional connectivity in neonates. *Neuroimage* 59(3)**,** 2529-2538. doi: 10.1016/j.neuroimage.2011.08.094.

White, B.R., Snyder, A.Z., Cohen, A.L., Petersen, S.E., Raichle, M.E., Schlaggar, B.L., et al. (2009). Resting-state functional connectivity in the human brain revealed with diffuse optical tomography. *Neuroimage* 47(1)**,** 148-156. doi: 10.1016/j.neuroimage.2009.03.058.

Winocur, G., Moscovitch, M., and Bontempi, B. (2010). Memory formation and long-term retention in humans and animals: convergence towards a transformation account of hippocampal-neocortical interactions. *Neuropsychologia* 48(8)**,** 2339-2356. doi: 10.1016/j.neuropsychologia.2010.04.016.

Wise, R.G., Ide, K., Poulin, M.J., and Tracey, I. (2004). Resting fluctuations in arterial carbon dioxide induce significant low frequency variations in BOLD signal. *Neuroimage* 21(4)**,** 1652-1664. doi: 10.1016/j.neuroimage.2003.11.025.

Wong, C.W., DeYoung, P.N., and Liu, T.T. (2016). Differences in the resting-state fMRI global signal amplitude between the eyes open and eyes closed states are related to changes in EEG vigilance. *Neuroimage* 124(Pt A)**,** 24-31. doi: 10.1016/j.neuroimage.2015.08.053.

Wong, C.W., Olafsson, V., Tal, O., and Liu, T.T. (2013). The amplitude of the resting-state fMRI global signal is related to EEG vigilance measures. *Neuroimage* 83**,** 983-990. doi: 10.1016/j.neuroimage.2013.07.057.

Xia, X., Jiang, Q., McDermott, J., and Han, J.J. (2018). Aging and Alzheimer's disease: Comparison and associations from molecular to system level. *Aging Cell* 17(5)**,** e12802. doi: 10.1111/acel.12802.

Xiong, J., Parsons, L.M., Gao, J.H., and Fox, P.T. (1999). Interregional connectivity to primary motor cortex revealed using MRI resting state images. *Hum Brain Mapp* 8(2-3)**,** 151-156. doi: 10.1002/(sici)1097-0193(1999)8:2/3<151::aid-hbm13>3.0.co;2-5.

Xu, Y., Graber, H.L., and Barbour, R.L. (Year). "nirsLAB: A Computing Environment for fNIRS Neuroimaging Data Analysis", in: *Biomedical Optics 2014*: Optical Society of America), BM3A.1.

Yang, G.J., Murray, J.D., Glasser, M., Pearlson, G.D., Krystal, J.H., Schleifer, C., et al. (2017). Altered Global Signal Topography in Schizophrenia. *Cereb Cortex* 27(11)**,** 5156-5169. doi: 10.1093/cercor/bhw297.

Ye, J.C., Tak, S., Jang, K.E., Jung, J., and Jang, J. (2009). NIRS-SPM: Statistical parametric mapping for near-infrared spectroscopy. *NeuroImage* 44(2)**,** 428-447. doi: https://doi.org/10.1016/j.neuroimage.2008.08.036.

Yeo, B.T., Krienen, F.M., Sepulcre, J., Sabuncu, M.R., Lashkari, D., Hollinshead, M., et al. (2011). The organization of the human cerebral cortex estimated by intrinsic functional connectivity. *J Neurophysiol* 106(3)**,** 1125-1165. doi: 10.1152/jn.00338.2011.

Yuan, H., Ding, L., Zhu, M., Zotev, V., Phillips, R., and Bodurka, J. (2016). Reconstructing Large-Scale Brain Resting-State Networks from High-Resolution EEG: Spatial and Temporal Comparisons with fMRI. *Brain Connect* 6(2)**,** 122-135. doi: 10.1089/brain.2014.0336.

Yuan, H., Phillips, R., Wong, C.K., Zotev, V., Misaki, M., Wurfel, B., et al. (2018). Tracking resting state connectivity dynamics in veterans with PTSD. *Neuroimage Clin* 19**,** 260-270. doi: 10.1016/j.nicl.2018.04.014.

Yuan, H., Young, K.D., Phillips, R., Zotev, V., Misaki, M., and Bodurka, J. (2014). Resting-state functional connectivity modulation and sustained changes after real-time functional magnetic resonance imaging neurofeedback training in depression. *Brain connectivity* 4(9)**,** 690-701. doi: 10.1089/brain.2014.0262.

Yuan, H., Zotev, V., Phillips, R., and Bodurka, J. (2013). Correlated slow fluctuations in respiration, EEG, and BOLD fMRI. *Neuroimage* 79**,** 81-93. doi: 10.1016/j.neuroimage.2013.04.068.

Yuan, H., Zotev, V., Phillips, R., Drevets, W.C., and Bodurka, J. (2012). Spatiotemporal dynamics of the brain at rest--exploring EEG microstates as electrophysiological signatures of BOLD resting state networks. *Neuroimage* 60(4)**,** 2062-2072. doi: 10.1016/j.neuroimage.2012.02.031.

Yuxuan, C., Farrand, J., Tang, J., Yafen, C., O'Keeffe, J., Guofa, S., et al. (2017). Relationship between amplitude of resting-state fNIRS global signal and EEG vigilance measures. *Conf Proc IEEE Eng Med Biol Soc* 2017**,** 537-540. doi: 10.1109/EMBC.2017.8036880.

Zang, Y., Jiang, T., Lu, Y., He, Y., and Tian, L. (2004). Regional homogeneity approach to fMRI data analysis. *NeuroImage* 22(1)**,** 394-400. doi: https://doi.org/10.1016/j.neuroimage.2003.12.030.

Zarahn, E., Aguirre, G., and D'Esposito, M. (1997). A trial-based experimental design for fMRI. *Neuroimage* 6(2)**,** 122-138. doi: 10.1006/nimg.1997.0279.

Zeff, B.W., White, B.R., Dehghani, H., Schlaggar, B.L., and Culver, J.P. (2007). Retinotopic mapping of adult human visual cortex with high-density diffuse optical tomography. *Proc Natl Acad Sci U S A* 104(29)**,** 12169-12174. doi: 10.1073/pnas.0611266104.

Zhang, D., and Raichle, M.E. (2010). Disease and the brain's dark energy. *Nat Rev Neurol* 6(1)**,** 15-28. doi: 10.1038/nrneurol.2009.198.

Zhang, H., Duan, L., Zhang, Y.J., Lu, C.M., Liu, H., and Zhu, C.Z. (2011). Test-retest assessment of independent component analysis-derived resting-state functional connectivity based on functional near-infrared spectroscopy. *Neuroimage* 55(2)**,** 607-615. doi: 10.1016/j.neuroimage.2010.12.007.

Zhang, H., Zhang, Y.-J., Lu, C.-M., Ma, S.-Y., Zang, Y.-F., and Zhu, C.-Z. (2010). Functional connectivity as revealed by independent component analysis of resting-state fNIRS measurements. *NeuroImage* 51(3)**,** 1150-1161. doi: https://doi.org/10.1016/j.neuroimage.2010.02.080.

Zhang, H.Y., Wang, S.J., Xing, J., Liu, B., Ma, Z.L., Yang, M., et al. (2009a). Detection of PCC functional connectivity characteristics in resting-state fMRI in mild Alzheimer's disease. *Behav Brain Res* 197(1)**,** 103-108. doi: 10.1016/j.bbr.2008.08.012.

Zhang, Q., Brown, E.N., and Strangman, G.E. (2007). Adaptive filtering to reduce global interference in evoked brain activity detection: a human subject case study. *J Biomed Opt* 12(6)**,** 064009. doi: 10.1117/1.2804706.

Zhang, Q., Strangman, G.E., and Ganis, G. (2009b). Adaptive filtering to reduce global interference in non-invasive NIRS measures of brain activation: how well and when does it work? *Neuroimage* 45(3)**,** 788-794. doi: 10.1016/j.neuroimage.2008.12.048.

Zhang, X., Noah, J.A., and Hirsch, J. (2016). Separation of the global and local components in functional near-infrared spectroscopy signals using principal component spatial filtering. *Neurophotonics* 3(1)**,** 015004. doi: 10.1117/1.NPh.3.1.015004.

Zhang, Y., Brooks, D.H., Franceschini, M.A., and Boas, D.A. (2005). Eigenvector-based spatial filtering for reduction of physiological interference in diffuse optical imaging. *J Biomed Opt* 10(1)**,** 11014. doi: 10.1117/1.1852552.

Zhang, Y., van Drongelen, W., and He, B. (2006). Estimation of in vivo brain-to-skull conductivity ratio in humans. *Applied physics letters* 89(22)**,** 223903-2239033. doi: 10.1063/1.2398883.

Zonneveld, H.I., Pruim, R.H.R., Bos, D., Vrooman, H.A., Muetzel, R.L., Hofman, A., et al. (2019). Patterns of functional connectivity in an aging population: The Rotterdam Study. *NeuroImage* 189**,** 432-444. doi: https://doi.org/10.1016/j.neuroimage.2019.01.041.

Zou, Q.-H., Zhu, C.-Z., Yang, Y., Zuo, X.-N., Long, X.-Y., Cao, Q.-J., et al. (2008a). An improved approach to detection of amplitude of low-frequency fluctuation (ALFF) for resting-state fMRI: Fractional ALFF. *Journal of Neuroscience Methods* 172(1)**,** 137-141. doi: https://doi.org/10.1016/j.jneumeth.2008.04.012.

Zou, Q.H., Zhu, C.Z., Yang, Y., Zuo, X.N., Long, X.Y., Cao, Q.J., et al. (2008b). An improved approach to detection of amplitude of low-frequency fluctuation (ALFF) for resting-state fMRI: fractional ALFF. *J Neurosci Methods* 172(1)**,** 137-141. doi: 10.1016/j.jneumeth.2008.04.012.

Zuo, X.-N., Di Martino, A., Kelly, C., Shehzad, Z.E., Gee, D.G., Klein, D.F., et al. (2010). The oscillating brain: Complex and reliable. *NeuroImage* 49(2)**,** 1432-1445. doi: https://doi.org/10.1016/j.neuroimage.2009.09.037.